Evaluation Of Dynamic Properties For Asymmetric Linear System

By

Anukant Singh Jadeja

16MCLC01

DEPARTMENT OF CIVIL ENGINEERING

INSTITUTE OF TECHNOLOGY

NIRMA UNIVERSITY

AHMEDABAD-382481

May 2018

Evaluation Of Dynamic Properties For Asymmetric Linear System

Major Project

Submitted in partial fulfillment of the requirements

for the degree of

Master of Technology

in

Civil Engineering

(Computer Aided Structural Analysis and Design)

By

Anukant Singh Jadeja

16MCLC01

Under the guidance of

Dr. Sharad P Purohit

Department of Civil Engineering

Institute of Technology

Nirma University

Ahmedabad-382 481

May 2018

Declaration

This is to certify that

a. The thesis comprises my work towards the Degree of Master of Technology in Civil Engineering (Computer Aided Structural Analysis and Design) at Nirma University and has not been submitted elsewhere for a degree.

b. Due acknowledgment has been made in the text to all source material used.

Anukant Singh Jadeja

Certificate

This is to certify that Major Project entitled **"Evaluation of Dynamic Properties for Asymmetric Linear system"** submitted by **Anukant Singh Jadeja (16MCLC01)**, towards the partial fulfillment of the requirements for the degree of Master of Technology in Civil Engineering (Computer Aided Structural Analysis and Design) of Nirma University, Ahmedabad is the record of work carried out by him under my supervision and guidance. In my opinion, the submitted work has reached a level required for being accepted for examination. The results embodied in this major project, to the best of my knowledge, haven't been submitted to any other university or institution for award of any degree or diploma.

Dr. Sharad Purohit
Guide and Professor,
Dept. of Civil Engg.,
Institute of Technology,
Nirma University,
Ahmedabad.

Prof. Utsav Koshti
Co-Guide and Assistant Professor,
Dept. of Civil Engg.,
Institute of Technology,
Nirma University,
Ahmedabad.

Dr. P. V. Patel
Professor and Head,
Dept. of Civil Engg.,
Institute of Technology,
Nirma University,
Ahmedabad.

Dr. Alka Mahajan
Director,
Institute of Technology,
Nirma University,
Ahmedabad.

_____
Examiner

_____
Date of Examination

Abstract

The asymmetry in the building arises due to unsymmetrical distribution of mass, stiffness, damping and strength. Asymmetric building frame is characterized by coupling between translational and torsional degrees of freedom under the influence of an earthquake. And thus, it is susceptible not only to bending oscillations, but also torsional oscillations that can lead to failure of the building frame. If oscillations of such an asymmetric building frame are beyond acceptable limits, they need to be control by some control techniques. There are three types of Response control techniques which are widely adopted in the practice, namely, Passive damping, Active damping and Hybrid damping techniques. All techniques have distinct advantages and disadvantages and is adopted based on dynamics of the Problem.

In the present study asymmetric building with planar and geometrical irregularity are considered. Asymmetric building is modelled as Single Degree of Freedom (SDOF) System with L- and T- shaped scaled model fabricated using aluminium material as well as Aluminium model with one column of mild steel. To characterize coupling between translation and torsion degrees of freedom, SDOF models are subjected to base excitation at varied angle of incident using Uniaxial Shake Table. SDOF models are instrumented with Uni-axial Accelerometers and Data Acquisition Systems to capture translational and torsional response of the test models. Mathematical formulation is developed to compare experimental and analytical results. It has been found that no significant influence of angle of incident of base excitation is observed for the SDOF models with planar and material asymmetry. Existence of coupling between translational and torsional degree of freedom for Planar and Material Irregular models is established through response measurements. Air based Pneumatic Damper and Elastic and Friction based Piston Type Damper categorized as Passive Dampers are developed. Both types of Passive Dampers are characterized under displacement controlled cyclic loading and Equivalent Damping ratio () is determined at Civil Engineering Department, Institute of Technology, Nirma University. It has been observed that both passive dampers show hysteric behaviour under cyclic loading and hence capable of dissipation of energy to reduce seismic response. These passive dampers are then installed in asymmetric SDOF models and are tested under free and forced vibration. It has been observed that significant increase in damping value of SDOF models with passive dampers yields substantial reduction in the response.

Acknowledgement

I would like to thank my guide **Dr. Sharad P. Purohit,** whose keen interest and knowledge base helped me to carry out the major project work. His constant support and guidance during my project work equipped me with a great understanding of different aspects of the project work. He has shown keen interest in this work right from beginning and has been a great motivating factor in outlining the flow of my work.

I would like to express my gratitude to my co-guide **Prof. Utsav Koshti,** Professor, Civil Engineering Department for his valuable support and help for not only my Major Project work but throughout two years of M.tech study.

My sincere thanks to **Dr. Paresh V. Patel,** Head of Department, Civil Engineering Department for his kind suggestions and motivational words throughout the major project.

A special thanks to **Dr. Alka Mahajan,** Hon'ble Director, Institute of Technology, Nirma University, Ahmedabad for providing required resources for my project and healthy research environment.

I would also like to thank my senior and JRF **Mr. Pawan Pandey** for his everlasting support and encouragement in all possible ways throughout the major project work. I also express my gratitude towards **Mr. P. N. Raval, Mr.Sunil Regar** and all my classmates for their timely help during the various stages of experiments.

Most important, my deepest appreciation and thanks to Almighty and my family for their unending love, affection and personal sacrifices during the whole tenure of my study at Nirma University.

Anukant Singh Jadeja

16MCLC01

Abbreviation Notation and Nomenclature

LabVIEW ..... Laboratory Virtual Instrument Engineering Workbench

SDOF ..... Single Degree of Freedom

MDOF ..... Multi Degree of Freedom

DMF ..... Dynamic Magnification Factor

DAQ ..... Data Acquisition System

TR ..... Transmissibility Ratio

CM ..... Centre of Mass

CS ..... Cenrtre of Stiffness

ξ ..... Damping Coefficient

ω_d ..... Damped Natural Frequency

ω_n ..... Natural Frequency

ω_f ..... Forcing Frequency

η ..... Frequency Ratio

m ..... Mass of Member

L ..... Length of Member

k ..... Stiffness of Member

c ..... Damping

c_{cr} ..... Critical Damping

M ..... Mass Matrix

K ..... Stiffness Matrix

r ..... Raduis of Gyration

E ..... Modulus of Elasticity

I ..... Moment of Inertia

λ ..... Eigen Value

Φ ..... Eigen Vector

δ ..... Logarithmic Decrement

Contents

List of Tables

List of Figures

,

Chapter 1

Introduction

1.1 General

Understanding of Dynamic response of structural systems in an important topic in structural engineering field. Retrofitting of structures requires thorough understanding of Structures under various dynamic loads such as wind and earthquake.

Practically all structures behave dynamically when they are subjected to dynamic loads. Structures intend to resist this dynamic load by producing an inertia force of opposite nature which can be determined using Newton's second law, i.e. the additional inertia forces are equal to the mass times the acceleration. If the dynamic load is applied very slowly then the inertia force produced can be neglected and static load analysis is sufficient. Thus, static analysis is one sense simple case of dynamic analysis.

In general, structural response to any dynamic loading is expressed basically in terms of the displacements of the structure. Thus, a deterministic analysis leads directly to displacement time histories corresponding to the prescribed loading history; other related response quantities, such as stresses, strains, internal forces, etc., are usually obtained as a secondary phase of the analysis. On the other hand, a non deterministic analysis provides only statistical information about the displacements resulting from the statistically defined loading; corresponding information on the related response quantities are then generated using independent non deterministic analysis procedures.

A concept of response reduction of structure under the earthquake excitation was developed 100 years ago by Prof. John Miller of Japan. He placed a wooden house on ball bearing to demonstrate isolation from ground shaking. In aircraft, structure sensitive avionics instruments are isolated by providing isolation damper. Seismic response control of structure is directly influenced by numbers of passive energy dissipation devices and their placement. Seismic response control of building using passive energy dissipation devices like viscous damper, viscoelastic damper and metallic yield damper was studied by Mr. Vijay Chachapara, M.Tech (CASAD), IT,NU during academic year (2010-11). His dissertation work includes seismic response control of building subjected to four different types of earthquake expiation, namely,EL Centro, Kobe, Loma Prieta and Northridge earthquake. Three different passive energy dissipation devices like viscous, VE and metallic yield damper were used. Response quantitative maximum displacement, maximum velocity, maximum acceleration, maximum intensity drift and maximum deformation were extracted for controlled and uncontrolled boundary. The scope of work as mentioned in the dissertation work of Mr.Vijay Chachapara pointed out study of placement of damper for seismic response control. In the present work.

1.2 Need of the Study

The dynamic response of a system differs from the static response as system will respond dynamically when subjected to the dynamic loads. Thus it is inevitable for the Structural Engineer to understand dynamic response of the structural system so as better and safe structural system can be designed.

Earthquake damage depends on many parameters, including intensity, duration and frequency content of ground motion, geologic and soil condition, quality of construction, etc. Building design must be such as to ensure that the building has adequate strength, high ductility, and will remain as one unit, even while subjected to very large deformation.

Dynamic behavior of structure can be analyzed both experimentally and analytically, but in some cases it is difficult to determine Dynamic properties analytically such as damping, therefore it is important to determine such properties experimentally.

1.3 Objective of the Study

The major objective of the present work is to assess effect of base motion directionality on Regular and Irregular building model. Apart, efficacy of passive damper to control structural response of regular building is to be studied experimentally on Shake table facility.

1.4 Scope of the Work

- To derive from first principle, equation of motion for regular and irregular building. Apart, derive equation for building under bi-directional base motion.
- Fabricate building models representing SDOF system with Planar and Material Irregularity from aluminum materials.
- Develop experimental setup to derive basic dynamic properties of SDOF building models with planar and material as-symmetry using accelerometer, Data acquisition system (DAQ), LabVIEW and computer system.
- To capture Acceleration response of SDOF system with planar and material irregularity under bi-directional base motion
- To characterize passive damper through an experiment.
- To fabricate regular building model with passive damper instrument at appropriate locations.
- To test regular building with passive damper on the shake table facility.
- To analyze results captured for various regular and irregular building models during different types of tests.

1.5 Organization of the Report

- Chapter 1 presents the introduction and overview of importance of understanding the dynamic behaviour of building, the need of study is discussed. It also includes

objectives of the study and scope of the work.

- Chapter 2, comprises of literature review covering various technical papers. It focuses on various experimental techniques developed to evaluate dynamic properties of actual building or building models and also comprises the experimental setup and procedure to characterize viscous dampers.

- Chapter 3 comprises of Dynamics of Asymmetric Structural system.In this section Problem Formulation of building model with Plan irregularities is stated analytically

- Chapter 4 comprises of instrumentation for experimental setup.Various instruments used in the evaluation of Geometrical and Dynamic Properties of Structural System and also characterization of Passive Damper Devices.

- Chapter 5 comprises of Experimental Evaluation of Geometrical and Dynamic Properties of Structural System. In this section Geometrical and dynamic properties of various regular and irregular building models have been evaluated and the effect of bi-directional base motion on the response of the irregular building models have been evaluated.

- Chapter 6 comprises of Characterization of Passive Damper Devices.Cyclic Load test on Pneumatic type damper and Piston type damper.

- Chapter 7 comprises of Structural Response control of Asymmetric Structural system using Pneumatic Damper.

- Chapter 8 Comprises of summary and conclusion of work done.

Chapter 2

Literature Review

2.1 General

Building systems subjected to time dependent loading. Each and every system subjected to such loading will behave differently. Under such loading its behavior is critical. Thus it is important to analyze the response of the structure analytically and experimentally.

Various paper and journals have been refereed to understand the behaviour of structure or its models and also to understand the importance of dynamic properties and to evaluate such properties experimentally. It also includes the experimental setup for the characterization of various energy dissipating devices. Present, literature review will discus the utilization of various instruments like shake table, accelerometers, DAQ (Data Acquisition System).

2.2 Literature Review

2.2.1 Dynamic Testing of Structural Systems

Manohar and Venkatesha[1] carried out experiment to understand the dynamics of a single bay, single storey -building frame which consists of a relatively rigid rectangular steel slab supported at the corners on three aluminum and one steel column. In this experimental setup the frame is mounted on the shake table such that the angle of in-

cidence of the base motion on to the frame can be varied over 0 to $\pi/2$. The objective of the experiment is to understand the dynamics of the frame as the frequency of the base motion is varied across the resonant frequency and also to understand the effect of base motion on the dynamic response of the frame.Figure 2.1 shows the Experimental setup for One-Storey building frame excited in X-direction to which accelerometers are connected which further is connected to the DAQ and computer system and Figure 2.2 shows the displacement of the steel slab in X,Y,θ direction when excited in X direction.

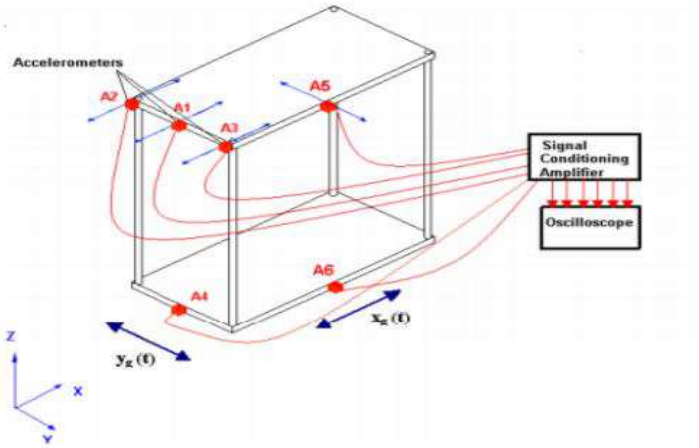

Figure 2.1: Experimental Setup for One-Story Building Frame excited in X-Direction

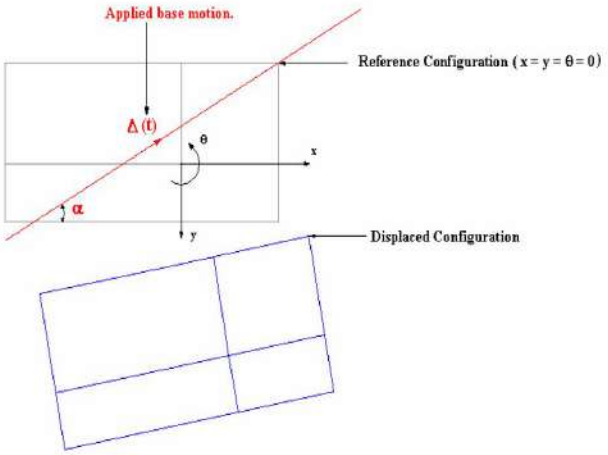

Figure 2.2: Displacement of the Steel Slab in X,Y,θ Direction

Table 2.1: Notations for Studies on One-story Building Frame

Accelerometer	Measurements
A1	Displacement along X axis ($\overline{X}$)
A2 & A3	Rotation ($\overline{X1}$, $\overline{X2}$)
A4	Base Motion ($\overline{Xg}$)
A5	Displacement along Y axis ($\overline{Y}$)
A6	Base Motion ($\overline{Yg}$)

Table 2.1 shows the displacement which will be measured by the accelerometer in their respective direction which can be seen in the table 2.1.Amplitude and phase spectra of absolute responses of one-story building frame subjected to harmonic base motion; where α =0; These responses along x, y and θ direction are shown in Figure 2.3.

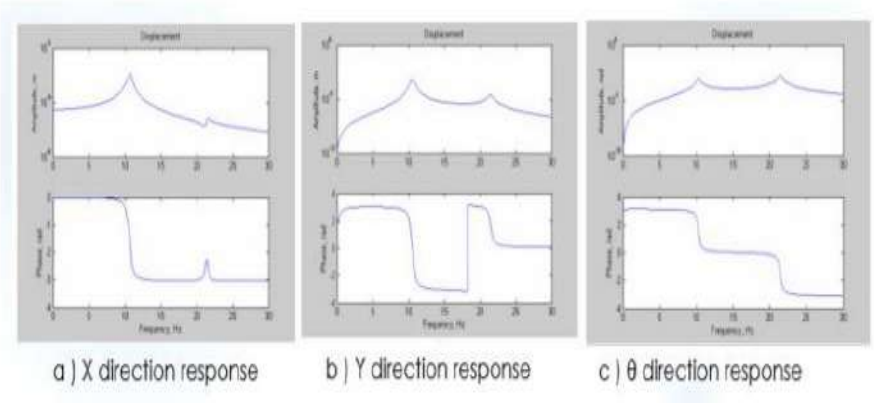

Figure 2.3: Amplitude and Phase Spectra of Absolute Responses of One-Story Building Frame

Panchal D. B.et al. [2] carried out experimental work to understand the control of dynamic response for a building model using different types of bracing like concentric, eccentric. The authors had carried out a small scale experiment was performed on a Shake Table in the laboratory. There were four types of building models were considered in experimental work: Uncontrolled SDOF, controlled SDOF, TDOF and MDOF. Response of all these model were studied in detail by conducting free and forced vibration test through uni axial shake table and Data Acquisition System LabVIEW 8.0. The dynamic properties like Natural Frequency and Damping co-efficient were obtained for both braced as well as unbraced building models. Figure 2.4 shows various types of bracing eccentric as well as concentric bracing were used. It has been observed that among all types of bracing V type bracing yields maximum reduction in response quantities without much affecting natural frequency of the system.

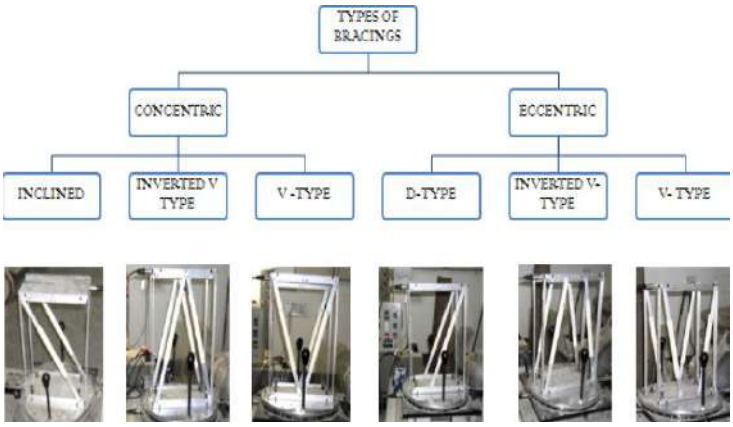

Figure 2.4: Concentric and Eccentric Types of Bracings

Patel H. Y.et al. [3] carried out experimental work to understand the control of dynamic response of MDOF a building model using different types of bracings like concentric, eccentric and tuned mass dampers like single tuned mass dampers and multi tuned mass dampers. MDOF model has been prepared from aluminum and small scale experiment was performed on shake table. Response of this MDOF model was studied in detail by conducting free and forced vibration test through uniaxial shake table and Data Acquisition System LabView 8.0.Natural frequency, damping coefficient for free and force vibrations were obtained. Various types of bracings were provided in MDOF building model. Eccentric bracing shows better reduction in all dynamic response quantities com-

pare to concentric bracings. Dynamic properties of MDOF system with single tuned mass dampers and multi tuned mass dampers were studied in detail. Both single TMD and multiple TMD shows maximum response reduction compare to bare model.

Umashankar K. S.et al. [4] have estimated the damping ratio of aluminum(Al) material manufactured through powder metallurgy process and compare it with commercially available cast aluminum material. Cantilever beams of 15 mm in width, 5 mm in depth and 100 mm length were prepared for experimental purpose. Figure 2.5 shows cantilever beam excited by sweep sine test and resulting response was stored and analyzed using half power bandwidth method for both sintered and cast aluminum material. Damping ratio was also estimated by performing free vibration test on cantilever beam. Free vibration tests also confirmed the damping ratios obtained by sweep sine method. It is observed that damping ratio of sintered aluminum is higher than cast aluminum. This may be due to increased porosity in former material. This can be accounted to the presence of pores which results in lower stiffness hence in turn lower elastic modulus.

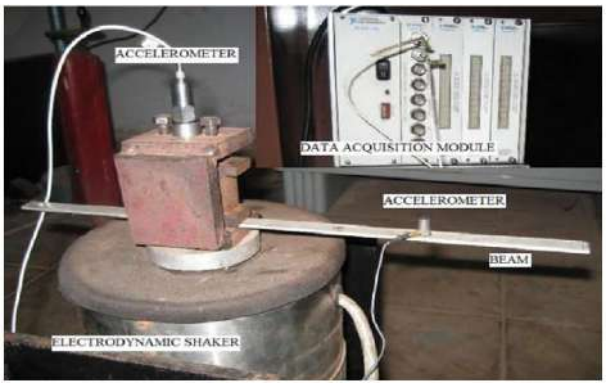

Figure 2.5: Aluminum Cantilever beam subjected to sweep sine test

Slifka D.L. [5] presents methods of double integrating acceleration data to find position data for the application of a vehicle road test. The acceleration of a body will be measured with an accelerometer, which is a more convenient to make measurements than the devices used to directly measure position. When performing the double integration, two problems arise The drift associated with real accelerometers. The initial conditions (initial position and initial velocity) of the system are unknown. Both of these problems can

cause major integration errors. Therefore, the designed double integration process must overcome these problems and provide an accurate measurement reading. The principle contributions of this thesis are the development of the double integration process and a thorough evaluation of this process tested on a physical system.

Shah D. [6]carried out the experiment to find out the dynamic property such as damping ratio of planar as-symmetry that is L and T shape planar irregular SDOF and MDOF building model and also found out the damping ratio of material irregular SDOF and MDOF building model.The author observed that L- shape building model shows larger acceleration response as compared to T-shape building model.Apart damping coefficient ζ is observed to be highest for building model with material irregularity followed by T-shaped building model and least is building with L- shape geometry.Forced vibration study on SDOF and MDOF systems indicates that for both the types transmissibility ratio is highest for L-shape building model.Transmissibility ratio for T shape building model is smaller than transmissibility ratio for L shape building model, but is slightly higher than transmissibility ratio of material irregularity building model.

2.2.2 Characterization of Dampers

Reza A and Mahmood Md. [7] presents a new passive earthquake damper termed as Bar Fuse Damper (BFD) is presented for frame structure. It is developed from common steel section such as hot rolled Square Hollow Sections (SHS).C-Channels,Plates and bars.The performance of the several full scaled BFD's was evaluated with a series of cyclic experiments. It has been observed that it has stable hysteric behavior under cyclic loading.The hysteric curves for different number,diameter and length of bar is shown in the figure 2.7.

Figure 2.6 shows the setup of the monotonic test subjected on to the Bar Fuse Damper (BFD) and its failure modes can be seen in the figure 2.6.Parametric study was done for different number, diameter and length of bar can be seen in the figure 2.7. To have an indication of the capability in order to evaluate and compare metallic damper, the parameter of the equivalent viscous damping ratio is defined as follows.

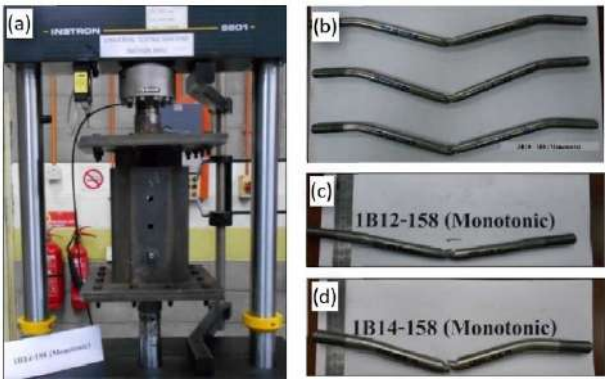

Figure 2.6: Setup of the monotonic tests and the failure modes

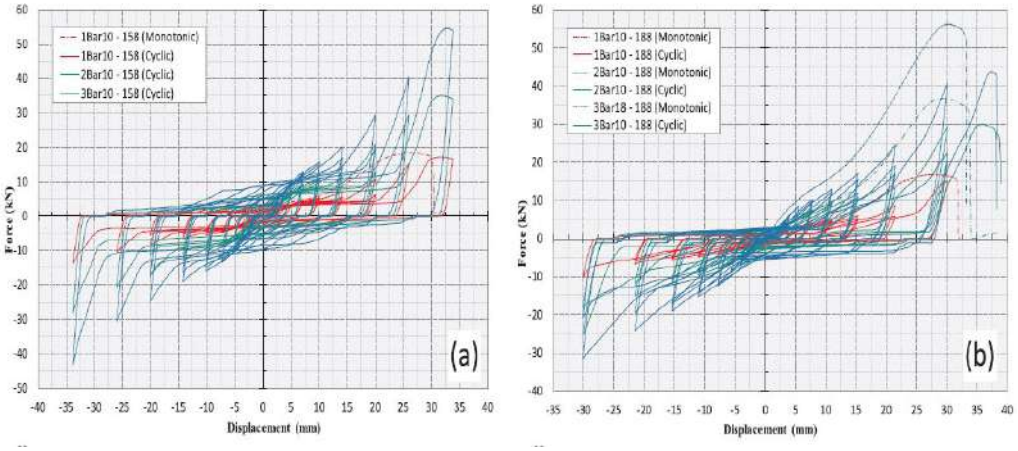

Figure 2.7: Hysteric curve for different number, diameter and length of bar.

$$\zeta = \frac{1}{4\prod}\frac{E_d}{E_s} = \frac{1}{2\prod}\frac{E_d}{K_{eff}D^2} \tag{2.1}$$

E_d is the dissipated energy in each cycle of hysteresis equal to the enclosed area of the complete cycle. E_s is the strain energy stored in an elastic spring with an equivalent stiffness K_{eff} and displacement D.Whose equation is $\frac{1}{2}K_{eff}D^2$.K_{eff} is the equivalent stiffness which can be calculated by the maximum strengths and displacements in both directions as in the formulae below:-

$$K_{eff} = \frac{|P_{max}| - |P_{min}|}{|D_{max}| - |D_{min}|} \tag{2.2}$$

Miyamoto H.et. al. [8] has considered a reinforced concrete moment resisting frame building of G+20 are considered . The building is intended to be in seismic zone V and

intended for commercial purpose. Two models are prepared with and without dampers providing all parameters using SAP 2000 software. Results shows that by using fluid viscous dampers to building can effectively reduce the building response by selecting optimum damping coefficients i.e when the building is connected to the fluid viscous dampers can control both acceleration and displacements of the building.Further Damper at appropriate Locations can significantly reduce the earthquake responses.

Mosqueda G.et al. [9] discusses the performance characterization of two fluid viscous dampers used in earthquake simulation tests of an isolated bridge model prior to these testing , the fluid viscous dampers were subjected to uni-axial compression-tension cycle consisting of sinusoidal tests,constant velocity tests and low-velocity friction tests.

Figure 2.8: Isolated Rigid Block with Dampers

Based on the uni-axial tests and the subsequent earthquake simulation tests of the damped isolated bridge model which is shown in the figure 2.8, recommendations regarding prototype testing and acceptance criteria for fluid viscous dampers are presented.

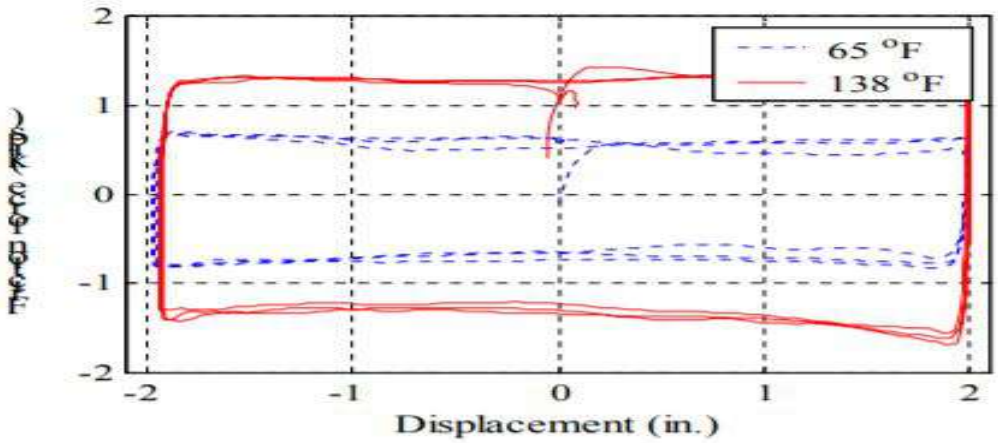

Figure 2.9: Force Displacement Curve of 10 Kip Taylor Damper

2.2.3 Summary

In this chapter Literature related to determination of dynamic properties of different building models has been presented, also experimental setup for characterization (i.e cyclic load test setup) of energy dissipating dampers has been presented and also understanding of properties of energy dissipating dampers has been developed based on literature.

Chapter 3

Dynamics of Asymmetric Structural Systems

3.1 General

Structural Dynamics deals with the time dependent forces and motions. When any structure is subjected to such time dependent force i.e.dynamic loading, it undergoes motion and produces internal forces. The dynamic equilibrium equation for these forces is achieved through D'Alembert's principle or Newton's second law of motion for various mass elements.

The seismic waves caused by an earthquake will make buildings sway and oscillate in various ways depending on the frequency and direction of ground motion, and the height and construction of the building. Seismic activity can cause excessive oscillations of the building which may lead to structural failure. To enhance the building's seismic performance, a proper building design is performed engaging various seismic vibration control technologies.Hence, Dampers are used to enhance the building's performance, for which properties of dampers are found out and its applicability in structures are carried out.Various Damper properties has been discussed in the following Chapter.

3.2 Dynamics of SDOF Systems

3.2.1 Free Vibrations of SDOF Systems

3.2.1.1 Undamped Free Vibrations

When a structure is disturbed from its static equilibrium position and then allowed to vibrate without any external dynamic excitation then it is known as free vibration of the structure.

Derivation of the Equation of Motion

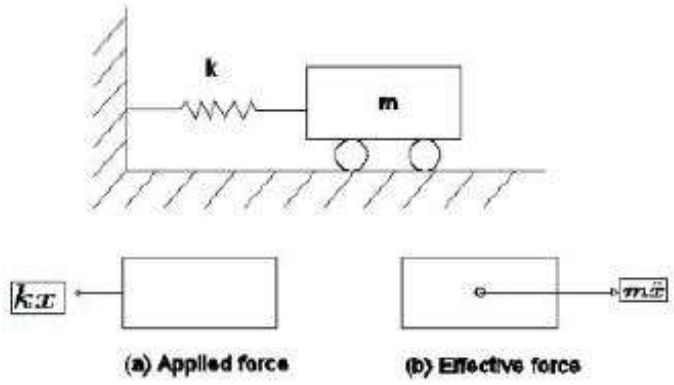

Figure 3.1: Free Body Diagram of undamped SDOF System

Figure 3.1 depicts the free body diagram of the undamped SDOF system having mass m and an spring constant k from which the equation of motion for the system can be derived,

$$m\ddot{x} = -kx \tag{3.1}$$

$$m\ddot{x} + kx = 0 \tag{3.2}$$

Free vibration is initiated by disturbing the system from its static equilibrium position by imparting on the mass, some displacements x(0) and velocity $\dot{x}(0)$ at time zero, defined as the instant the motion is initiated. x=x(0) and $\dot{x} = x(0)$ are the initial conditions.

The solution to the homogeneous differential equation 3.2 is obtained using initial conditions by standard methods.The solution of above differential equation 3.2 can be expressed as,

$$x\left(t\right) = A_1 cos\omega_n t + A_2 sin\omega_n t \tag{3.3}$$

Here $A_1 and A_2$ are arbitrary constant. Above equation can also be expressed in the terms of initial displacement and initial velocity.

$$x\left(t\right) = x\left(0\right) cos\omega_n t + \left[\dot{x}\left(0\right)/\omega_n\right] sin\omega_n t \tag{3.4}$$

Where

$$\omega_n = \sqrt{\frac{k}{m}} \tag{3.5}$$

Amplitude of motion

$$A = \sqrt{A_1^2 + A_2^2} \tag{3.6}$$

Phase angle

$$tan^{-1}\left(\frac{A_1}{A_2}\right) \tag{3.7}$$

The time required for the undamped system to complete one cycle of free vibration is the natural period of vibration T_n.

$$T_n = \frac{2\pi}{\omega_n} \tag{3.8}$$

$$f_n = \frac{1}{T_n} \tag{3.9}$$

Here $[f_n]$ is natural frequency in H_z.

3.2.1.2 Damped Free Vibrations

For free vibration of SDOF system with damping free body diagram is represented in Figure 3.2, governing differential equation is,

$$m\ddot{x} + c\dot{x} + kx = 0 \tag{3.10}$$

solution of this second order homogeneous differential equation is in the form of

$$x = e^{st} \tag{3.11}$$

Dividing equation by m gives

$$\ddot{x} + 2\zeta\omega_n\dot{x} + \omega_n^2 u = 0 \tag{3.12}$$

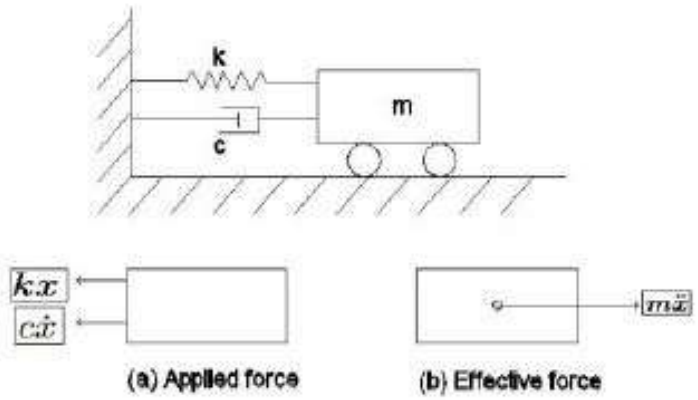

Figure 3.2: Free Body Diagram of Damped SDOF System

where

$$\zeta = \frac{c}{2m\omega_n} = \frac{c}{c_{cr}} = Damping\ Ratio$$

$$c_{cr} = 2m\omega_n = 2\sqrt{km} = Critical\ Damping\ Coefficient$$

roots of characteristic equation are

$$S_{1,2} = -\frac{c}{2m} \pm \sqrt{\left[\frac{c}{2m}\right]^2 - \frac{k}{m}} \tag{3.13}$$

$$S_{1,2} = (-\zeta \pm \sqrt{[\zeta^2 - 1]}\omega_n \tag{3.14}$$

The general solution of homogeneous equation can be written as,

$$x(t) = A_1 e^{s_1 t} + A_2 e^{s_2 t} \tag{3.15}$$

3.2.1.3 Types of Motion

The actual form of the solutions depends on the nature of roots given by equations 3.15 or 3.16. Depending on the nature of the roots of Eq. 3.15 and 3.16 ,i.e., imaginary(complex

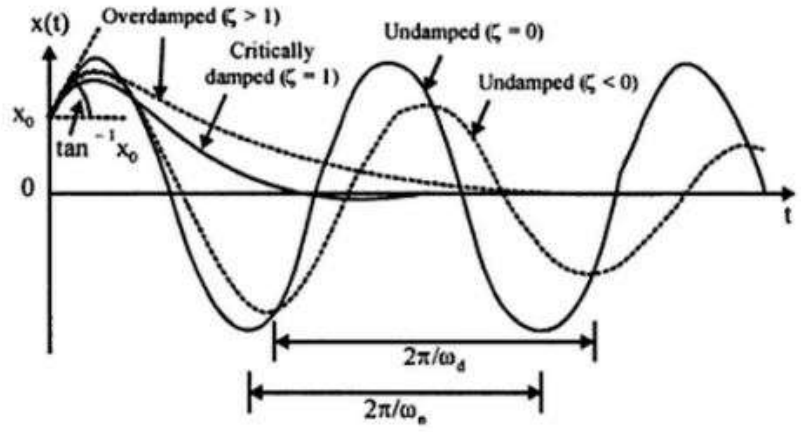

Figure 3.3: Response of Under Damped, Critically Damped and Overdamped Systems

conjugate roots), real distinct [$\zeta < 1$] roots or real repeated roots [$\zeta = 1$], three types of motions are presented in Figure 3.3.

CASE : 1 Under Damped System: If [$\zeta < 0$], the system is termed as under damped system. The roots of the characteristic equation are complex conjugates,corresponding to oscillatory motion with an exponential decay in amplitude. The solution can be obtained as,

$$x(t) = e^{-\zeta\omega_n t}[A_1 cos(\omega_d t) + A_2 sin(\omega_d t)] \tag{3.16}$$

Where [A_1] and [A_2] are arbitrary constants and can be determined by initial conditions of the system, and [ω_d] is the damped natural frequency of the system given by,

$$\omega_d = \omega_n\sqrt{(1-\zeta^2)} \tag{3.17}$$

From [A_1] and [A_2] can be determined

$$A_1 = \dot{x_0} \tag{3.18}$$

and

$$A_2 = \frac{x_0 + \dot{\zeta}\omega_n\dot{x_0}}{\omega_d} \tag{3.19}$$

This equation now can be written as in terms of [x_0] and [$\dot{x}_0$]

$$x(t) = e^{-\zeta\omega_n t}[x_0 cos(\omega_d t) + \frac{x_0 + \dot{\zeta}\omega_n\dot{x_0}}{\omega_d} sin(\omega_d t)] \tag{3.20}$$

Logarithmic Decrement: In the free vibration of an underdamped system,displacement amplitude decays exponentially with time which can be seen in figure 3.4. The rate of decrease depends on the damping ratio [ζ].

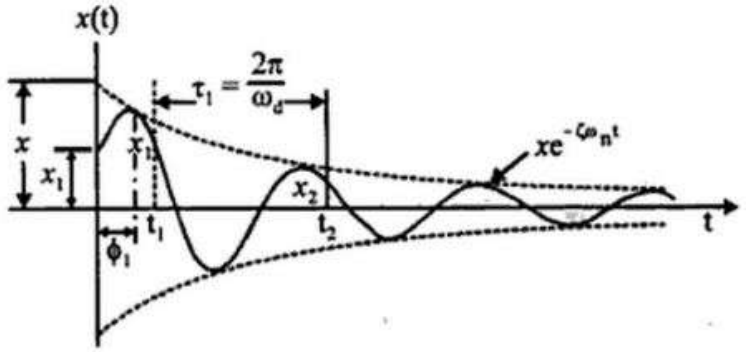

Figure 3.4: Displacement Response of SDOF System Under Free Vibration

if we consider displacement at time [t_1] by [x_1] [$\equiv$] [$x(t_1)$],then

$$x(t_1) = Ae^{-\zeta\omega_n t_1} sin(\omega_d t_1 + \phi) \tag{3.21}$$

The displacement at [$t_{1+\frac{2\pi}{\omega_d}}$] is given by

$$x(t_{1+\frac{2\pi}{\omega_d}}) = Ae^{-\zeta\omega_n t_{1+\frac{2\pi}{\omega_d}}} sin(\omega_d t_1 + \phi) \tag{3.22}$$

The ratio [$u(t_1)$] to [$t_{1+\frac{2\pi}{\omega_d}}$] provides the measure of the decrease in displacement over one cycle of motion. The ratio is constant and does not vary with time. Its natural log with time is called logarithmic decrement and is denoted as [δ]. The value of [δ] is given by,

$$\delta = ln(\frac{e^{\zeta\omega_n t_1}}{e^{-\zeta\omega_n t_{1+\frac{2\pi}{\omega_d}}} sin(\omega_d t_1 + \phi)}) \tag{3.23}$$

$$\delta = 2\pi\zeta\frac{\omega_n}{\omega_d} \tag{3.24}$$

$$\delta = 2\pi\frac{\zeta}{\sqrt{1-\zeta^2}} \tag{3.25}$$

For small values of [ζ] , [$\delta \approx 2\pi\zeta$]. If [δ] is obtained from measurements and [ζ] is to be evaluated, we can use,

$$\zeta = \frac{\delta}{2\pi} \tag{3.26}$$

$$\zeta = \frac{\delta}{\sqrt{4\pi^2 + \delta^2}} \tag{3.27}$$

CASE : 2 Critically Damped System: If $[\zeta = 0]$, the system is termed critically damped. The damping constant c is, in this case, denoted by $[c_{cr}]$ and its value is given by

$$c = c_{cr} = 2\sqrt{km} \tag{3.28}$$

$$c = c_{cr} = 2m\omega_n \tag{3.29}$$

The roots of Eq are now equal, so that

$$s_1 = s_2 = \frac{c_{cr}}{2m} = -\omega_n \tag{3.30}$$

The general solution is given by

$$x = (A_1 + A_2 t)e^{-\omega_n t} \tag{3.31}$$

Where $[A_1]$ and $[A_2]$ are arbitrary constants to be determined from initial conditions. Substitution of initial displacement and initial velocity, leads to the following values of $[A_1]$ and $[A_2]$.

$$A_1 = x_0 \tag{3.32}$$

$$A_2 = \frac{\dot{x_0}}{\omega_n} + x_0 \tag{3.33}$$

The general solution thus becomes,

$$x(t) = [x_0 + (\frac{\dot{x_0}}{\omega_n} + x_0)\omega_n t]e^{\omega_n t} \tag{3.34}$$

Since critical damping represents the limit of a-periodic damping, the motion returns to rest in the shortest time without oscillations. This property can be advantageously used

in many practical vibration problems such as large guns, measuring instruments and electrical meters.

CASE : 3 Over Damped System: If $[\zeta > 0]$ or damping is greater than $[c_{cr}]$ the system is termed over damped system. The roots of the characteristic equation are purely real and distinct, corresponding to simple exponentially decaying motion.

$$\zeta = \frac{c}{c_{cr}} \tag{3.35}$$

$$c = c_{cr}\zeta \tag{3.36}$$

$$c = 2m\omega_n\zeta \tag{3.37}$$

Substitution of values gives,

$$s_1 = -\omega_n\zeta + \omega_n\sqrt{\zeta^2 - 1} \tag{3.38}$$

$$s_1 = -\omega_n\zeta - \omega_n\sqrt{\zeta^2 - 1} \tag{3.39}$$

If we denote

$$\omega_n\sqrt{\zeta^2 - 1} = \bar{\omega} \tag{3.40}$$

The general solution becomes

$$x(t) = e^{-\omega_n\zeta t}(A_1 e^{\bar{\omega}t} + A_2 e^{\bar{\omega}t}) \tag{3.41}$$

Where the arbitrary constants $[A_1]$ and $[A_2]$ are again determined by initial conditions.

3.2.2 Forced Vibration of SDOF System

3.2.2.1 Undamped Force Vibrations

The response of any structural system subjected to external force called forced response.In figure 3.5 simple SDOF undamped system is shown.

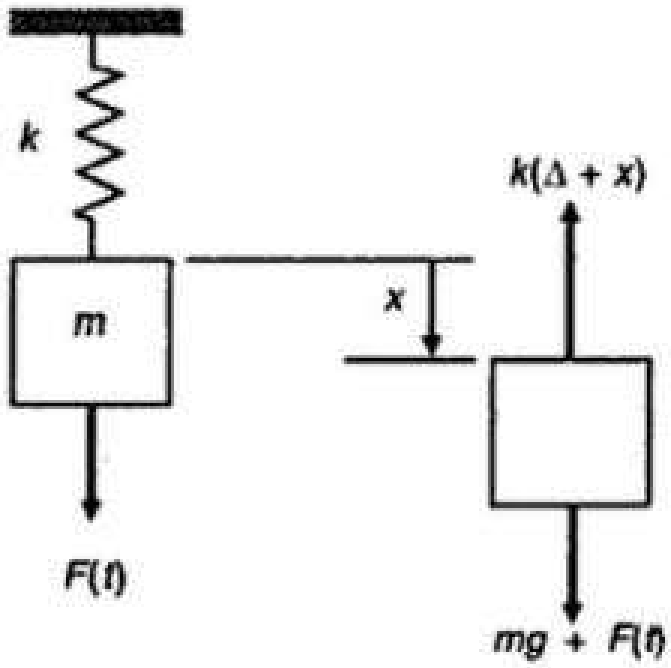

Figure 3.5: Forced Undamped Vibration of SDOF System

$$F(t) = F_0 sin\omega_f t \tag{3.42}$$

Equation of motion becomes,

$$m\ddot{x} + kx = F(t) \tag{3.43}$$

$$\ddot{x} + \frac{k}{m}x = \frac{F(t)}{m} \tag{3.44}$$

$$\ddot{x} + \frac{k}{m}x = \frac{F_0}{m} sin\omega_f t \tag{3.45}$$

Equation is a non homogeneous, second order differential equation with constant coefficients.Hence, the complete solution is the sum of homogeneous solution $x_h(t)$ and a particular solution $x_p(t)$ such that,

$$x(t) = x_h t + x_p t \tag{3.46}$$

where,

$$\ddot{x}_h + \frac{k}{m}x_h = 0 \tag{3.47}$$

and,

$$\ddot{x}_h + \frac{k}{m}x_p = \frac{F_0}{m}sin\omega_f t \tag{3.48}$$

Equation is a differential equation of motion for free vibration of simple harmonic oscillator, for which the solution is,

$$x_h(t) = A_1 cos\omega_f t + A_2 sin\omega_f t \tag{3.49}$$

In order to obtain the particular solution of equation, excitation force $[F(t)]$ is harmonic, the particular solution $[xp(t)]$ is also harmonic and has frequency $[\omega_f]$. Thus we assume the solution in the form,

$$x_p(t) = Xcos\omega_f t \tag{3.50}$$

Where X is the unknown constant, which is obtained such that the assumed solution does satisfy the differential equation. X denotes the maximum amplitude of $[xp(t)]$. Substituting equation in we obtain

$$X = \frac{\frac{F_0}{m}}{\frac{k}{m} - \omega_f^2} \tag{3.51}$$

Multiplying both numerator and denominator by m/k, we obtain

$$x = \frac{\frac{F_0}{k}}{1 - (\frac{m}{k})\omega_f^2} = \frac{\frac{F_0}{k}}{1 - (\frac{\omega_f}{\omega_n})^2} \tag{3.52}$$

Hence the particular solution is given by,

$$x_p(t) = \frac{\frac{F_0}{k}}{k(1 - (\frac{\omega_f}{\omega_n})^2)} \tag{3.53}$$

The complete solution for the motion of the mass is

$$x_p(t) = A_1 cos\omega_n t + A_2 sin\omega_n t + \frac{\frac{F_0}{k}}{k(1 - (\frac{\omega_f}{\omega_n})^2)} \tag{3.54}$$

The constants $[A_1]$ and $[A_2]$ are again determined by initial conditions. The result is

$$A_1 = x_0 - \frac{F_0}{k - m\omega_f^2} \tag{3.55}$$

$$A_2 = \frac{\ddot{x_0}}{\omega_n} \tag{3.56}$$

Hence the complete solution is

$$x(t) = (x_0 - \frac{F_0}{(k - m\omega_f^2)})cos\omega_f t + \frac{\ddot{x_0}}{\omega_n} sin\omega_f t + \frac{\frac{F_0}{k}}{k(1 - (\frac{\omega_f}{\omega_n})^2)} \tag{3.57}$$

The maximum amplitude can also be expressed as

$$\frac{x}{\delta_{st}} = \frac{1}{1 - (\frac{\omega_f}{\omega_n})^2} \tag{3.58}$$

Where,

$$\frac{x}{\delta_{st}} = \frac{F_0}{k} \tag{3.59}$$

denotes the static deflection of the mass under a force $[F_0]$. The quantity $[\frac{x}{\delta_{st}}]$ represents the ratio of the dynamic to the static amplitude of motion and is called magnification factor.

3.2.2.2 Forced Damped Vibrations

Consider a viscously damped SDOF spring-mass system shown in Figure 3.6.

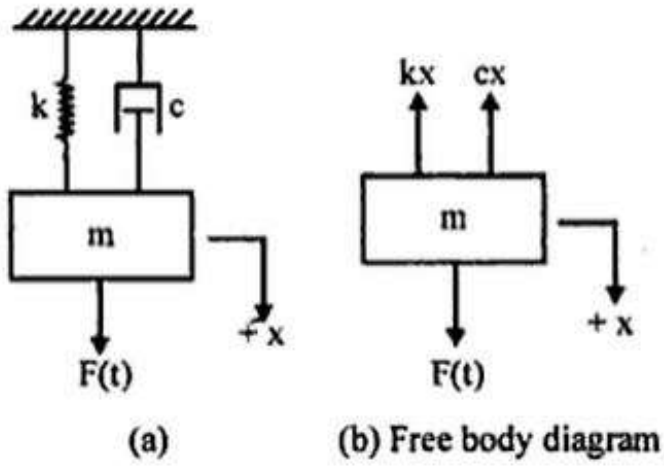

Figure 3.6: Forced Damped Vibration of SDOF System

equation of motion is

$$m\ddot{x} + c\dot{x} + kx = F_0 sin\omega_f t \tag{3.60}$$

$$\ddot{x} + \frac{c}{m\ddot{x}} + \frac{k}{mx} = \frac{F_0}{m} sin\omega_f t \tag{3.61}$$

This is a homogeneous equation. The particular solution or the steady state solution $[x_p]$ can be assumed in the form,

$$x_p = A_1 sin\omega_f t + A_2 cos\omega_f t \tag{3.62}$$

which gives the following equations for the velocity and acceleration

$$\dot{x_p} = \omega_f A_1 cos\omega_f t - \omega_f A_2 sin\omega_f t \tag{3.63}$$

$$\ddot{x_p} = \omega_f^2 A_1 cos\omega_f t - \omega_f^2 A_2 sin\omega_f t \tag{3.64}$$

$$[(k - \omega_f^2 m)A_1 - c\omega_f A_2]sin\omega_f t + [(k - \omega_f^2 m)A_2 + c\omega_f A_1]cos\omega_f t = F_0 sin\omega_f t \tag{3.65}$$

Two algebraic equations in $[A_1]$ and $[A_2]$

$$[(k - \omega_f^2 m)A_1 - c\omega_f A_2] = F_0 \tag{3.66}$$

$$[(k - \omega_f^2 m)A_2 + c\omega_f A_1] = 0 \tag{3.67}$$

Dividing by stiffness coefficient

$$(1 - \eta^2)A_1 - 2\zeta\eta A_2 = X_0 \tag{3.68}$$

$$(1 - \eta^2)A_2 - 2\zeta\eta A_1 = 0 \tag{3.69}$$

Where

$$\eta = \frac{\omega_f}{\omega_n} \tag{3.70}$$

$$\zeta = \frac{c}{c_{cr}} = \frac{c}{2m\omega_n} \tag{3.71}$$

$$X_0 = \frac{F_0}{k} \tag{3.72}$$

where, $[c_{cr}] = [2m\omega_n]$ is the critical damping coefficient. Solving these two algebraic equations simultaneously gives the values of $[A_1]$ and $[A_2]$.

$$A_1 = \frac{((1-\eta^2))X_0}{(1-\eta^2)^2 + (2\zeta\eta)^2} \tag{3.73}$$

$$A_1 = \frac{(-2\zeta\eta)X_0}{(1-\eta^2)^2 + (2\zeta\eta)^2} \tag{3.74}$$

Hence, the steady state solution can be written as

$$x_p = \frac{X_0}{(1-\eta^2)^2 + (2\zeta\eta)^2}[(1-\eta^2)sin\omega_f t - (2\zeta\eta)cos\omega_f t] \tag{3.75}$$

This can be written as

$$x_p = \frac{X_0}{(1-\eta^2)^2 + (2\zeta\eta)^2} sin(\omega_f t - \phi) \tag{3.76}$$

$[X_0]$ is the amplitude and $[\phi]$ is the phase angle

$$\phi = tan^{-1}[\frac{2\zeta\eta}{(1-\eta^2)}] \tag{3.77}$$

$$x_p = X_0\beta sin(\omega_f t - \phi) \tag{3.78}$$

Where, $[\beta]$ is known as Magnification factor. Fig shows plot of Dynamic magnification factor versus Frequency ratio $[\eta]$.

3.2.3 Forced Vibration Test: Half Power Bandwidth

In this method, SDOF models are subjected to forced vibration. Considering frequency ratios of excitation applied to natural frequency of system, dynamic magnification and response is extracted which is seen in figure 3.7. Tracking peak value of response, damping is estimated Response Spectra v/s Frequency ratio plot for forced vibration can be seen in figure 3.8. Estimation of damping in a structure can be carried in frequency domain

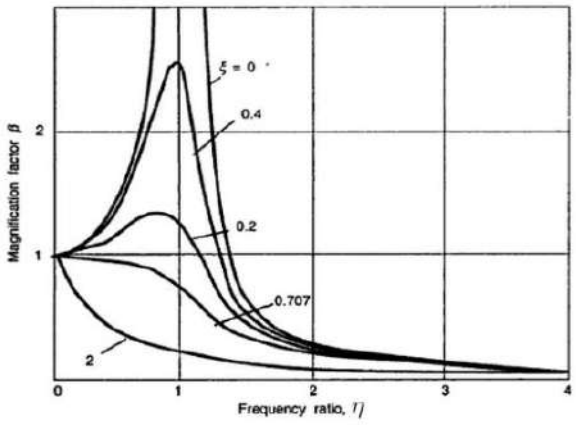

Figure 3.7: Forced Damped Vibration of SDOF System

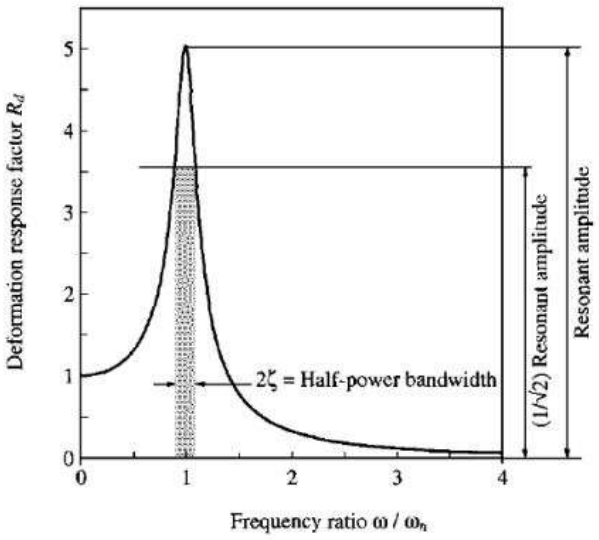

Figure 3.8: Half Power Bandwidth Method

through half power band width approach. In this method, two forcing frequencies $[\omega_a]$ and $[\omega_b]$ are extracted on either side of the resonant frequency considering amplitude $[A_2 = \frac{1}{\sqrt{2}}]$ times the amplitude of resonant frequency amplitude $[A_1]$. For small value of $[\xi]$,

$$2\zeta = \frac{\omega_a - \omega_b}{\omega_n} \tag{3.79}$$

3.3 Types of Irregularities in Building

3.3.1 Types of Structural Irregularities

Regular Structures and Irregular Structures behave differently when they are subjected to dynamic loading.

- **Symmetric or regular structures:** Mass and stiffness is uniformly distributed in plan as well as in elevation.
- **Asymmetric or irregular structure:** Mass and stiffness is not distributed uniformly in plan as well as in elevation.

  Buildings having irregularities show major damage during earthquakes. There are various types of irregularities given in IS 1893 : 2002 (PART 1)[10] which are also shown in figure 3.9.

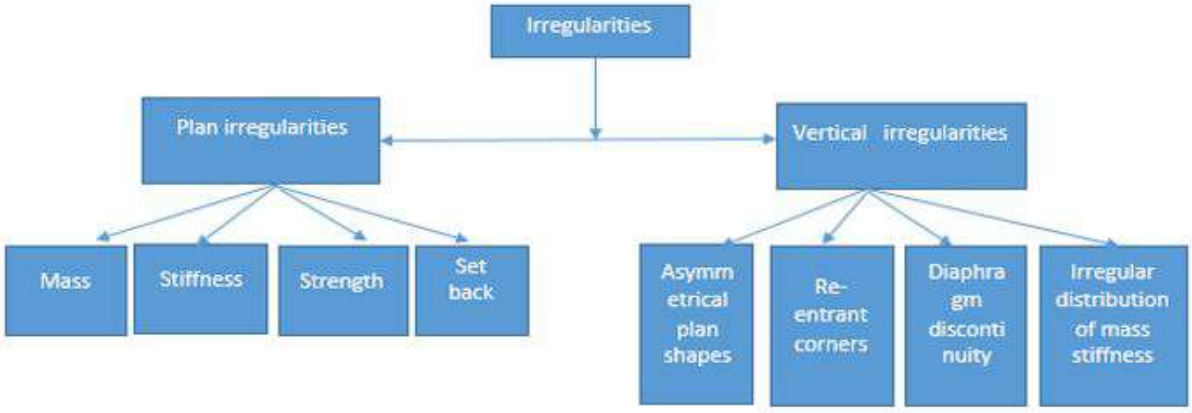

Figure 3.9: Types of Irregularities

3.3.2 Definitions of Irregular Buildings — Plan Irregularities

Plan irregularities for a building includes Torsional Irregularity, Re-entrant Corners, Diaphragm Discontinuity, Out of Plane Offsets and Non Parallel Systems. In the following section each of these irregularities are discussed in brief.

- **Torsion Irregularity**

  To be considered when floor diaphragms are rigid in their own plan in relation to

the vertical structural elements that resist the lateral forces. Torsional irregularity to be considered to exist when the maximum storey drift, computed with design eccentricity, at one end of the structures transverse to an axis is more than 1.2 times the average of the storey drifts at the two ends of the structure.

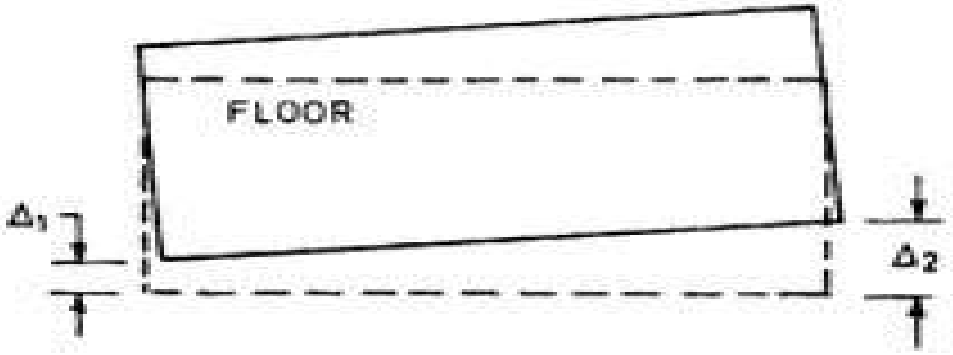

Figure 3.10: Torsional Irregularity of the Building Model

- **Re-entrant Corners**

  Plan configurations of a structure and its lateral force resisting system contain re-entrant corners, where both projections of the structure beyond the re-entrant corner are greater than 15 percent of its plan dimension in the given direction.Examples of planar irreegularity having re-entrant cornaers can be seen in figure 3.11.

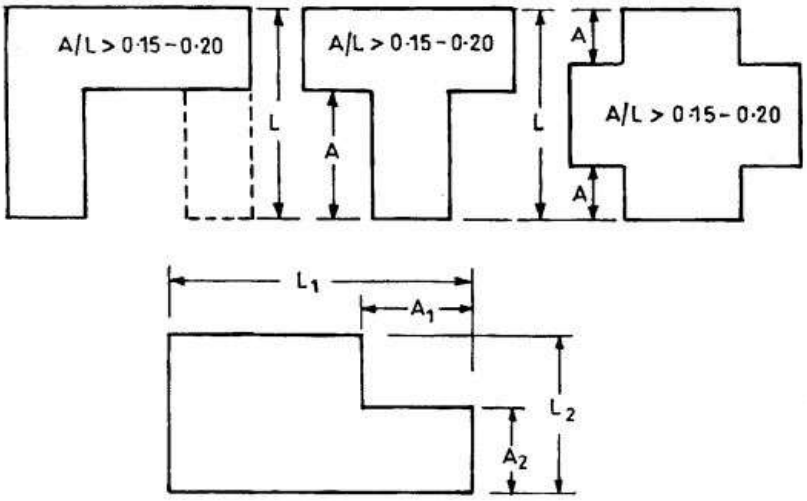

Figure 3.11: Re-entrant Corners for the Building

- **Diaphragm Discontinuity**

  Diaphragms with abrupt discontinuities or variations in stiffness, including those having cut-out or open areas greater than 50 percent of the gross enclosed diaphragm area, or changes in effective diaphragm stiffness of more than 50 percent from one storey to the next.Examples of rigid diagphrams can be seen in figure 3.12.

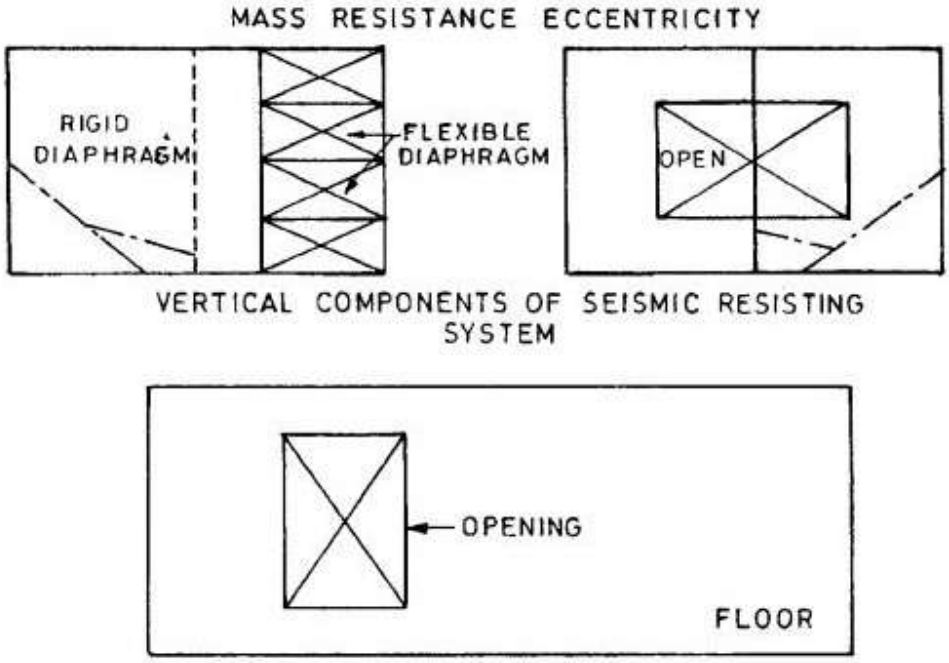

Figure 3.12: Diaphragm Discontinuity for Building

- **Out-of-Plane Offsets**

  Discontinuities in a lateral force resistance path, such as out-of-plane offsets of vertical elements.

- **Non-parallel Systems**

  The vertical elements resisting the lateral force are not parallel to or symmetric about the major orthogonal axes or the lateral force resisting elements.

3.3.3 Definitions of Irregular Buildings — Vertical Irregularities

- **Mass Irregularity**

  Mass Irregularities shall be considered to exist where the seismic weight of any storey is more than 200 percent of that of its adjacent storeys. The irregularity need not

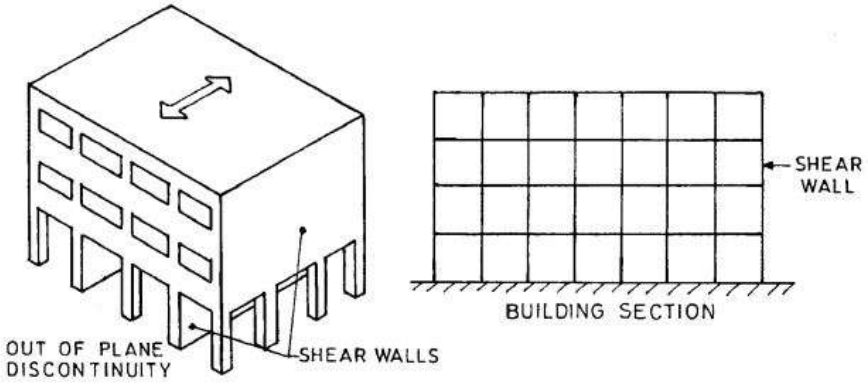

Figure 3.13: Out-of-Plane Offsets

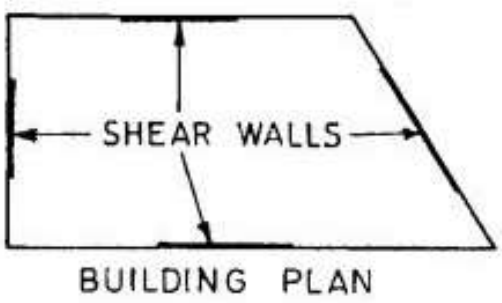

Figure 3.14: Non-parallel Systems for a Building

be considered in case of roofs.

- **Stiffness Irregularity**

  A soft storey is one in which the lateral stiffness is less than 70 percent of that in the storey above or less than 80 percent of the average lateral stiffness of the three storeys above.

  A extreme soft storey is one in which the lateral stiffness is less than 60 percent of that in the storey above or less than 70 percent of the average stiffness of the three storeys above. For example, buildings on STILTS will fall under this category.

- **Vertical Geometric Irregularity**

  Vertical Geometric Irregularity shall be considered to exist where the horizontal

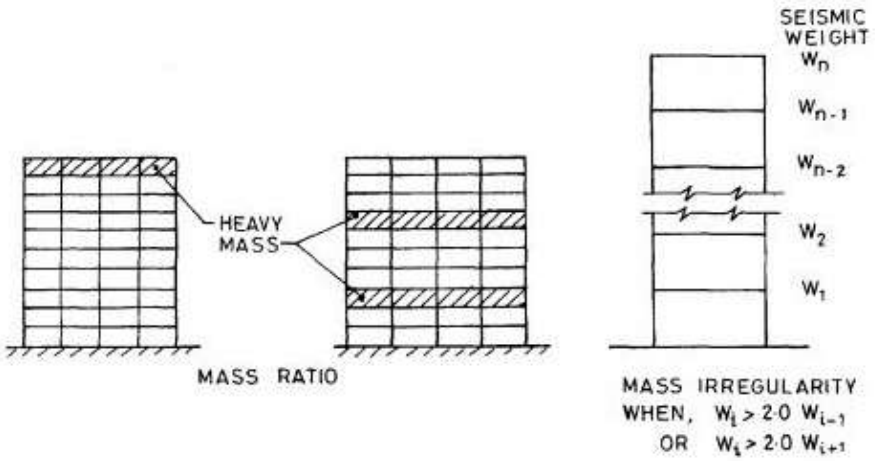

Figure 3.15: Mass Irregularity of Building

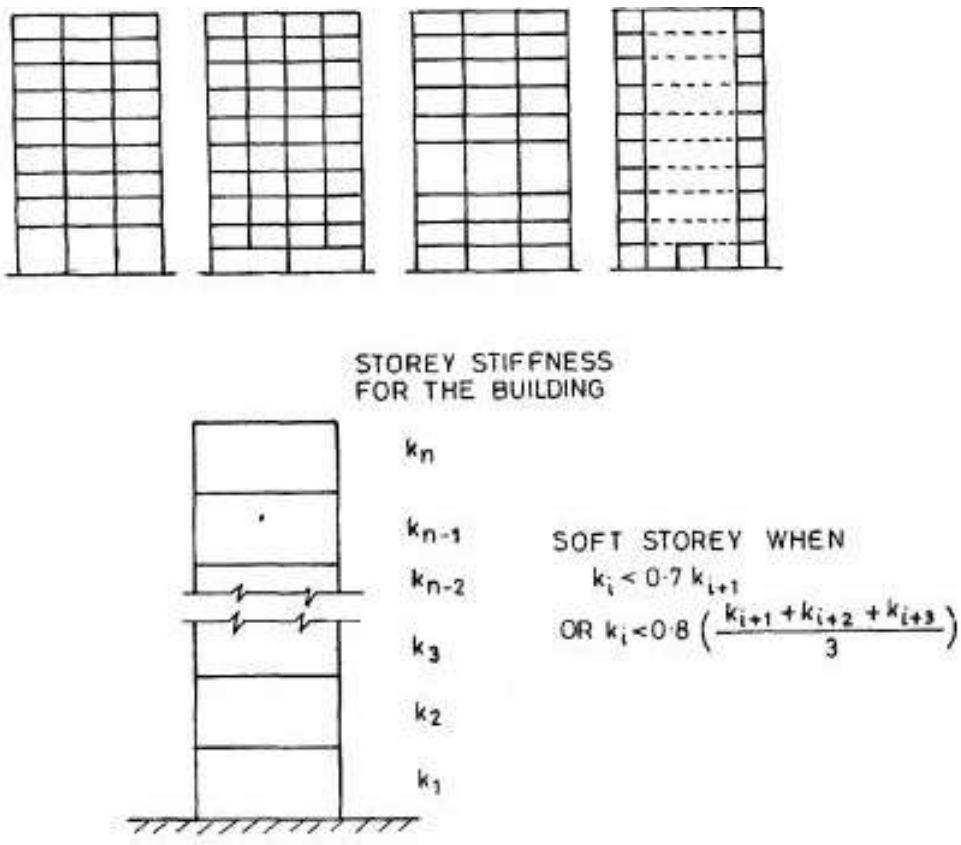

Figure 3.16: Stiffness Irregularity

dimension of the lateral force resisting system in any storey is more than 150 percent of that in its adjacent storey.

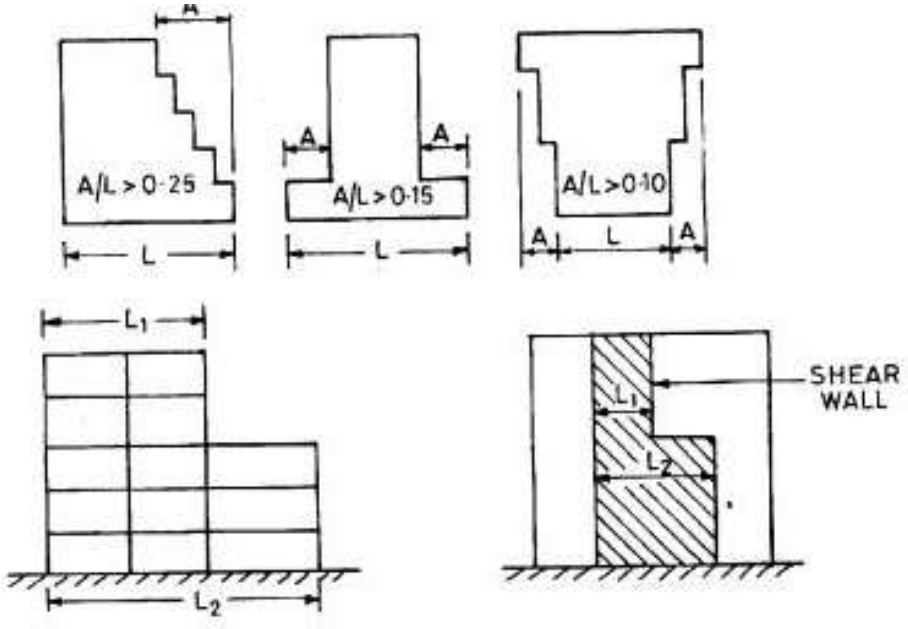

Figure 3.17: Vertical Geometric Irregularity

- **Discontinuity in Capacity — Weak Storey**

  A weak storey is one in which the storey lateral strength is less than 80 percent of that in the storey above, The storey lateral strength is the total strength of all seismic force resisting elements sharing the storey shear in the considered direction.

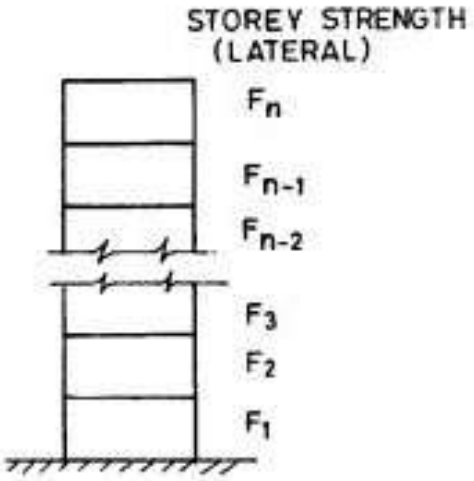

Figure 3.18: Discontinuity in Capacity — Weak Storey

- **In-Plane Discontinuity in Vertical Elements Resisting Lateral Force**

  An in-plane offset of the lateral force resisting elements greater than the length of those elements.

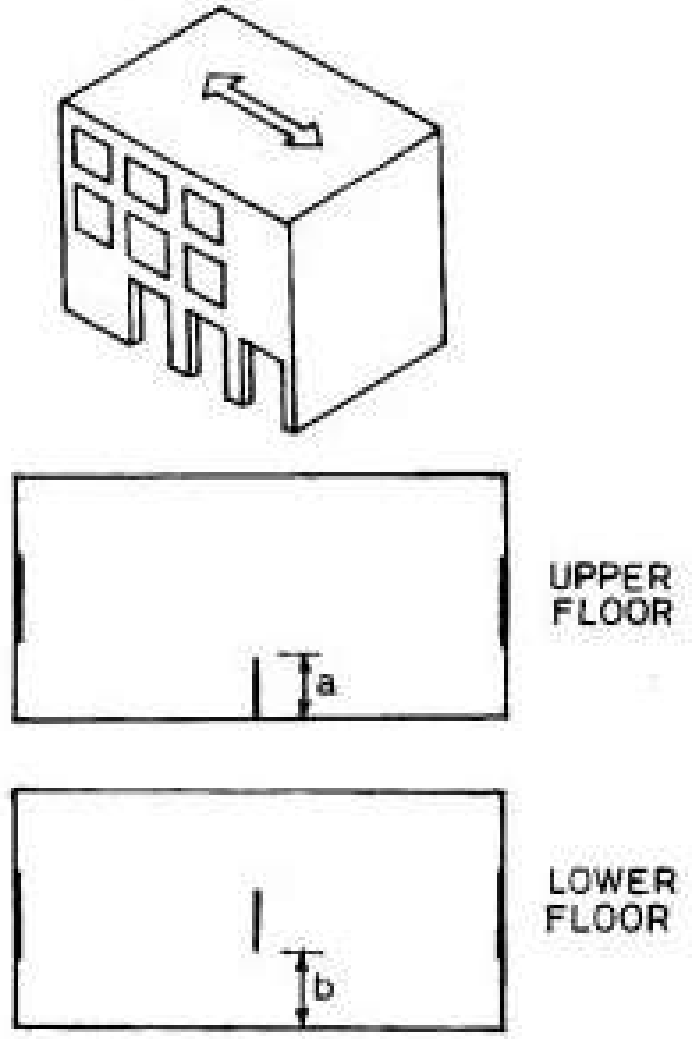

Figure 3.19: In-Plane Discontinuity in Vertical Elements Resisting Lateral Force

3.4 Analytical Problem Formulation

In this section Problem Formulation & Building model with plan irregularities is stated analytically. Analytical approach to determine mass and stiffness matrix of Building model is given in detail. By calculating Eigen values and Eigen Vectors for these space frame structures, natural frequencies and mode shapes can be obtained.

To analyze the structure, floors are considered as rigid diaphragm that leads to diagonal mass matrix and stiffness matrix can be calculated from unsymmetrical stiffness distribution that leads to coupled stiffness matrix.The effect of unsymmetrical stiffness distribution emphasis on torsional coupling.The motion of the each slab is defined by three dynamic degrees of freedom defined at the center of mass and whole mass of the structure is confined at the slab.However distribution of the mass can be done evenly to the adjacent floors.

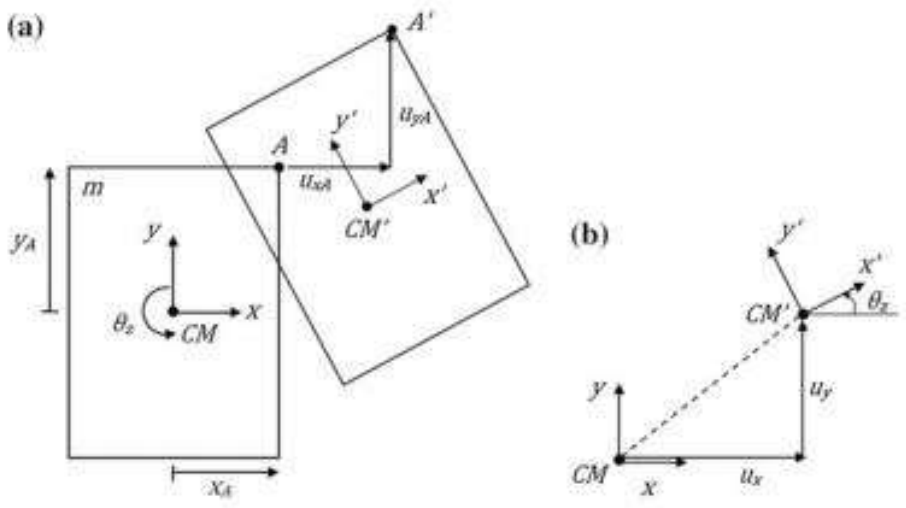

Figure 3.20: (a) Motion of a Rigid Slab in its Own Plane, (b) Motion of the Centre of Mass

3.4.1 Analytical Solution of Single Storey 3 DOF Structure

To carry out analytical solution of single storey structure mass and stiffness matrix has been prepared and eigen values can be determined.

Mass matrix can be calculated by considering two translation masses in both the x and y direction . It is shown as $[m_i]$ and mass moment of inertia $[I_i]$ can be calculated about z-axis.As the translational and rotational masses of each story represents the translational and rotational dynamic degrees of freedom of that story, mass matrix can be constructed as a diagonal matrix since and hence there is no translational-rotational coupling between the mass coefficients.

$$\begin{bmatrix} m_1 & 0 & 0 \\ 0 & m_2 & 0 \\ 0 & 0 & I_1 \end{bmatrix}$$

Stiffness matrix can be calculated by applying direct stiffness matrix and by choosing three DOFs at the centre of the mass.The i^{th} column is located at distances x_i and y_i from the co-ordinate center. Direct stiffness method is applied for each DOF separately.

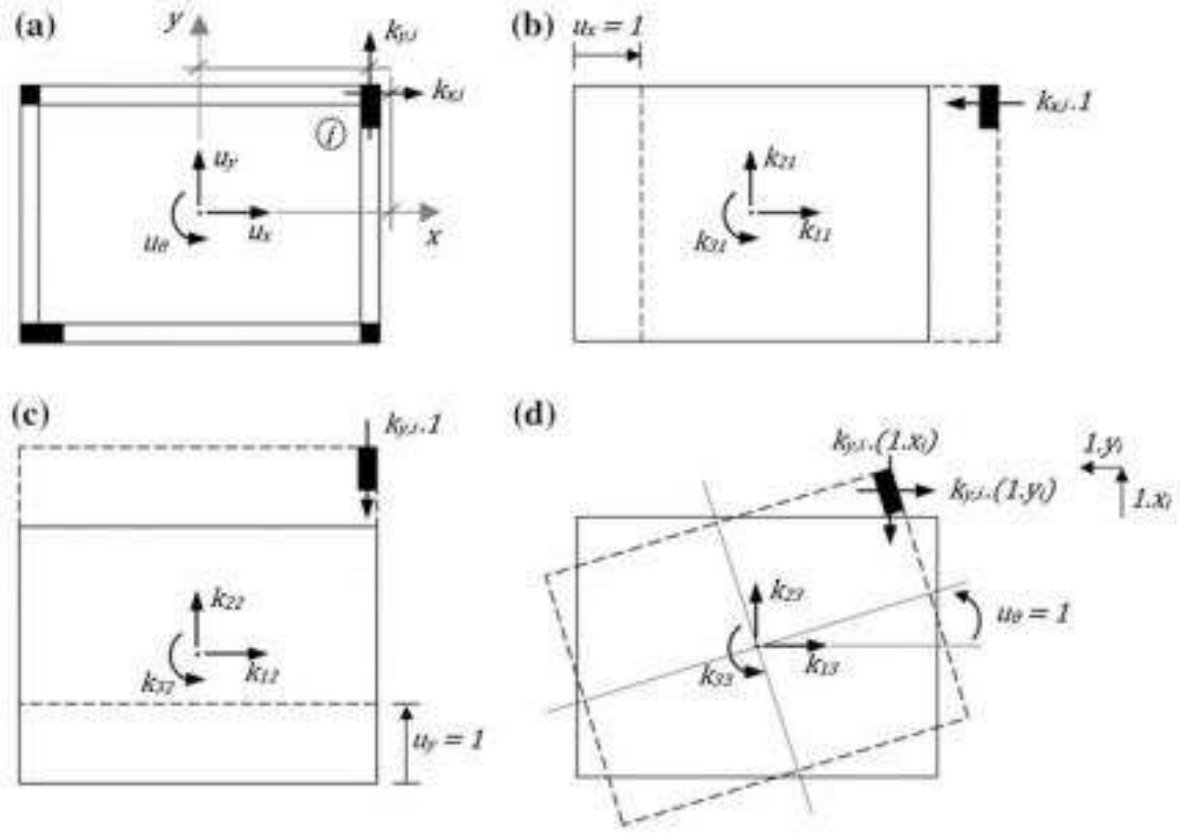

Figure 3.21: Calculation of Stiffness Coefficients for One Storey Space Frame

First of all applying unit displacement in x direction (u_x=1, u_y=0 , u_z=0). All column will resist this motion and inducing force $k_{xi}.1 = k_{xi}$. Where as k_{xx} , k_{yx}, $k_{\theta x}$ are the coordinates that constrain the displacement in u_x]=1, u_y =0 , u_z. This can be represented as,

$$k_{xx} = \sum k_{xi}, k_{yx} = 0, k_{\theta x} = \sum(-k_{xi}.y_i) \tag{3.80}$$

Same way applying unit displacement in y direction (u_x=0, u_y=1 , u_z =0) and calculating coordinates.

$$k_{xy} = 0, k_{yy} = \sum k_{yi}, k_{\theta y} = \sum(k_{yi}.x_i) \tag{3.81}$$

when unit rotation is given in z direction (u_x = 0,u_y=0,u_z =1), coordinated can be calculated as below.

$$k_{x\theta} = \sum(-k_{xi}.y_i), k_{y\theta} = \sum(k_{yi}.x_i), k_{\theta\theta} = \sum[(k_{xi}.y_i^2) + (k_{yi}.x_i^2)] \tag{3.82}$$

The complete stiffness matrix can be written as

$$\begin{bmatrix} \sum k_{xi} & 0 & \sum(-k_{xi}.y_i) \\ 0 & \sum k_{yi} & \sum(k_{yi}.x_i) \\ \sum(-k_{xi}.y_i) & \sum(k_{yi}.x_i) & \sum[(k_{xi}.y_i^2) + (k_{yi}.x_i^2)] \end{bmatrix}$$

3.5 Dynamic Response Solution of Asymmetric Structural System

To a first approximation, the building frame can be modeled as a three-dof system as shown in figure 3.22. The origin of reference is taken to coincide with the mass center of the frame. Figure 3.22 shows the idealized physical model in which the slab is assumed to be rigid and it is taken to displace in its own plane with two translations and one rotation. The four columns are replaced by a set of springs and dampers. Half of the mass of columns could be taken to participate in offering inertia. Figure 3.23 shows the free body diagram with all the forces acting on the slab explicitly displayed.The following equations have been taken from the videos of Stochastic Structural Dynamics by Dr C.S.Manohar IISc Bangalore NPTEL videos. The equation of motion can thus be deduced as

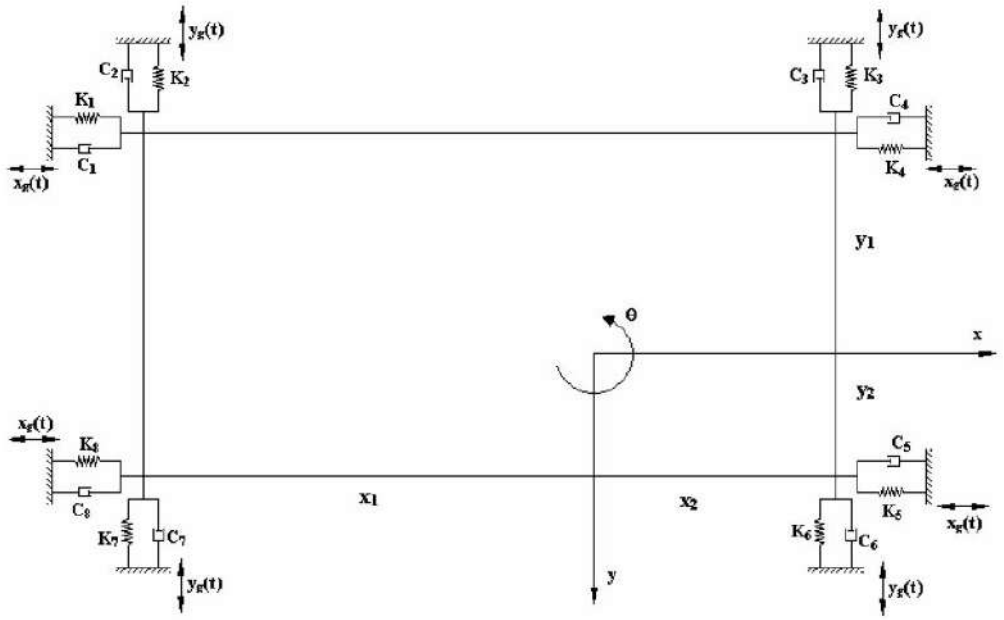

Figure 3.22: Rigid Mass-Damper Spring Model Representation of the frame subjected to Harmonic Base Motion

Figure 3.23 shows the free body diagram with all the forces acting on the slab explicitly displayed.The following equations have been taken from the videos of Stochastic Structural Dynamics by Dr C.S.Manohar IISc Bangalore NPTEL videos. The equation of motion can thus be deduced as

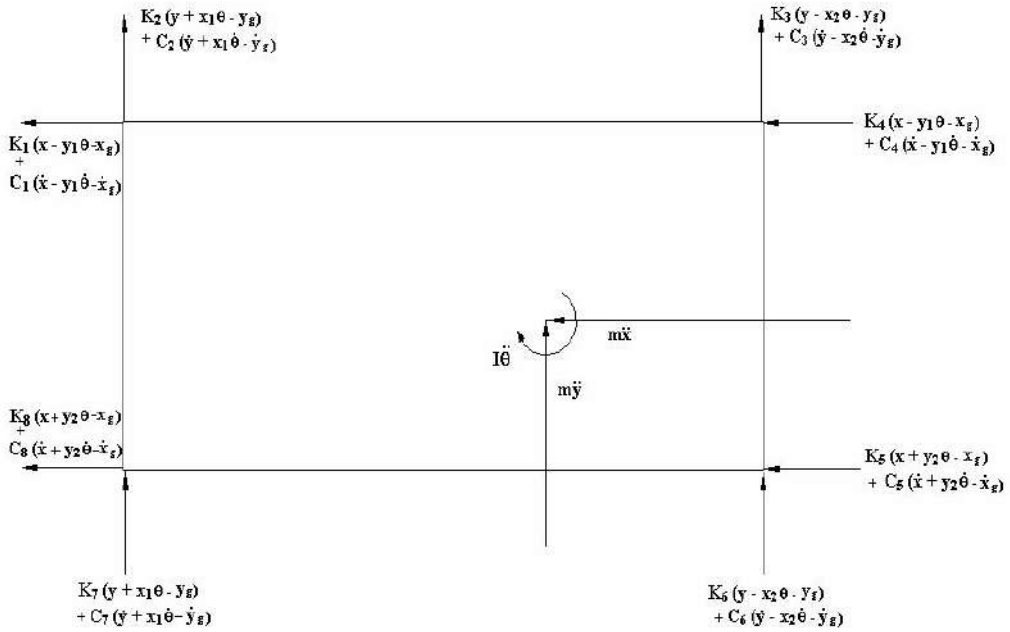

Figure 3.23: Free Body Diagram Showing the forces acting on the frame

$$m\ddot{x} + k_1(x - y_1\theta - x_g) + c_1(\dot{x} - y_1\dot{\theta} - \dot{x}_g) + k_4(x - y_1\theta - x_g) + c_4(\dot{x} - y_1\dot{\theta} - \dot{x}_g) + \\ + k_8(x + y_2\theta - x_g) + c_8(\dot{x} + y_2\dot{\theta} - \dot{x}_g)k_5(x + y_2\theta - x_g) + c_5(\dot{x} + y_2\dot{\theta} - \dot{x}_g) = 0 \tag{3.83}$$

$$m\ddot{y} + k_2(y + x_1\theta - y_g) + c_2(\dot{y} - x_1\dot{\theta} - \dot{y}_g) + k_7(y - x_1\theta - y_g) + c_7(\dot{y} - x_1\dot{\theta} - \dot{y}_g) + \\ k_3(y - x_2\theta - y_g) + c_3(\dot{y} + x_2\dot{\theta} - \dot{y}_g) + k_6(y - x_2\theta - y_g) + c_6(\dot{y} + x_2\dot{\theta} - \dot{y}_g) = 0 \tag{3.84}$$

$$I\ddot{\theta} + x_1[k_2(y + x_1\theta - y_g) + c_2(\dot{y} + x_1\dot{\theta} - \dot{y_g}) + k_7(y + x_1\theta - y_g) + c_7(\dot{y} + x_1\dot{\theta} - \dot{y_g})] \\ - x_2[k_3(y - x_2\theta - y_g) + c_3(\dot{y} - x_2\dot{\theta} - \dot{y_g}) + k_6(y - x_2\theta - y_g) + c_6(\dot{y} - x_2\dot{\theta} - \dot{y_g})] \\ + y_2[k_8(x + y_2\theta - x_g) + c_8(\dot{x} + y_2\dot{\theta} - \dot{x_g}) + k_5(x + y_2\theta - x_g) + c_5(\dot{x} + y_2\dot{\theta} - \dot{x_g})] \\ - y_1[k_1(x - y_1\theta - x_g) + c_1(\dot{x} - y_1\dot{\theta} - \dot{x_g}) + k_4(x - y_1\theta - x_g) + c_4(\dot{x} - y_1\dot{\theta} - \dot{x_g})] = 0 \tag{3.85}$$

The mass, Stiffness and Damping matrices are given,respectively,by

$$\begin{bmatrix} m & 0 & 0 \\ 0 & m & 0 \\ 0 & 0 & I \end{bmatrix}$$

$$\begin{bmatrix} k_1+k_4+k_8+k_5 & 0 & y_2(k_5+k_8)-y_1(k_1+k_4) \\ 0 & k_2+k_3+k_6+k_7 & x_1(k_2+k_7)-x_2(k_3+k_6) \\ y_2(k_5+k_8)-y_1(k_1+k_4) & x_1(k_2+k_7)-x_2(k_3+k_6) & [x_1^2(k_2+k_7)+x_2^2(k_3+k_6) \\ & & +y_1^2(k_1+k_4)+y_2^2(k_8+k_5)] \end{bmatrix}$$

$$\begin{bmatrix} c_1+c_4+c_8+c_5 & 0 & y_2(c_5+c_8)-c_1(c_1+c_4) \\ 0 & c_2+c_3+c_6+c_7 & x_1(c_2+c_7)-x_2(c_3+c_6) \\ y_2(c_5+c_8)-y_1(c_1+c_4) & x_1(c_2+c_7)-x_2(c_3+c_6) & [x_1^2(c_2+c_7)+x_2^2(c_3+c_6) \\ & & +y_1^2(c_1+c_4)+y_2^2(c_8+c_5)] \end{bmatrix}$$

$$M\ddot{x}+C\ddot{x}+Kx=f(t) \tag{3.86}$$

$$X(\omega)=\int_{-\infty}^{\infty}x(\tau)exp(i\omega\tau)\mathrm{d}\tau \tag{3.87}$$

$$X(\tau)=\frac{1}{2\pi}\int_{-\infty}^{\infty}X(\omega)exp(-i\omega t)\mathrm{d}\omega \tag{3.88}$$

$$M[\int_{-\infty}^{\infty}-\omega^2X(\omega)exp(i\omega t)d\omega]+C[\int_{-\infty}^{\infty}i\omega X(\omega)exp(-i\omega t)d\omega]+K[\int_{-\infty}^{\infty}X(\omega)exp(i\omega t)d\omega]= \int_{-\infty}^{\infty}F(\omega)exp(-i\omega t)d\omega \tag{3.89}$$

Here we have used Integral transform techniques, such as, Laplace transforms,to solve the problem . For the special case in which the excitation is harmonic, that is, f(t)=$f_0$exp(iλ t), and interest is focused on steady state behaviour

$$X(\omega)=[-\omega^2M+i\omega C+K]^{-1}F(\omega) \tag{3.90}$$

$$H(\omega) = [-\omega^2 M + i\omega C + K]^{-1} \tag{3.91}$$

The Matrix H(ω)=[-ω^2M+iω C+K] can be called as the dynamic stiffness matrix.This matrix is a complex valued symmetric matrix that is dependent upon the driving frequency ω.

Uncoupling of Equation of Motion is done now to obtain response of the building model which is another method used other than Laplace Transformations

$$M\ddot{x} + C\dot{x} + Kx = Fexp(i\omega t) \tag{3.92}$$

$X_{rs}(t)$ = response of the r^{th} co-ordinate due to unit harmonic driving at S-th Cordinate

$$lim_{t\to\infty} X(t) = X_0 exp(i\omega t) \tag{3.93}$$

$$\dot{x}(t) = X_0 i\omega exp(iwt) \tag{3.94}$$

$$\ddot{x}(t) = -X_0\omega^2 exp(i\omega t) \tag{3.95}$$

$$-Mx_0\omega^2 exp(i\omega t) + Cx_0 i\omega exp(i\omega t) + Kx_0 exp(i\omega t) = Fexp(i\omega t) \tag{3.96}$$

$$[-\omega^2 M + i\omega C + K]x_0 exp(i\omega t) = Fexp(i\omega t) \tag{3.97}$$

$$[-\omega^2 M + i\omega C + K]x_0 = F \tag{3.98}$$

$$X(t) = x_0 exp(i\omega t) = \phi Z_0 exp(i\omega t) \tag{3.99}$$

$$\phi^t M\phi = I \tag{3.100}$$

$$\phi^t K\phi = \lambda \tag{3.101}$$

$$\phi^t C\phi = \gamma \tag{3.102}$$

$$\gamma_{nn} = 2\eta_n\omega_n \tag{3.103}$$

γ is an Diagonal Matrix with entry on the nth row being $2\eta_n\omega_n$

$$[-\omega^2 M + i\omega c + K]\phi Z_0 = F \tag{3.104}$$

$$\phi^t[-\omega^2 M + i\omega C + K]\phi Z_0 = \phi^t F \tag{3.105}$$

$$[-\omega^2 I + i\omega\gamma + \lambda]Z_0 = \phi^t F Z_{0n} = \sum_{k=1}^{N} \frac{(\phi_{nk})^t F_k}{(\omega_n)^2 - \omega^2 + i2\eta_n\omega_n\omega} \tag{3.106}$$

$$Z_{0n} = \sum_{k=1}^{N} \frac{(\phi_{kn})F_k}{(\omega_n)^2 - \omega^2 + i2\eta_n\omega_n\omega} Z_{0n} = \frac{\phi_{sn}}{\omega_n^2 - \omega^2 + i2\eta_n\omega_n\omega} \tag{3.107}$$

$$lim_{t\to\infty} = \phi z_0 exp(i\omega t) = \sum_{n=1}^{N} \phi_{rn} Z_{0n} exp(i\omega t) = \sum_{N=1}^{N} \frac{\phi_{sn}\phi_{rn} exp(i\omega t)}{\omega_n^2 - \omega^2 + i2\eta_n\omega_n\omega} \tag{3.108}$$

$$X_{rs}(t) = H_{rs}(\omega) exp(i\omega t) \tag{3.109}$$

$$H_{rs}(\omega) = \sum_{n=1}^{N} \frac{\phi_{sn}\phi_{rn}}{\omega_n^2 - \omega^2 + i2\eta_n\omega_n\omega} \tag{3.110}$$

$$X_{rs}(\omega) = \sum_{n=1}^{N} \frac{\phi_{sn}\phi_{rn} exp(i\omega t)}{\omega_n^2 - \omega^2 + i2\eta_n\omega_n\omega} \tag{3.111}$$

$$H(\omega) = [\sum_{n=1}^{N} \frac{\phi_{sn}\phi_{rn}}{\omega_n^2 - \omega^2 + i2\eta_n\omega_n\omega}] = [-\omega^2 M + i\omega C + K]^{-1} \tag{3.112}$$

The Equation obtained from uncoupling of equation of motion is computationally easier to implement and it is not required to include all modes in the equation, the response equation obtained from Laplace transformation is Conceptually simple but it is computationally difficult to implement.

3.6 Summary

Detailed fundamental study of single degree of freedom system has been carried out for free and forced Vibration.In this chapter various types of irregularities in building model have been discussed and an analytical approach has been carried out to determine mass and stiffness matrix of asymmetric building model and also mathematical model has been solved for asymmetric building model with irregularity in order to obtain the response of the asymmetric building model. It is evident that damping plays very significant role in the dynamic behaviour of structural system.

Chapter 4

Instrumentation for Experimental Setup

4.1 General

This Chapter deals with the various instruments used for measuring various dynamic properties. Experimental Determination of various quantities like natural frequencies and damping requires measurement of acceleration.This physical quantity can be captured using:-

1 Shake Table

2 Accelerometers

3 Data Acquisition System

4 LabVIEW 8.0

A description of all the above instruments has been given in this chapter with their working principle and following sections explain each one of them in sufficient details. Following figure 4.1 shows the overall process of acquiring vibration data and convert them into digital form using the instruments stated above.

Figure 4.1: Experimental Setup

4.2 Shake Table

Shake table is a basic testing facility for development of earthquake resistant techniques. The Shake table is an instrument to simulate the conditions of the earthquake.
Figure 4.2 shows the shake table purchased by Nirma Institute of Technology. It is a uniaxial shake table having a design capacity of 30 kg which can be used to simulate sine sweeps. Table 4.1 and Table 4.2 shows the specification of the Shake Table.

Table 4.1: specifications of shake table

1	Motion	Horizontal
2	Load capacity	30 KG
3	Operating frequency	0-25Hz
4	Frequency control	(+/- 3)
5	Amplitude	0-10 mm
6	Resolution	1 mm
7	Table size	400 x 400 mm
8	Rotating table diameter	390 mm

Figure 4.2: Uni- Axial Shake Table

Table 4.2: Amplitude v/s frequency table for shake table

	Amplitude (mm)	Frequency up to (Hz)
1	(+/- 0.5)	25.00
2	(+/- 1.0)	16.50
3	(+/- 1.5)	12.50
4	(+/- 2.0)	10.50
5	(+/- 2.5)	9.00
6	(+/- 3.0)	8.00
7	(+/- 3.5)	7.25
8	(+/- 4.0)	6.75
9	(+/- 4.5)	6.10
10	(+/- 5.5)	5.75

4.3 Accelerometers

The basic principle of the measurement by the accelerometer is that it measures the force exerted by a body as a result of a change in the velocity of the body (i.e. which leads to acceleration). A moving body possesses an inertia which tends to resist change in velocity. The force caused by vibration or a change in motion causes the mass to "squeeze" the piezoelectric material which produces an electrical charge that is proportional to the force exerted upon it. Since the charge is proportional to the force, and the mass is a constant, hence the change is proportional to the acceleration.

The most commonly used device is the piezoelectric accelerometer. As the name suggests, it uses the principle of piezoelectric effect. The device consists of a piezoelectric quartz crystal on which an accelerative force, whose value is to be measured, is applied.Due to the special self-generating property, the crystal produces a voltage that is proportional to the accelerative force.

Figure 4.3 shows an accelerometer having sensitivity 106 mV/g. which is attached to the SDOF building model using the help of an adhesive.

Figure 4.3: IMI Accelerometer attached to the Mass of SDOF System

4.4 Data Acquisition System

Data acquisition is the process of sampling signals that measure real world physical conditions and convert them into digital numeric values that can be manipulated by a computer. These real conditions may be temperature, pressure, wind, distance, acceleration, etc. In civil Engineering applications the most common types of sensors measure displacement, acceleration, force and strain. Data acquisition systems (abbreviated with the acronym DAS or DAQ) convert analog waveforms into digital values for processing. In automated data acquisition systems the sensors transmit a voltage or current signal directly to a computer via a data acquisition board.Figure 4.4 shows an National Instrument's Data Acquisition System(DAQ).

The purpose of data acquisition is to measure an electrical or physical phenomenon such as voltage, current, temperature, pressure, or sound. PC-based data acquisition uses a combination of modular hardware, application software, and a computer to take measurements. While each data acquisition system is defined by its application requirements, every system shares a common goal of acquiring, analyzing, and presenting information.Data acquisition systems incorporate signals, sensors, actuators, signal conditioning, data acquisition devices, and application software.

The components of measurement and data acquisition systems include

1 Sensors that convert physical parameters to electrical signals,

2 Signal conditioning circuitry to convert sensor signals into a form that can be converted to digital values

3 Analog-to-digital converters, which convert conditioned sensor signals to digital values.

When the voltage signal from the accelerometer is sent to the data acquisition system, it converts the signal to a mechanical vibration data (acceleration) and stores it to the computer.The benefits of automated systems are improved accuracy of recording and increased frequency with which measurements can be taken.

Figure 4.4: DAQ System

4.4.1 Acquiring Signal In NI-Daqmx

NI-DAQmx is a programming interface which can be used to communicate with data acquisition devices. Using this system we can create NI-DAQmx task that continuously takes voltage reading and plots the data on a waveform graph. In NI-DAQmx, a task is a collection of one or more channels, which contains timings, triggering and other properties. Conceptually a task represents a measurement or generation you want to perform. DAQ Hardware turns your PC into a measurement and automation system.

4.5 LabVIEW

LabVIEW programs are called virtual instruments, or VIs, because their appearance and operation imitate physical instruments, such as oscilloscopes and multimeters. LabVIEW contains a comprehension tools for acquiring,analyzing,displaying,and storing data,as well as tools to help you troubleshoot code you write.

LabVIEW stands for Laboratory Virtual Instrument Engineering Workbench. It is a graphical programming language that allows for instrument control, data acquisition, and pre/post processing of acquired data. Lab VIEW relies on graphical symbols rather than textual language to describe programming actions. LabVIEW programs are called Virtual Instruments (VIs) because their appearance and operation imitate actual instruments. LabVIEW is programmed with a set of graphical icons (called “G”) which are connected with “wires”. The combination of a DAQ board and LabVIEW software makes a virtual instrument or VI.

In LabVIEW, we build a user interface, or front panels,with controls and indicators. Control are Knobs,push buttons,dials and other input mechanisms.Indicators are graphs,LEDs,and

other output display's.After you build the front panel, you add code using VIs and structures to control the front panel objects which can be seen in Figure 4.5.The block diagram controls the code which can be seen in Figure 4.6.

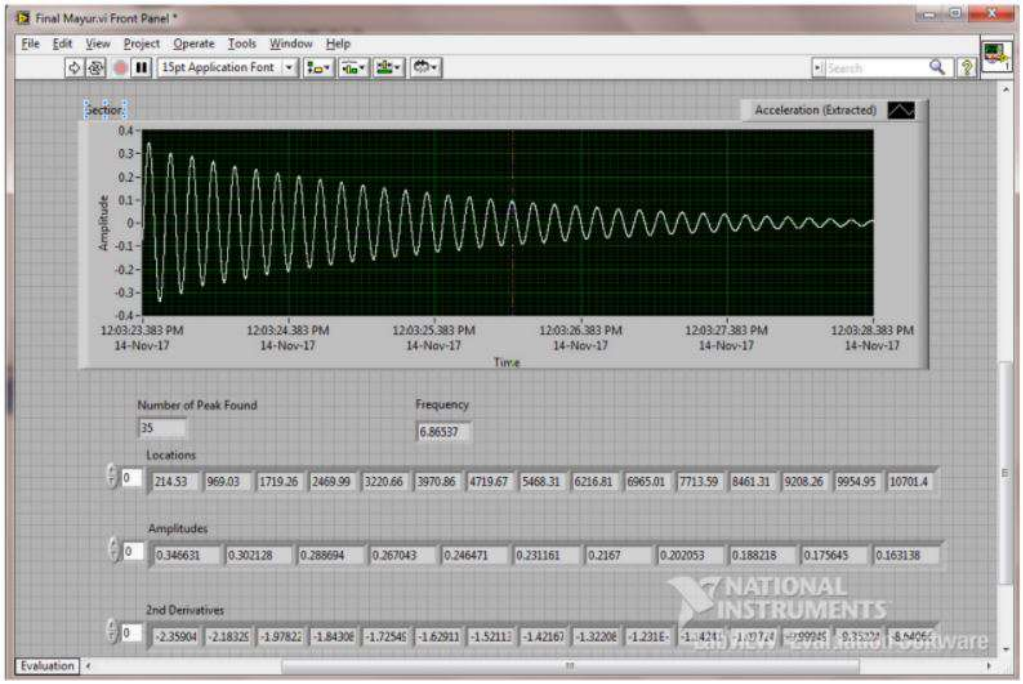

Figure 4.5: Front Panel Of LabVIEW

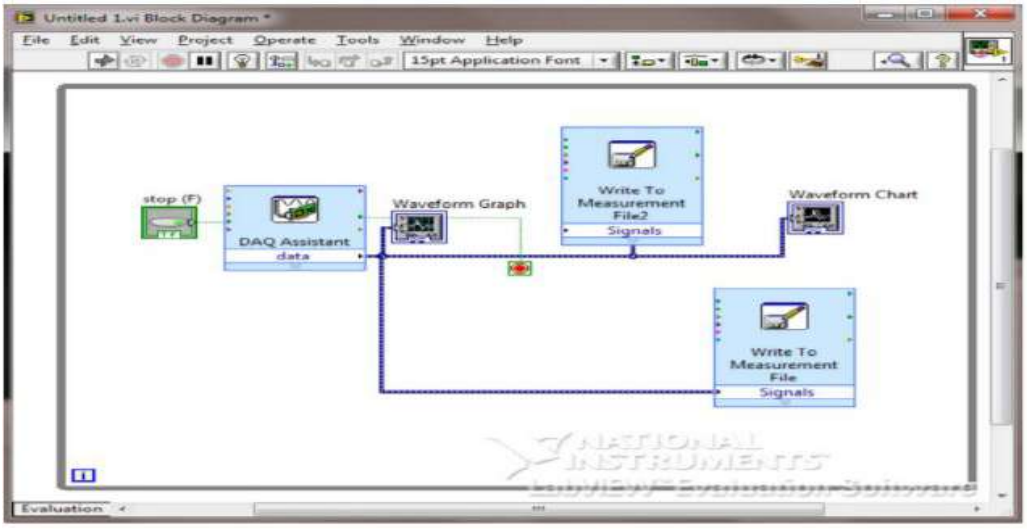

Figure 4.6: Block Diagram Of LabVIEW

4.6 Experimentation for Cyclic Test

4.6.1 Load Cell

Figure 4.7 shows an S-Type Load cell for measuring force, The force is measured in Kg and its Least count is 0.05 Kg.

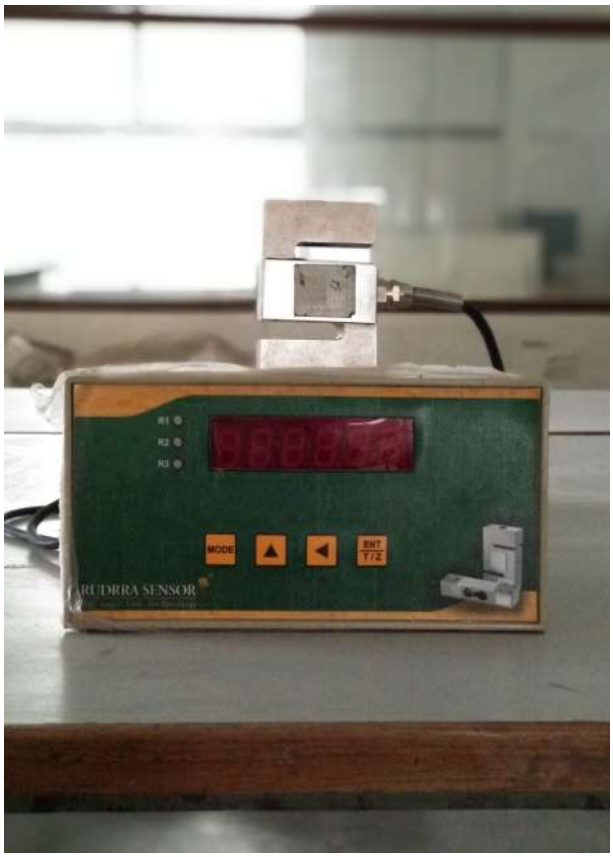

Figure 4.7: S-Type Load Cell

S type Load cell can measure both Tension and compression, There are grooves which are given in S-Type Load cell using which we have to attach the material in which the measurement of force is to be taken.

4.6.2 Dial Gauge

To measure the displacement, dial gauge is used with maximum displacement capacity of 50 mm with least-count of 0.01 mm. Dial gauge is shown in fig.4.8.

Figure 4.8: Dial Gauge

4.6.3 Unconfined Compression Testing Machine

The figure 4.9 shows an unconfined Compression testing machine which is available in Geo technical lab in Nirma University, It is used to apply Cyclic load, We can change the rate of loading at 1.25mm/min, 1.5mm/min and 2.5mm/min,Lever can be seen in Figure 4.10b through which we can change the rate , Figure 4.10a shows the knob using which we can change the direction of loading i.e in forward and Reverse direction.

Figure 4.9: Unconfined Compression Testing Machine

(a) Knob

(b) Lever

Figure 4.10: Lever and Knob in Unconfined Compression Testing Machine

4.7 Summary

In this chapter basic instruments that are required to determine dynamic properties of structure, experimentally, are discussed in detail. Functional and technical specifications for each of the instruments used for dynamic measurements are incorporated in the chapter.

Chapter 5

Experimental Evaluation of Geometrical and Dynamic Properties of Structural Systems

5.1 General

The stiffness, k, is the resistance to the deformation in response of the force applied to the body, for an elastic body with a single degree of freedom,stiffness can be defined as:-

$$k = \frac{F}{\delta} \tag{5.1}$$

Where,

F is the force applied on the body.

δ is the displacement produced by the force along the same degree of freedom .

An elastic modulus (also known as modulus of elasticity) is a number that measures an object or substance's resistance to being deformed elastically (i.e.,non-permanently) when a stress is applied to it. The elastic modulus of an object is defined as the slope of its stress–strain curve in the elastic deformation region. A stiffer material will have a higher elastic modulus. An elastic modulus has the form:

$$E = \frac{Stress}{Strain} \tag{5.2}$$

Natural frequency is the frequency at which a system naturally vibrates once it has been set into motion. In other words, natural frequency is the number of times a system will oscillate between its original position and its displaced position without any external interference. The natural frequency can be calculated using the formula,

$$f = \frac{1}{2\pi}\sqrt{\frac{k}{m}} \tag{5.3}$$

Where, k is the beam stiffness in N/m.

5.2 Evaluation of Modulus of Elasticity

An elastic modulus (also known as modulus of elasticity) is a number that measures an object or substance's resistance to being deformed elastically (i.e.,non-permanently) when a stress is applied to it. The elastic modulus of an object is defined as the slope of its stress–strain curve in the elastic deformation region The experimental setup has been showed in the figure 5.1 and analytically it can be expressed .

$$E = \frac{(P \times x^2) \times ((3 \times l) - x)}{6 \times \delta_x \times I} \tag{5.4}$$

where, P = Load applied in gm. x = Deflection measured from fixed joint. l = Length of Cantilever beam. δ_x = Deflection at x.

Figure 5.1: Test Setup For Modulus of Elasticity

5.2.1 Modulus of Elasticity of Aluminum

Load P(N)	Deflection (mm)	I (mm4)	Length l(mm)	x (mm)	E (MPa)	Average E(MPa)
1.962	4.13	52.5	417	210	69235.32	
3.924	8.27	52.5	417	210	69151.6	
5.886	12.4	52.5	417	210	69179.49	
7.848	16.54	52.5	417	210	69151.6	69163.45
9.81	20.68	52.5	417	210	69134.88	
11.772	24.81	52.5	417	210	69151.6	
13.734	28.95	52.5	417	210	69139.66	

5.2.2 Modulus of Elasticity Steel

Load P(N)	Deflection δx (mm)	I (mm4)	Length l(mm)	x (mm)	E (MPa)	Average E(MPa)
0.4905	0.55	52.5	417	285	222143	
0.981	1.05	52.5	417	285	232721.2	
1.4715	1.64	52.5	417	285	223497.5	
1.962	2.37	52.5	417	285	206208.7	210725.7
2.4525	3.24	52.5	417	285	188547.3	
2.943	3.61	52.5	417	285	203067	
3.4335	4.3	52.5	417	285	198895.5	

Equation 5.4 has been used to find out the Modulus of Elasticity at a distance x from the fixed end, Deflection at distance x has been found out using Dial Gauge which is represented as δ_x in the above Equation.

Modulus of Elasticity of Aluminum is found out to be as 6.9×10^{10} N/m^2 and Modulus of Elasticity of Steel is found out to be as 2.1×10^{11} N/m^2.

5.3 Evaluation of Stiffness and Natural Frequency of SDOF System

For evaluation of stiffness and natural frequency of SDOF, three methods are adopted. They are as follows.

1) Experimental procedure using load deflection curve.

2) Using theoretical formula.

3) Using shake table.

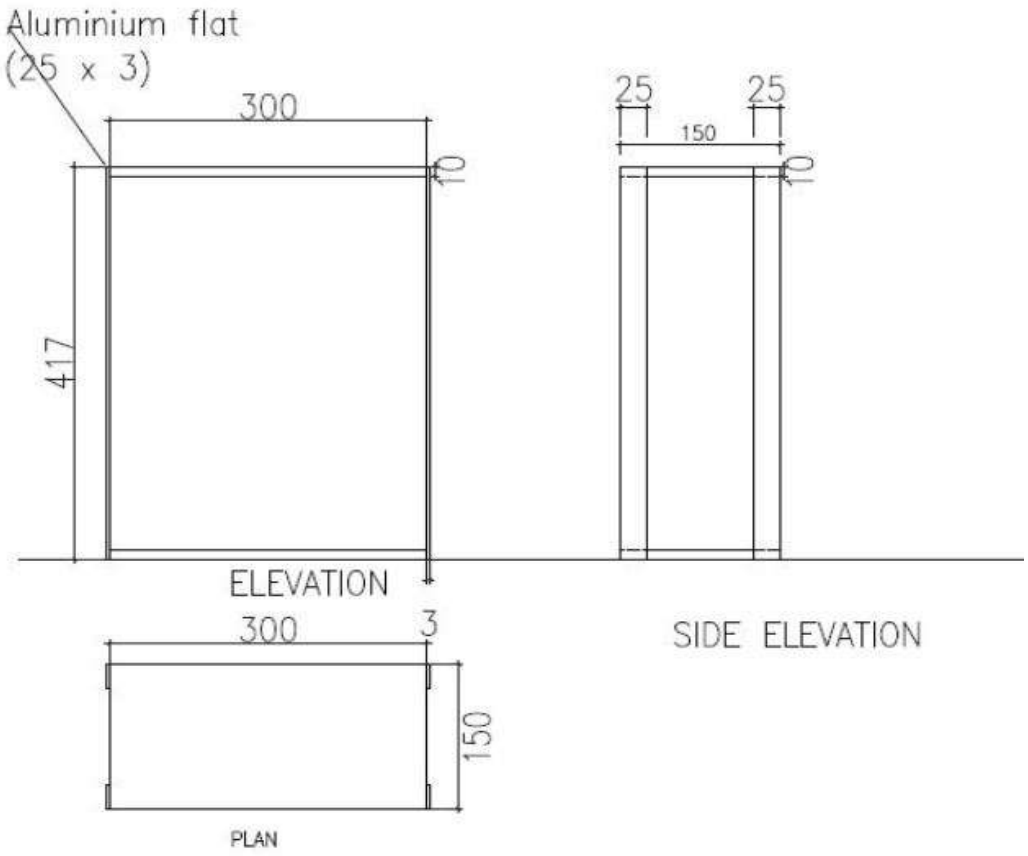

Figure 5.2: SDOF System Configuration

Figure 5.3: Photograph of SDOF model

5.3.1 Load Displacement Curve Obtained From Experiment

SDOF System has been clamped to the shake table using allen screws.SDOF system was further attached to the supporting assembly through string,Loading was applied to the string at the other end, Dial Gauge was used to measure the deflection of the SDOF system, The above description of the Test Setup can be seen in the Figure 5.4 . Further Load v/s Deflection curve was made through which Stiffness was found out.

Mass of SDOF = 1.7425 kg

Height = 417 mm

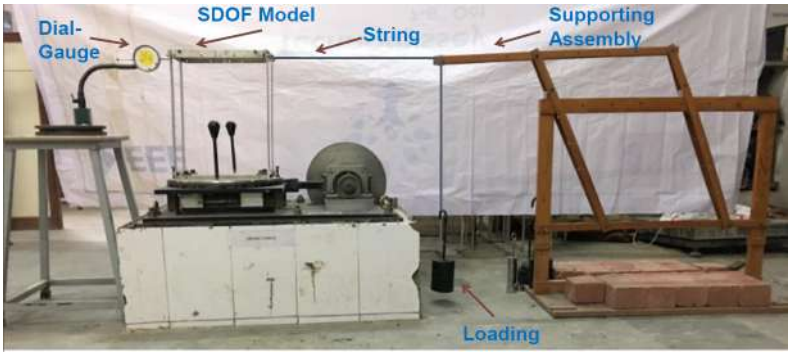

Figure 5.4: Test Setup to Evaluate Stiffness

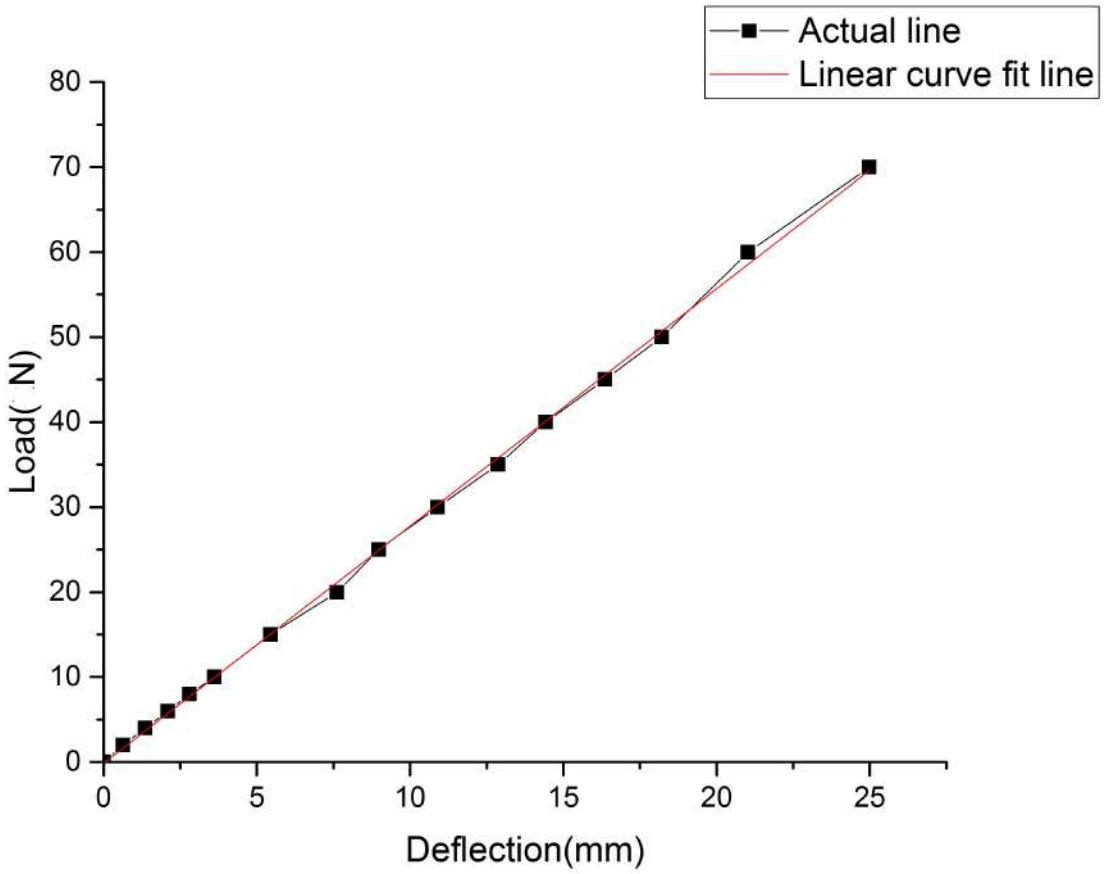

Figure 5.5: Load vs Deflection Curve

From figure 5.5, Stiffness k = 2752 N/m Frequency f_n = 6.12 Hz

5.3.2 Theoretical Calculations

Mechanical properties of Aluminum are calculated using analytical equations.

5.3.2.1 Stiffness

Stiffness of Aluminum is calculated and presented below

$$k = \frac{12EI}{L^3} = 2569.24N/m \tag{5.5}$$

where, E =$69 \times 10^9 N/m^2$

I =$225mm^4$

L =417 mm

5.3.2.2 Natural Frequency

Natural frequency of Aluminum is calculated and presented below

$$\omega_n = \sqrt{\frac{k}{m}} = \sqrt{\frac{2569.24}{1.7425}} = 38.398 rad/sec = 6.111 Hz \tag{5.6}$$

5.3.3 Experimental Frequency Obtained from Shake Table

Resonance in the building is a phenomenon in which if the building vibrates with its natural frequency, then the displacements of a structure will reach maximum called resonance, The greater the displacements,the greater the stresses that are developed in the framing members and connection of the structure.

In this context, SDOF system is clamped on shake table. Shake table is attached to the power supply. Shake table is allowed to vibrate at different frequencies. At certain frequency, resonance phenomena occurs i.e. SDOF vibrates with maximum amplitude. This frequency at which resonance occurs is the natural frequency of system. From the experiment performed, natural frequency of system was found to be i.e. f = 6.59 Hz

5.3.4 Comparison of Results

Table 5.1: Natural frequency obtained by experiments

Method	K (N/m)	$\omega_n(rad/sec)$	f(Hz)
Experimental	2573	38.42	6.13
Theoretical	2569	38.398	6.111
Using Shake-table	2996	41.46	6.59

5.4 Free Vibration Test

To determine the dynamic properties like Natural Frequency and Coeffcient of Damping more precisely Free Vibration Test was performed on regular building model as well as irregular SDOF building model.
Coefficient of damping is found out using Logarithmic decrement method, which is explained in Chapter [3] Dynamics of Asymmetric structural system .

5.4.1 Evaluation of Damping of Aluminum Column Strip

Aluminum column strip was clamped to the shake table using an angle section and a plate as shown in Figure 5.6.Aluminum column strip was subjected to free vibration and the acceleration response was captured using LabVIEW software.

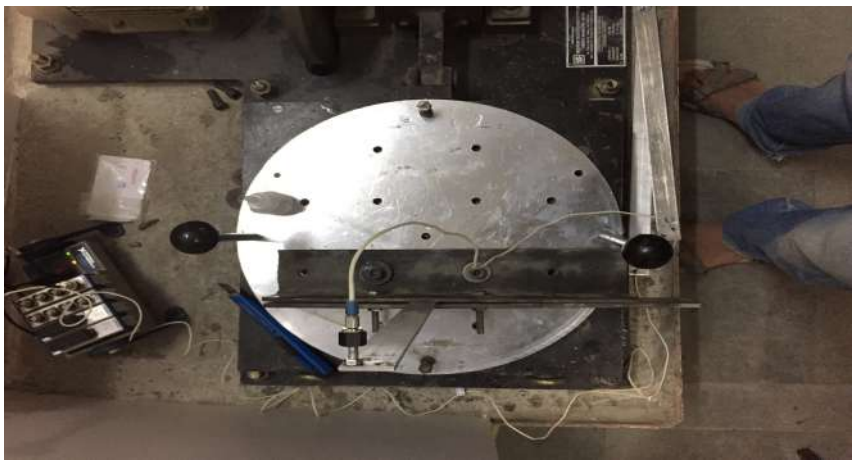

Figure 5.6: Uni-axial Accelerometer attached to aluminum column strip

Figure 5.7 shows the acceleration response of Aluminum column strip captured using LabVIEW and Figure 5.8 shows the extracted acceleration response of Aluminum column strip captured using LabVIEW.

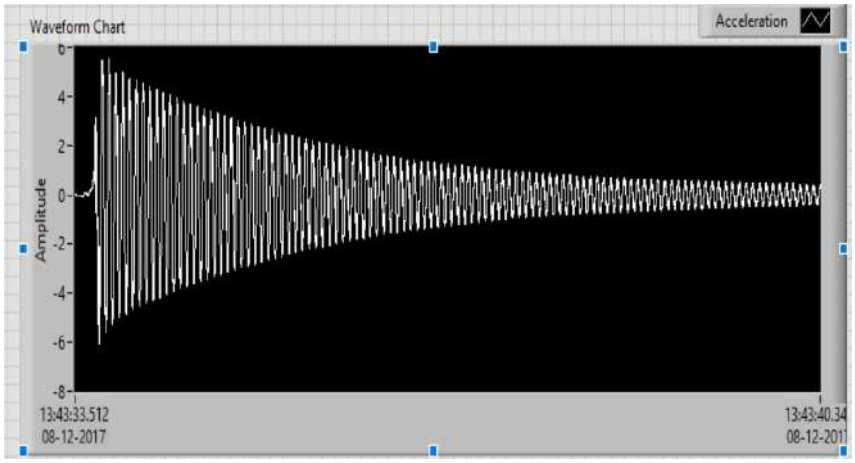

Figure 5.7: Acceleration Response of Aluminum Strip with Undergoing Free Vibration

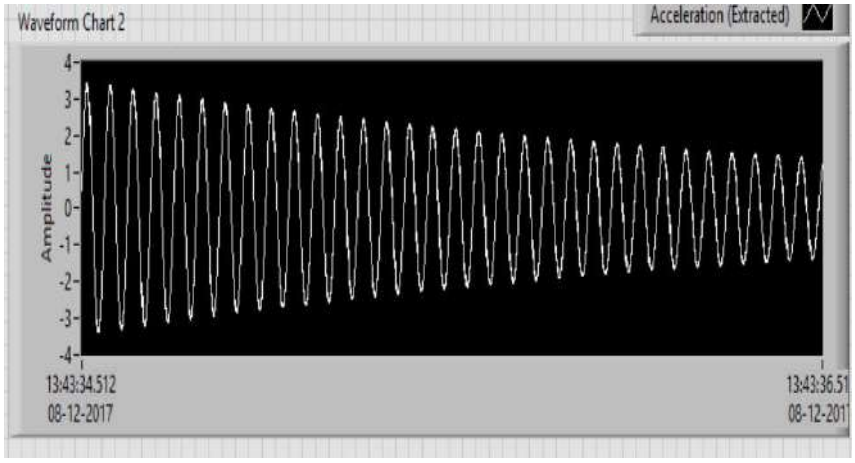

Figure 5.8: Extracted Acceleration Response of Aluminum Strip with Undergoing Free Vibration

Here gradual decrements in the acceleration response can be observed.Coefficient of damping (ζ) is found using Logarithmic Decrement method and is found out to be 0.4 %.

Table 5.2: Calculation of damping ratio (ζ) from logarithmic decrement method Aluminum Column strip

Peak	**Amplitude**	**Number of consecutive cycles**								
0	3.439	0.432	0.428	0.432	0.436	0.44	0.446	0.447	0.449	0.451
1	3.347	0.425	0.433	0.438	0.442	0.449	0.45	0.451	0.454	
2	3.259	0.441	0.445	0.448	0.455	0.455	0.456	0.458		
3	3.17	0.449	0.452	0.46	0.459	0.458	0.461			
4	3.082	0.456	0.465	0.462	0.461	0.463				
5	2.995	0.475	0.465	0.463	0.465					
6	2.907	0.456	0.457	0.461						
7	2.825	0.457	0.463							
8	2.745	0.469								
9	2.665									

5.4.2 Evaluation of Damping of Steel Column Strip

Steel column strip was clamped to the shake table using an angle section and a plate just like aluminum column strip was clamped as shown in Figure 5.6.Steel column strip was subjected to free vibration and the acceleration response was captured using LabVIEW software.

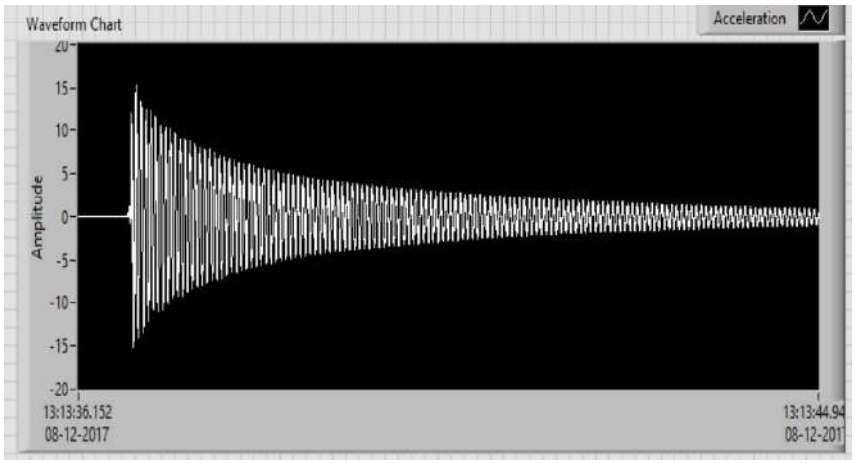

Figure 5.9: Acceleration Response of Steel Strip with Undergoing Free Vibration

Figure 5.9 shows the acceleration response of Steel column strip captured using LabVIEW and Figure 5.10 shows the extracted acceleration response of Steel column strip captured using LabVIEW.

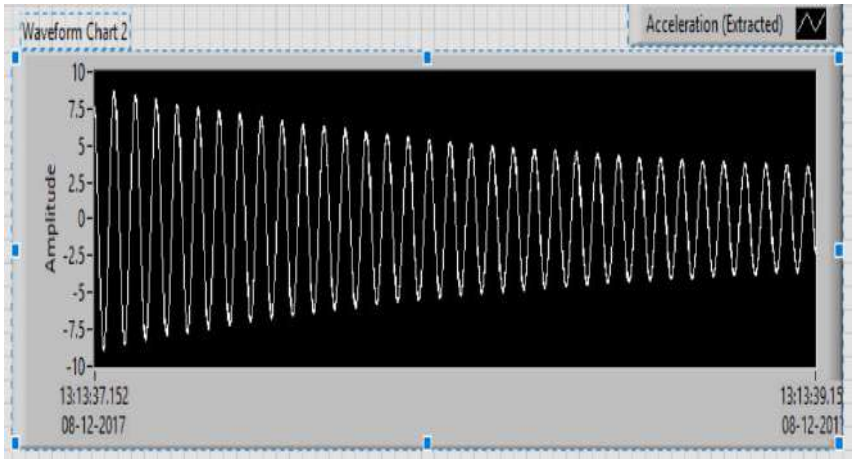

Figure 5.10: Extracted Acceleration Response of Steel Strip with Undergoing Free Vibration

Here gradual decrements in the acceleration response can be observed.Coefficient of damping (ζ) is found using Lgarithmic Decrement method and is found out to be 0.7 %.

Table 5.3: Calculation of damping ratio (ζ) from logarithmic decrement method Steel Column Strip

Peak	Amplitude	Number of consecutive cycles								
0	8.718	0.745	0.704	0.72	0.717	0.727	0.729	0.725	0.721	0.721
1	8.32	0.665	0.708	0.708	0.723	0.726	0.722	0.717	0.71	
2	7.98	0.752	0.73	0.743	0.741	0.734	0.726	0.725		
3	7.612	0.708	0.738	0.738	0.729	0.721	0.721			
4	7.281	0.769	0.753	0.736	0.724	0.724				
5	6.938	0.736	0.721	0.703	0.712					
6	6.624	0.704	0.695	0.704						
7	6.338	0.670	0.705							
8	6.07	0.722								
9	5.801									

5.4.3 Free Vibration test on Simple Bare single storey building model

Simple SDOF Bare building model was mounted on the Shake table and subjected to Free ex-citations. Experimental response was captured in LabVIEW and is shown in Figure 5.11 . Here gradual decrement in the Amplitude of the signal can be seen clearly.Extracted acceleration response can be seen in Figure 5.12.

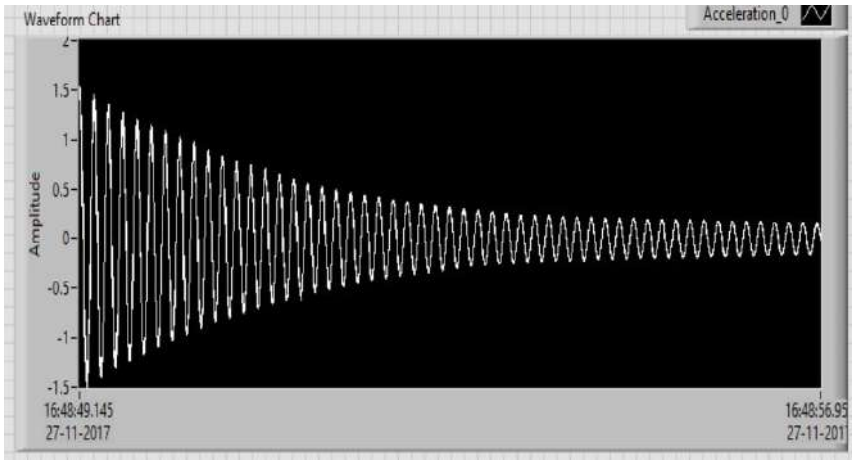

Figure 5.11: Acceleration Response of Single Story building model Undergoing Free Vibration

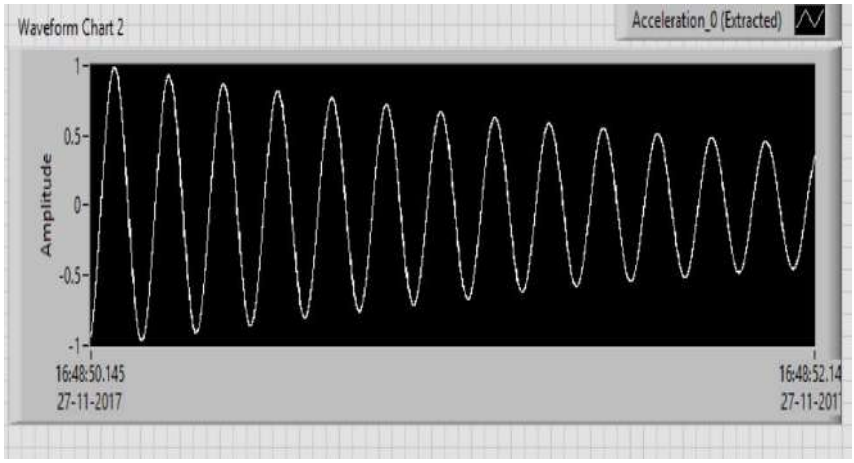

Figure 5.12: Extracted Acceleration Response of Single Story building model Undergoing Free Vibration

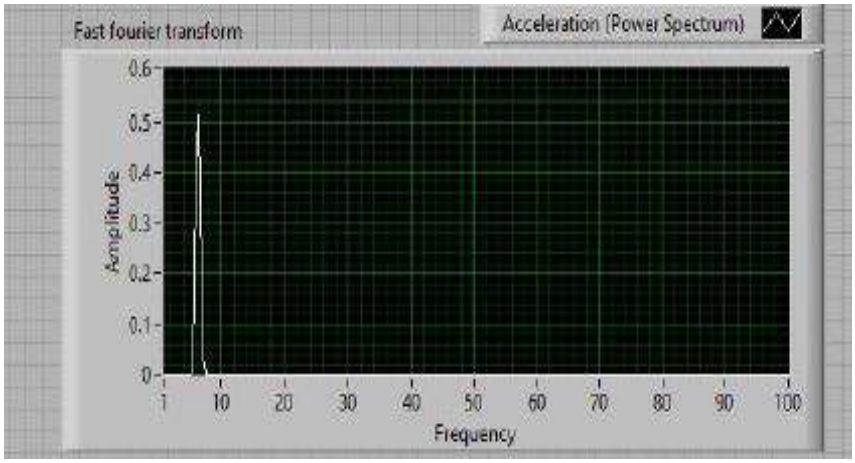

Figure 5.13: Fundamental Frequency Extraction for Bare Regular SDOF Model Through Fast Fourier Transform Techniques

After getting Acceleration Response of building model, Fast Fourier Transform can be produced in LabVIEW software. It is shown in Figure 5.13. Natural Frequency of the structure is 6.3 Hz. After capturing the Natural frequency of the structure Coefficient of damping is evaluated using Logarithmic Decrement method and is found out to be 0.757 %.

Table 5.4: Calculation of damping ratio (ζ) from logarithmic decrement method bare SDOF aluminum building model

Peak	Amplitude	Number of consecutive cycles								
0	0.835	0.782	0.76	0.757	0.754	0.754	0.752	0.748	0.739	0.742
1	0.795	0.739	0.745	0.744	0.747	0.746	0.742	0.733	0.737	
2	0.759	0.751	0.747	0.749	0.747	0.743	0.732	0.736		
3	0.724	0.742	0.748	0.746	0.741	0.728	0.734			
4	0.691	0.755	0.748	0.74	0.724	0.732				
5	0.659	0.742	0.733	0.714	0.727					
6	0.629	0.725	0.701	0.722						
7	0.601	0.676	0.720							
8	0.576	0.764								
9	0.549									

5.4.4 Free Vibration test on SDOF Model with Material Irregularity

Single storey building model with three aluminum column and one column of steel was mounted on the Shake table and subjected to Free ex-citations. Experimental response was captured in Lab-VIEW.The filtered extracted signal of SDOF building model with material irregularity can be seen in Figure 5.14 and the extracted acceleration response can be seen in figure 5.15 Here gradual decrements in the Amplitude of the signal can be seen clearly.

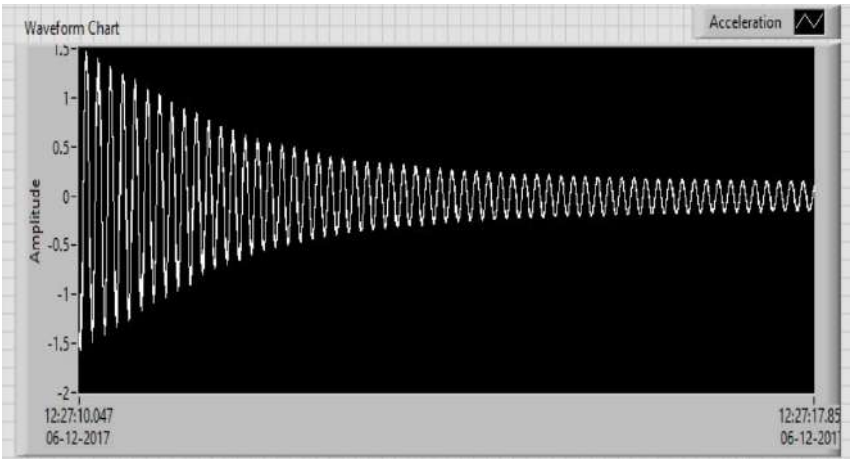

Figure 5.14: Acceleration Response of Single Story building model with material Irregularity Undergoing Free Vibration

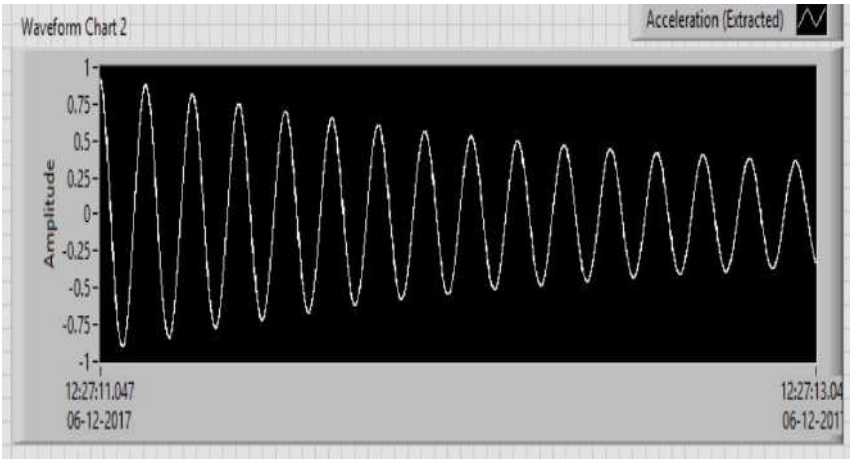

Figure 5.15: Extracted Acceleration Response of Single Story building model with material Irregularity Undergoing Free Vibration

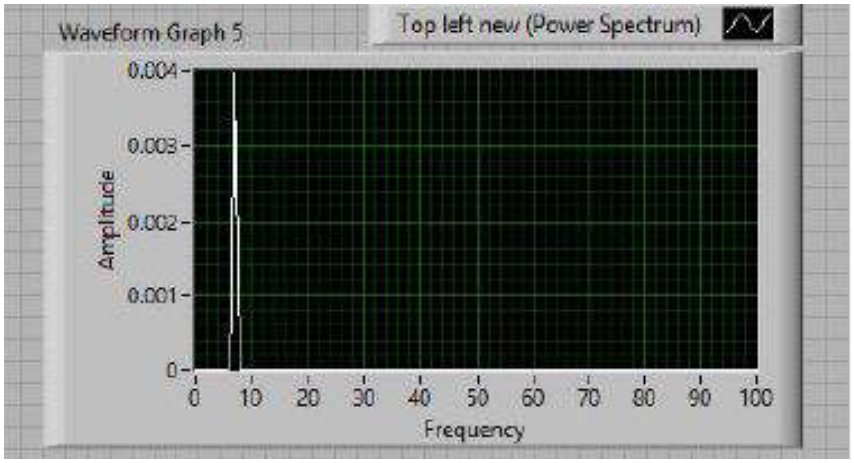

Figure 5.16: Fundamental Frequency Extraction for SDOF Building Model with Material Irregularity Through Fast Fourier Transform Techniques

After getting Acceleration Response of building model, Fast Fourier Transform can be produced in LabVIEW software. It is shown in Figure 5.16. Natural Frequency of the structure is 6.3 Hz. After capturing the Natural frequency of the structure Coefficient of damping is evaluated using Logarithmic Decrement method and is found out to be 1.05%.

Table 5.5: Calculation of damping ratio (ζ) from logarithmic decrement method for building model with Material Irregularity

Peak	Amplitude	Number of consecutive cycles								
0	0.885	1.569	1.371	1.268	1.259	1.238	1.234	1.171	1.14	1.131
1	0.802	1.166	1.116	1.153	1.101	1.162	1.102	1.079	1.075	
2	0.745	1.065	1.146	1.079	1.160	1.089	1.0645	1.0618		
3	0.697	1.226	1.086	1.192	1.095	1.064	1.061			
4	0.645	0.945	1.175	1.051	1.023	1.028				
5	0.60	1.404	1.104	1.049	1.048					
6	0.556	0.804	0.871	0.929						
7	0.529	0.939	0.992							
8	0.499	1.046								
9	0.467									

5.4.5 Free Vibration test on SDOF Model with L-Shape Planar asymmetry

Single storey building model having planar asymmetry L-shape was mounted on the Shake table and subjected to Free ex-citations. Experimental response was captured in Lab-VIEW.The filtered extracted signal of SDOF building model with Planar irregularity L-shape can be seen in Figure 5.17 and the extracted acceleration response can be seen in figure 5.18 Here gradual decrements in the Amplitude of the signal can be seen clearly.

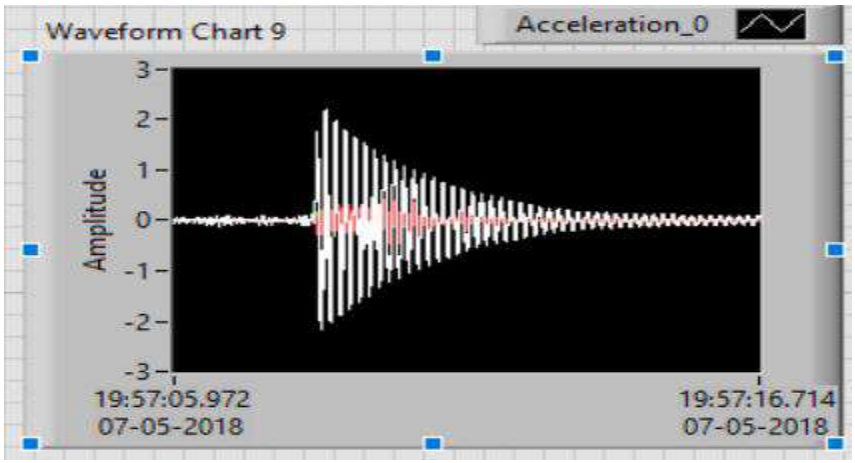

Figure 5.17: Acceleration Response of Single Story building model with Planar Irregularity of L-Shape Undergoing Free Vibration

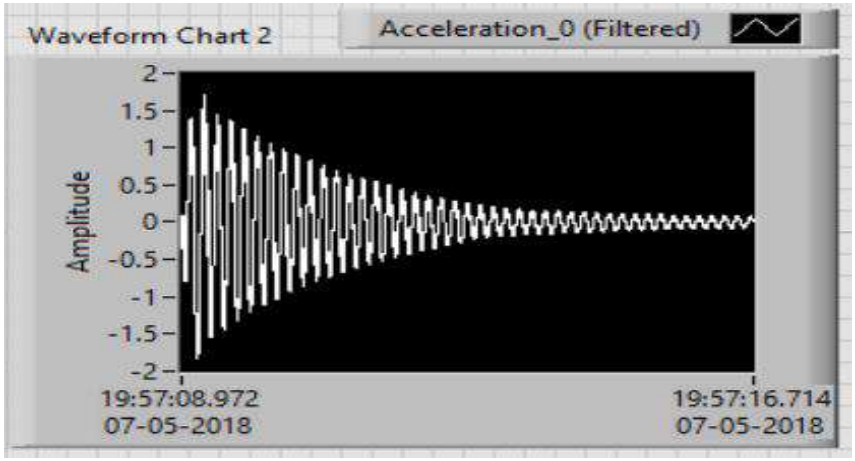

Figure 5.18: Extracted Acceleration Response of Single Story building model with Planar Irregularity of L-Shape Undergoing Free Vibration

After getting Acceleration Response of building model, Fast Fourier Transform can be produced in LabVIEW software. It is shown in Figure 5.19. Natural Frequency of the

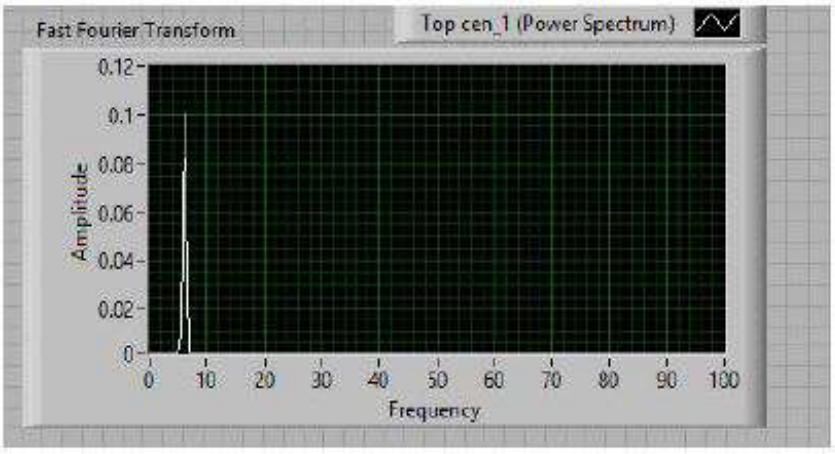

Figure 5.19: Fundamental Frequency Extraction for SDOF Building Model with Planar Irregularity of L-Shape Through Fast Fourier Transform Techniques

structure is 6.4 Hz. After capturing the Natural frequency of the structure Coefficient of damping is evaluated using Logarithmic Decrement method and is found out to be 1.07%.

Table 5.6: Calculation of damping ratio (ζ) from logarithmic decrement method for building model with Planar Irregularity of L Shape

Peak	Amplitude	Number of consecutive cycles								
0	1.442	0.908	1.3049	1.205	1.232	1.252	1.181	1.186	1.113	1.046
1	1.362	1.701	1.354	1.341	1.339	1.236	1.233	1.143	1.064	
2	1.224	1.007	1.16	1.218	1.119	1.139	1.05	0.973		
3	1.149	1.314	1.324	1.157	1.172	1.059	0.967			
4	1.058	1.334	1.078	1.125	0.995	0.898				
5	0.973	0.823	1.02	0.882	0.789					
6	0.924	1.217	0.912	0.778						
7	0.856	0.607	0.559							
8	0.824	0.511								
9	0.798									

5.4.6 Free Vibration test on SDOF Model with T-Shape Planar asymmetry

Single storey building model having planar asymmetry T-shape was mounted on the Shake table and subjected to Free ex-citations. Experimental response was captured in Lab-VIEW.The filtered extracted signal of SDOF building model with Planar irregularity T-shape can be seen in Figure 5.20 and the extracted acceleration response can be seen in figure 5.21 Here gradual decrements in the Amplitude of the signal can be seen clearly.

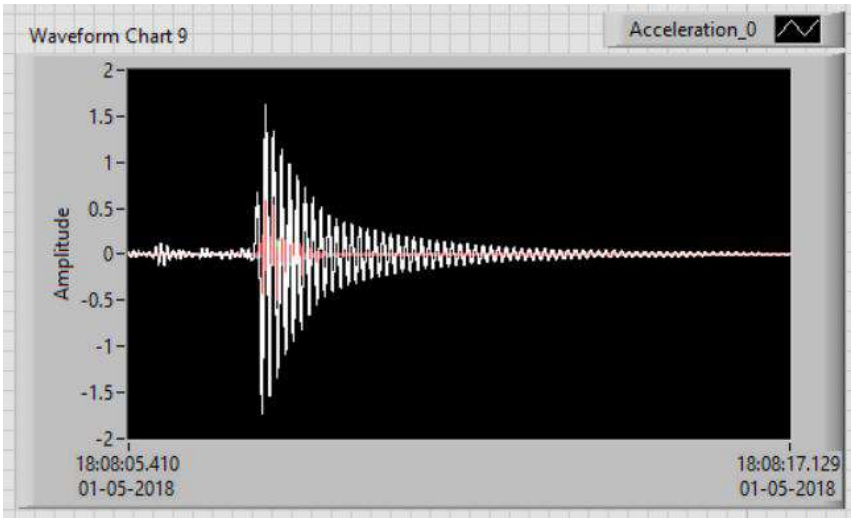

Figure 5.20: Acceleration Response of Single Story building model with Planar Irregularity of T-Shape Undergoing Free Vibration

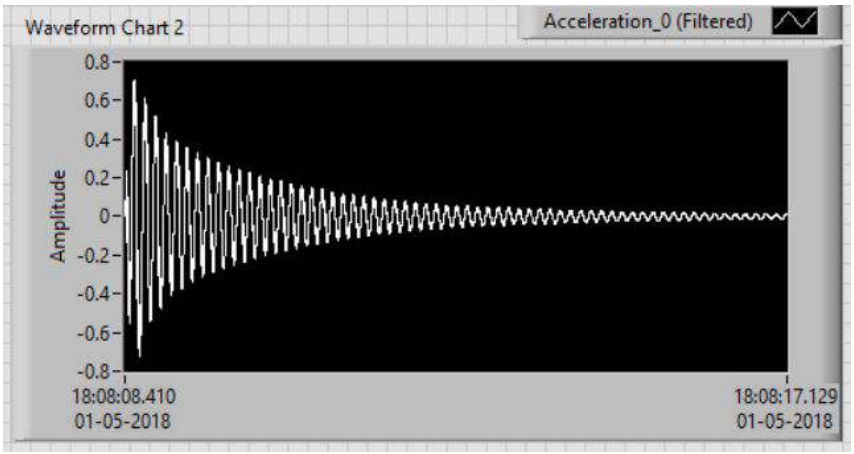

Figure 5.21: Extracted Acceleration Response of Single Story building model with Planar Irregularity of T-Shape Undergoing Free Vibration

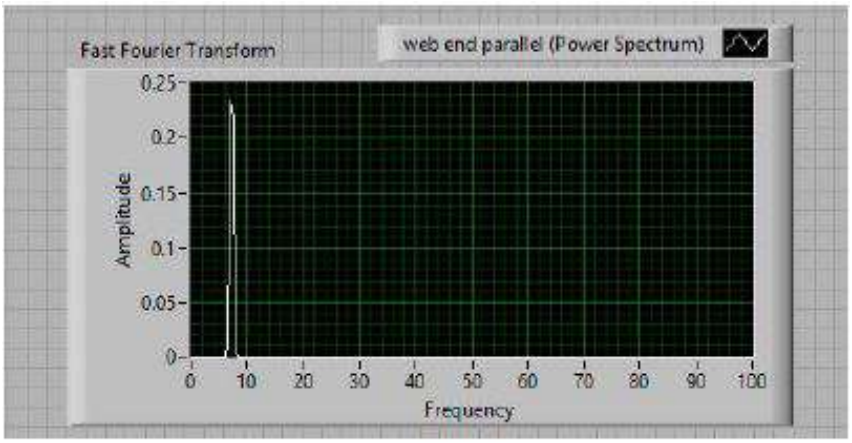

Figure 5.22: Fundamental Frequency Extraction for SDOF Building Model with Planar Irregularity of T-Shape Through Fast Fourier Transform Techniques

After getting Acceleration Response of building model, Fast Fourier Transform can be produced in LabVIEW software. It is shown in Figure 5.22. Natural Frequency of the structure is 7.14 Hz. After capturing the Natural frequency of the structure Coefficient of damping is evaluated using Logarithmic Decrement method and is found out to be 1.63%.

Table 5.7: Calculation of damping ratio (ζ) from logarithmic decrement method for building model with Planar Irregularity of T-Shape

Peak	Amplitude	Number of consecutive cycles								
0	0.706	2.223	2.435	2.607	2.342	2.172	2.035	1.932	1.848	1.774
1	0.614	2.646	2.799	2.382	2.159	1.997	1.883	1.794	1.57	
2	0.52	2.952	2.25	1.996	1.834	1.731	1.652	1.416		
3	0.432	1.547	1.518	1.462	1.425	1.313	1.16			
4	0.392	1.489	1.419	1.384	1.258	1.08				
5	0.357	1.349	1.332	1.176	0.981					
6	0.328	1.315	1.09	0.858						
7	0.302	0.0866	0.631							
8	0.286	0.395								
9	0.279									

5.5 Forced Vibration Test on Asymmetric Structural System

The earthquake response of building frames that are asymmetric in plan is characterized by coupling between transnational and torsional degree of freedom(dofs).The present experiment is done to understand the dynamics of the frame as the frequency of base motion is varied across the resonant frequencies of the frame and tried to understand the influence of the angle of incidence of the base motion on the dynamic response of the frame.

5.5.1 One Storey Building Model Frame with Material Irregularity

As explained in the Chapter 3 [3.4] Mass matrix, Stiffness Matrix has been formulated below and by using Eigen value analysis, Natural Frequency of the system has been found below.

Mass Matrix in Kg is generated as below

$$M = \begin{bmatrix} 1.634 & 0 & 0 \\ 0 & 1.634 & 0 \\ 0 & 0 & 0.01946 \end{bmatrix}$$

Stiffness matrix in N/m is generated as below.

$$K = \begin{bmatrix} 3788.698 & 0 & 64.582 \\ 0 & 263104.045 & -9787.6404 \\ 64.583 & -9787.641 & 5579.427 \end{bmatrix}$$

Natural Frequency in Hz can be obtained by Eigen value analysis.

$$\omega_n = \begin{bmatrix} 7.664 \\ 59.649 \\ 88.232 \end{bmatrix}$$

5.5.1.1 Experimental Setup of the One Storey Building Model Frame with Material Irregularity

The building frame is mounted on the electric motor driven shake table in which By varying the speed of the motor the frequency of the harmonic base motion could be varied , also the mounting device is capable of swiveling about the vertical axis, which would permit us to mount the frame at different angles relative to the axis of the base motion. Figure 5.23 shows experimental setup for one storey building frame.

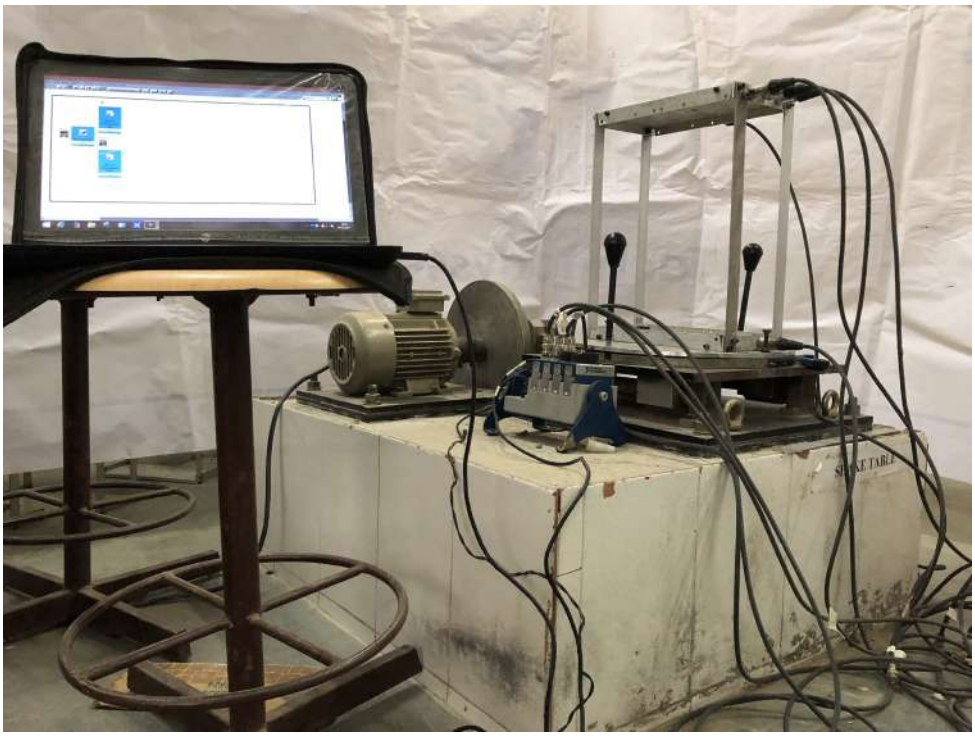

Figure 5.23: Experimental setup for one storey asymmetric building frame

5.5.1.2 Studies with Fixed Angle of Incidence of Base Motion ($\alpha = 0$)

The base motion test is run on the frame at different values of frequency making sure that readings at resonant frequencies are not missed , for a given motion frequency the frame is allowed to oscillate for a few seconds.

With the help of labview software we were able to transform the acceleration measured from accelerometer to displacement from which we were able to capture the responses in X,Y and θ, we have applied integration to the acceleration response but it has to be made sure to apply filter before applying the integration as mentioned in the literature review by Slifka D.L [5], and then the measured value was compared theoretically from the Equation give in Chapter [3.5] Dynamic Response Solution of Asymmetric Structural System .

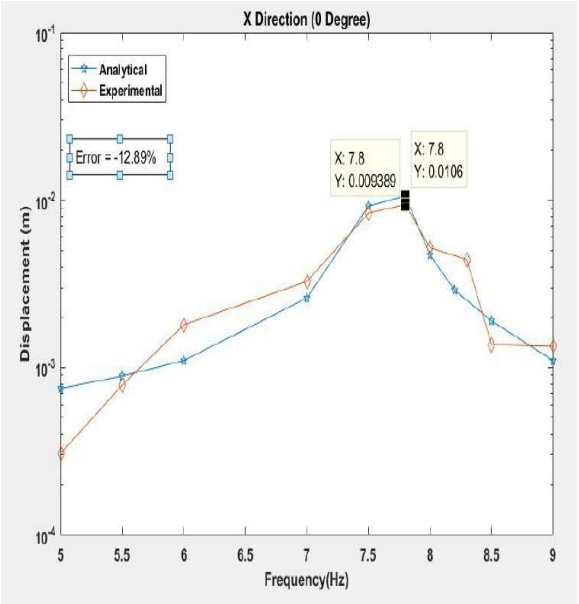

(a) Response of Material irregular SDOF model in X Direction

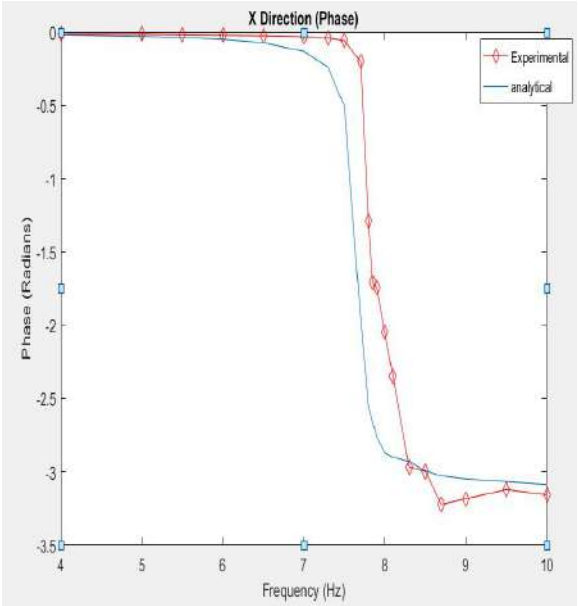

(b) Phase Spectra Material irregular SDOF model in X Direction

Figure 5.24: Comparison of Amplitude Spectra and Phase Spectra in X- Direction

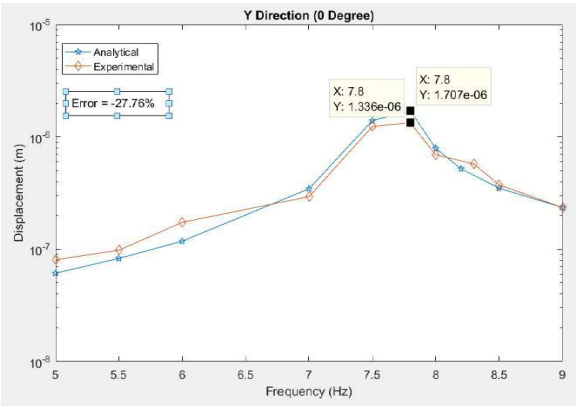

(a) Response of Material irregular SDOF model in Y Direction

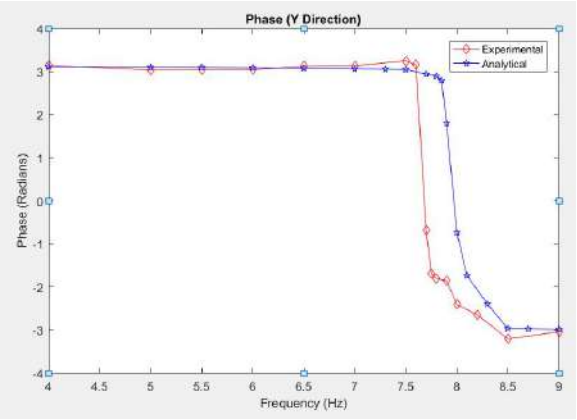

(b) Phase Spectra Material irregular SDOF model in Y Direction

Figure 5.25: Comparison of Amplitude Spectra and Phase Spectra in Y- Direction

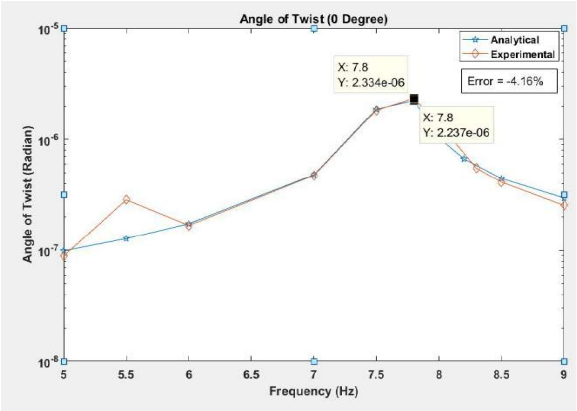

(a) Response of Material irregular SDOF model in θ Direction

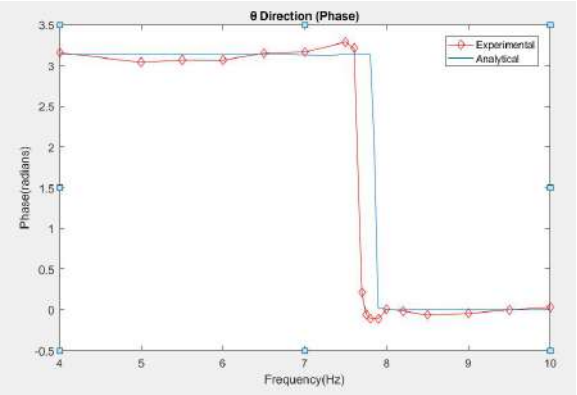

(b) Phase Spectra Material irregular SDOF model in θ Direction

Figure 5.26: Comparison of Amplitude Spectra and Phase Spectra in θ- Direction

In the above section we have made an attempt to experimentally derive the response of the planar asymmetry one storied building frame and then were able to compare it with the responses obtained analytically , and it is also observed that when the building frame reaches Resonance there is a shift in phase which is clearly visible in the response graphs obtained from both analytical and experimental results.

5.5.1.3 Studies with Varying Angle of Incidence of Base Motion

In this section we have tried to understand the influence of angle of incidence on the response of the motion of the SDOF building model with material irregularity.

Here we hold the motor RPM fixed and vary angle of incidence of the base motion by mounting the frame on the table at a desired angle in the range of 0 to $\pi/2$.

Comparison of Analytical and experimental results are done and the results are compared in the following figures, Analytical results has been explained in Chapter 3 3.5 Dynamic Response Solution of Asymmetric Structural System and are compared with the experimental results as explained above.
Response in X Y and θ directions are captured in labVIEW and determined analytically which are shown in the graphs below

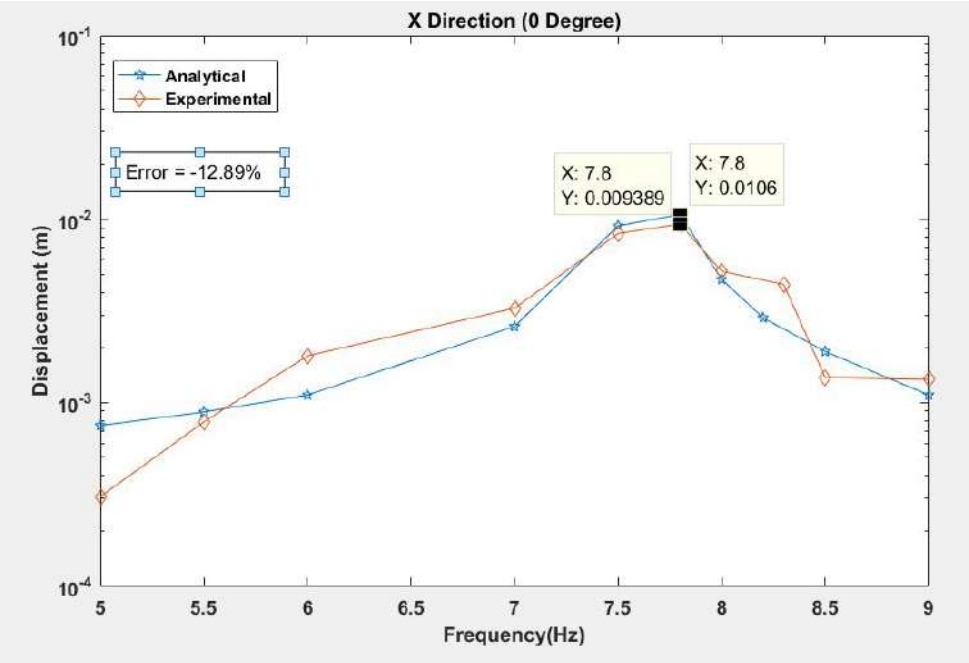

Figure 5.27: Response of SDOF building model with Material irregularity in X Direction along α= 0 degree

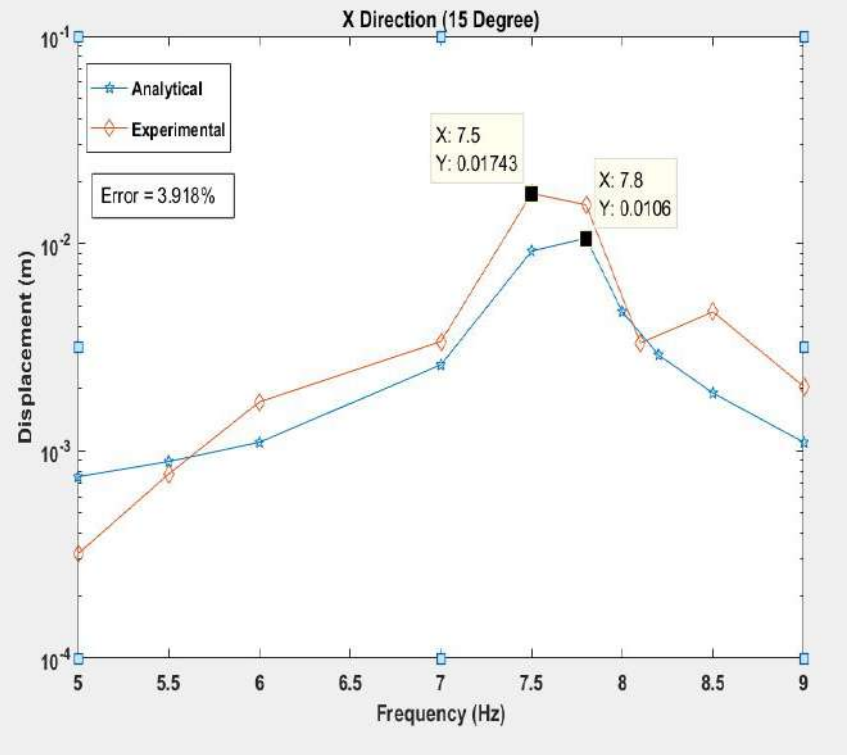

Figure 5.28: Response of SDOF building model with Material irregularity in X Direction along $\alpha = 15$ degree

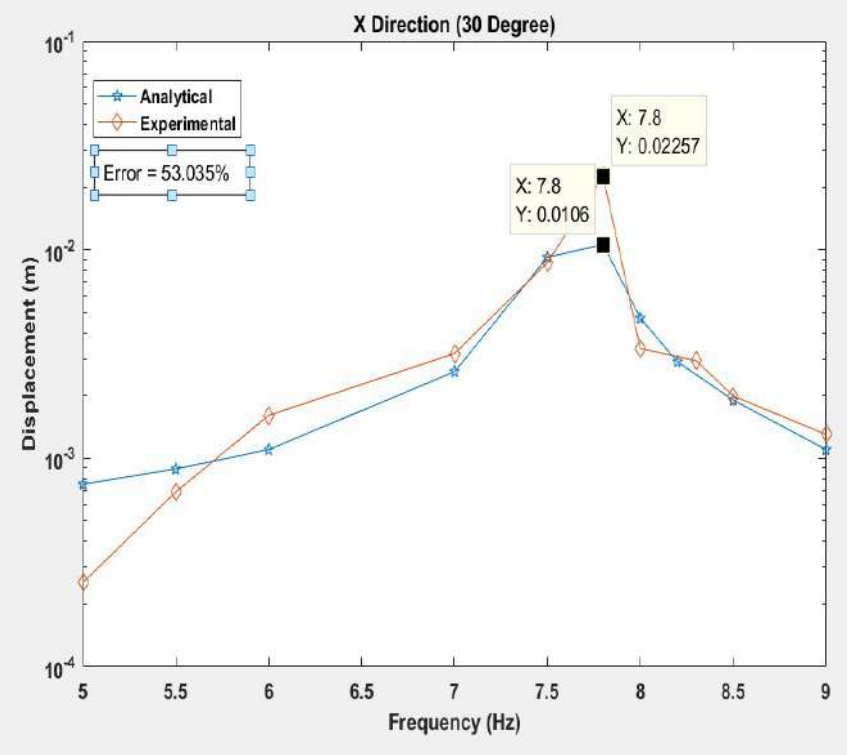

Figure 5.29: Response of SDOF building model with Material irregularity in X Direction along $\alpha = 30$ degree

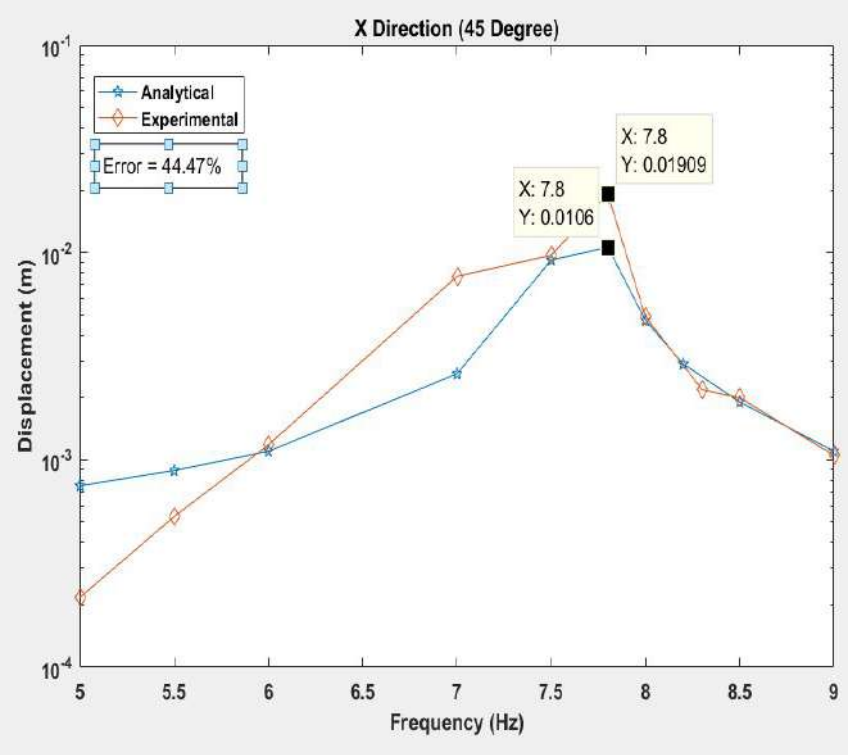

Figure 5.30: Response of SDOF building model with Material irregularity in X Direction along $\alpha = 45$ degree

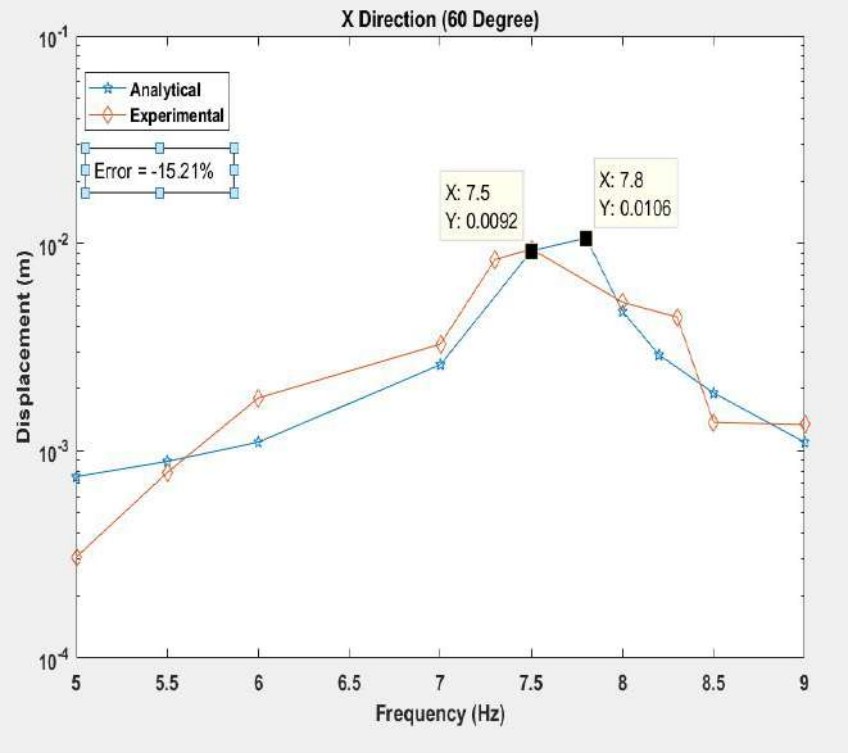

Figure 5.31: Response of SDOF building model with Material irregularity in X Direction along $\alpha = 60$ degree

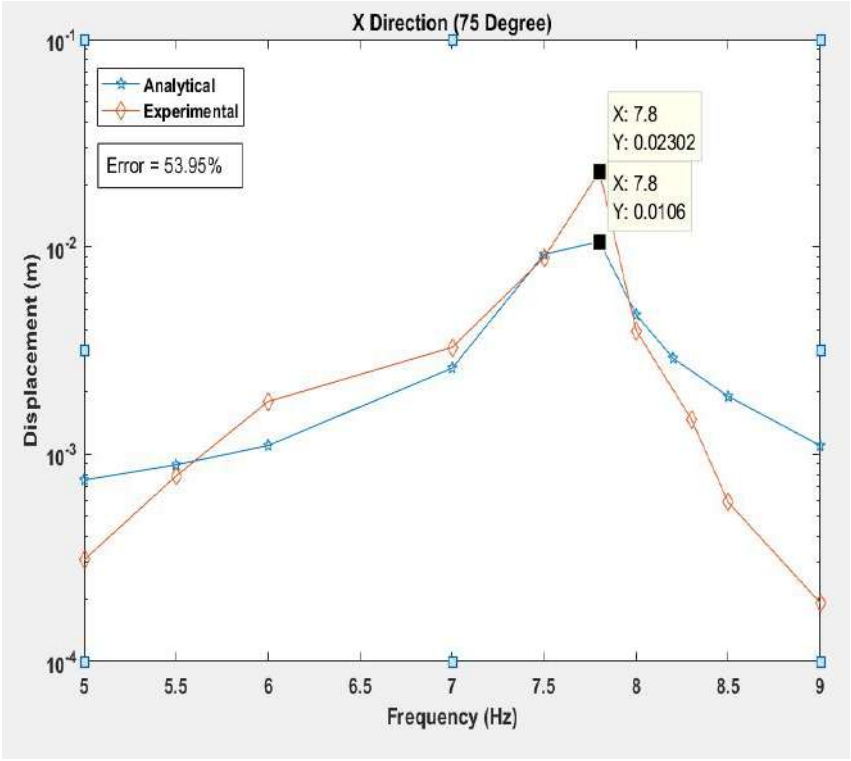

Figure 5.32: Response of SDOF building model with Material irregularity in X Direction along $\alpha = 75$ degree

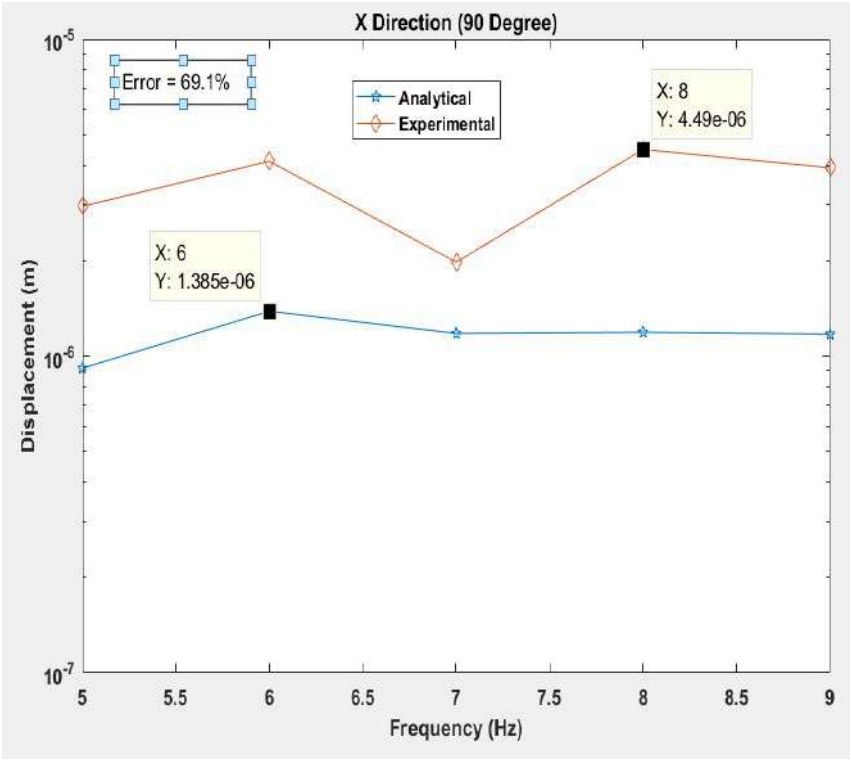

Figure 5.33: Response of SDOF building model with Material irregularity in X Direction along $\alpha = 90$ degree

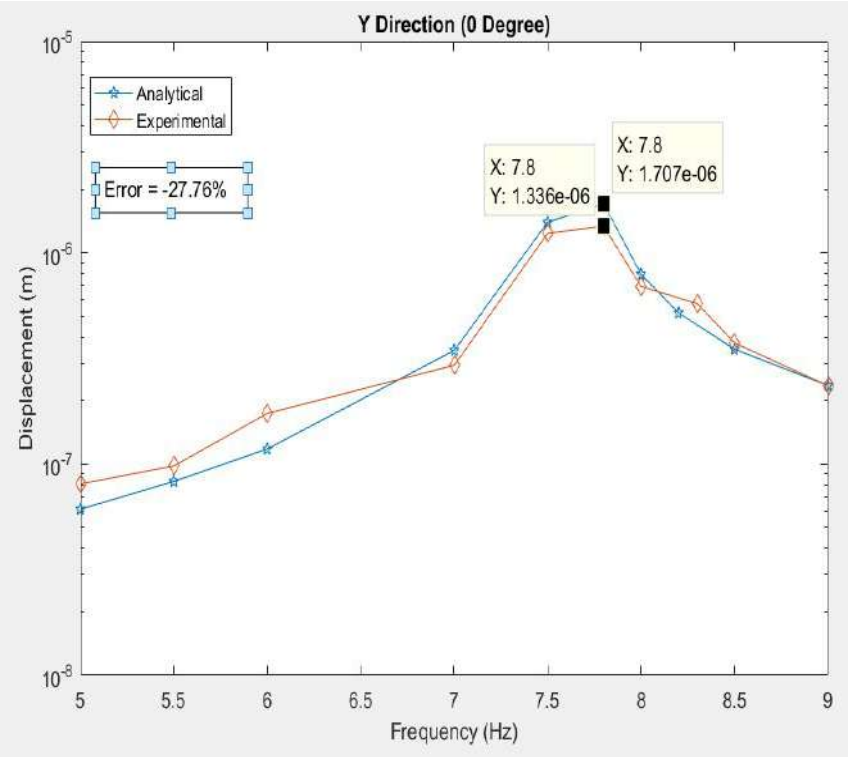

Figure 5.34: Response of SDOF building model with Material irregularity in Y Direction along $\alpha = 0$ degree

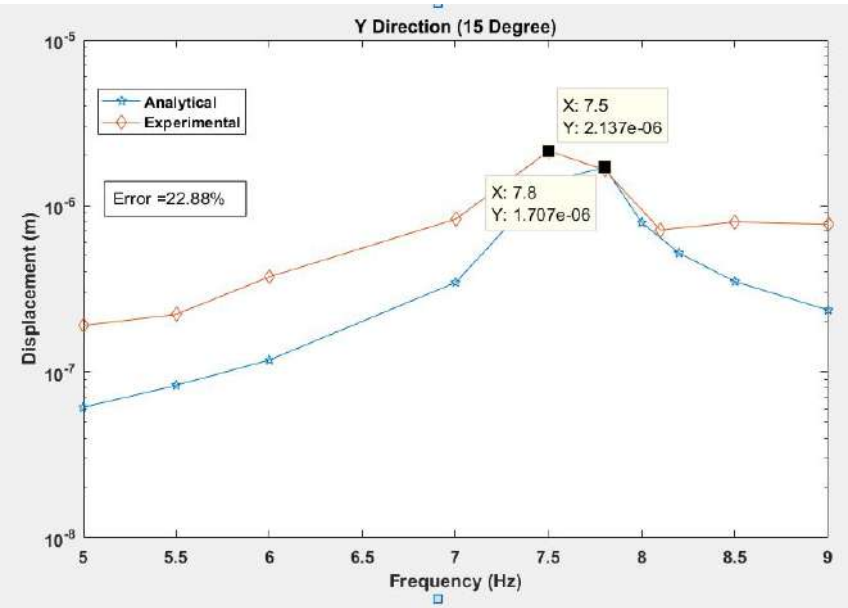

Figure 5.35: Response of SDOF building model with Material irregularity in Y Direction along $\alpha = 15$ degree

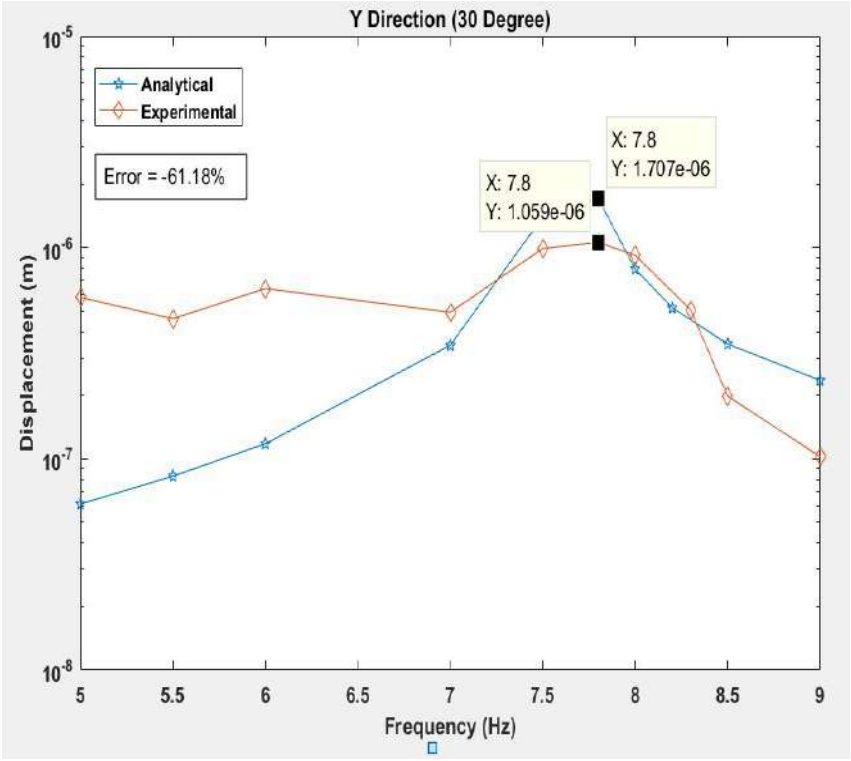

Figure 5.36: Response of SDOF building model with Material irregularity in Y Direction along $\alpha = 30$ degree

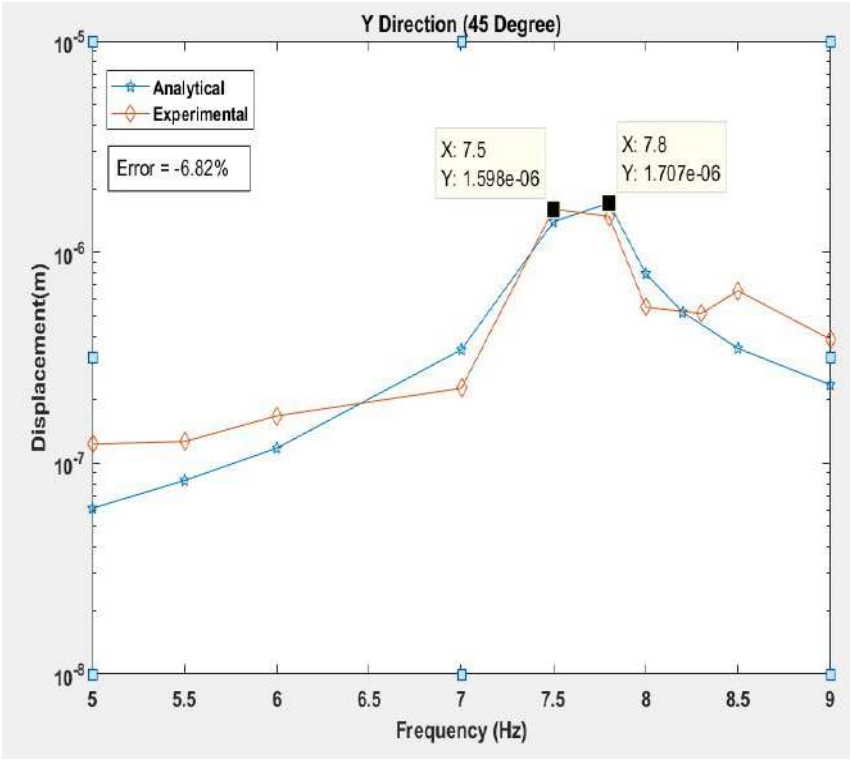

Figure 5.37: Response of SDOF building model with Material irregularity in Y Direction along $\alpha = 45$ degree

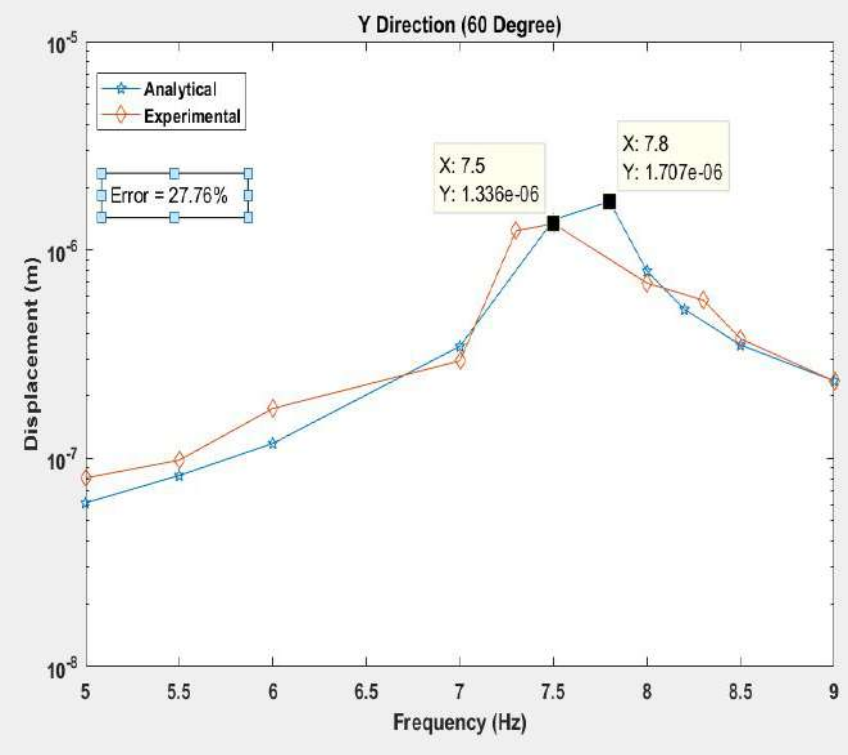

Figure 5.38: Response of SDOF building model with Material irregularity in Y Direction along $\alpha = 60$ degree

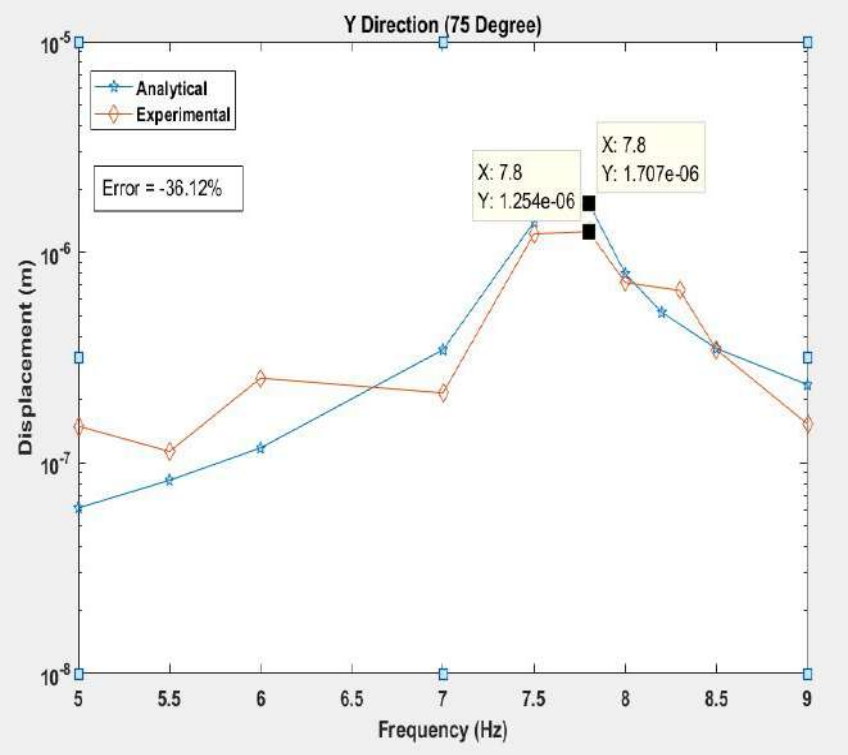

Figure 5.39: Response of SDOF building model with Material irregularity in Y Direction along $\alpha = 75$ degree

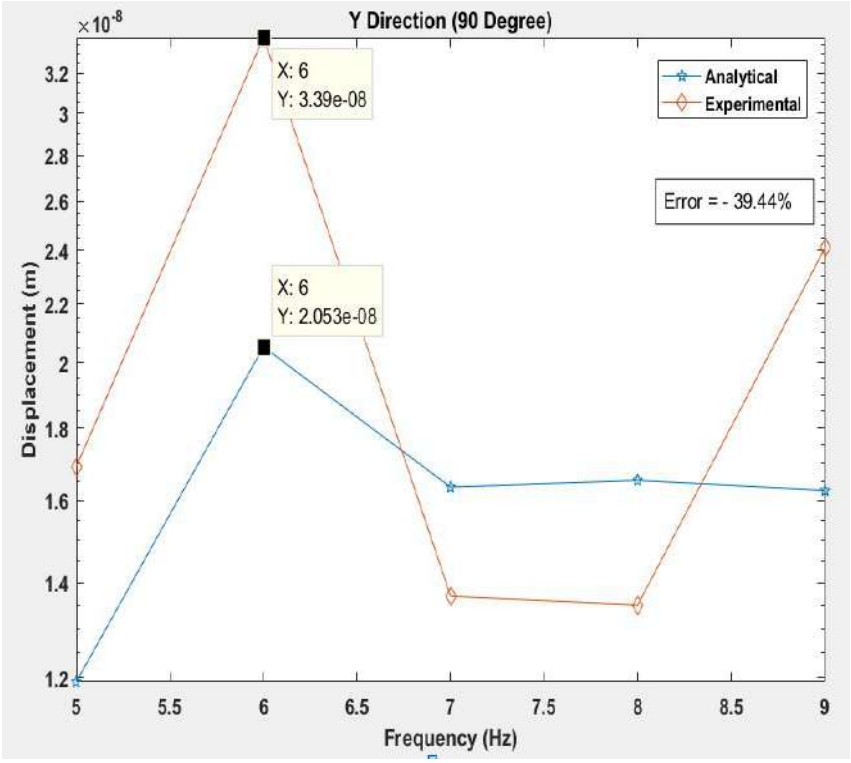

Figure 5.40: Response of SDOF building model with Material irregularity in Y Direction along $\alpha = 90$ degree

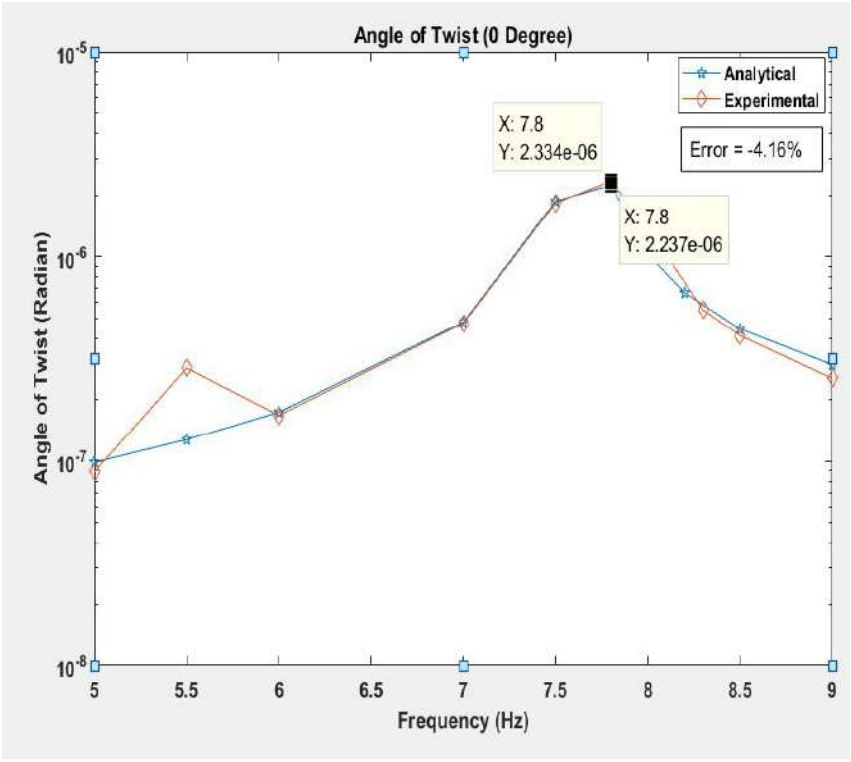

Figure 5.41: Response of SDOF building model with Material irregularity in θ Direction along $\alpha = 0$ degree

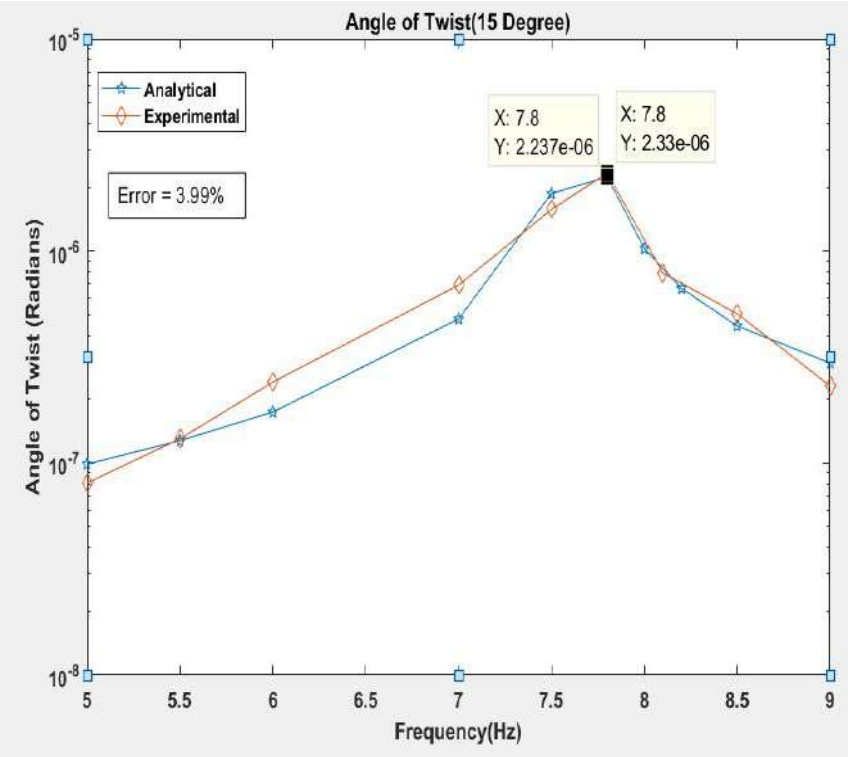

Figure 5.42: Response of SDOF building model with Material irregularity in θ Direction along $\alpha = 15$ degree

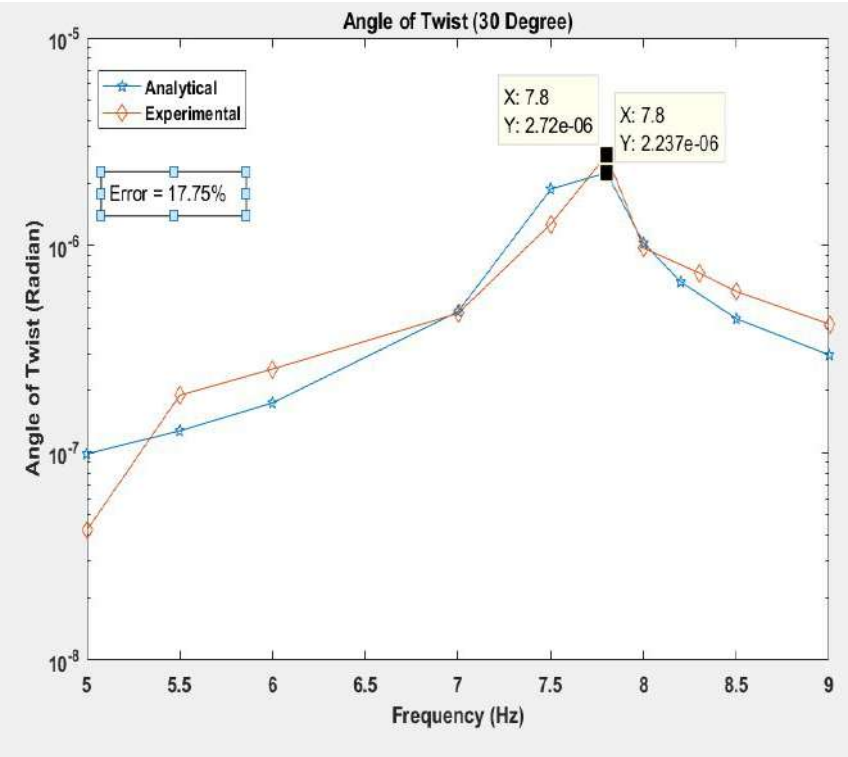

Figure 5.43: Response of SDOF building model with Material irregularity in θ Direction along $\alpha = 30$ degree

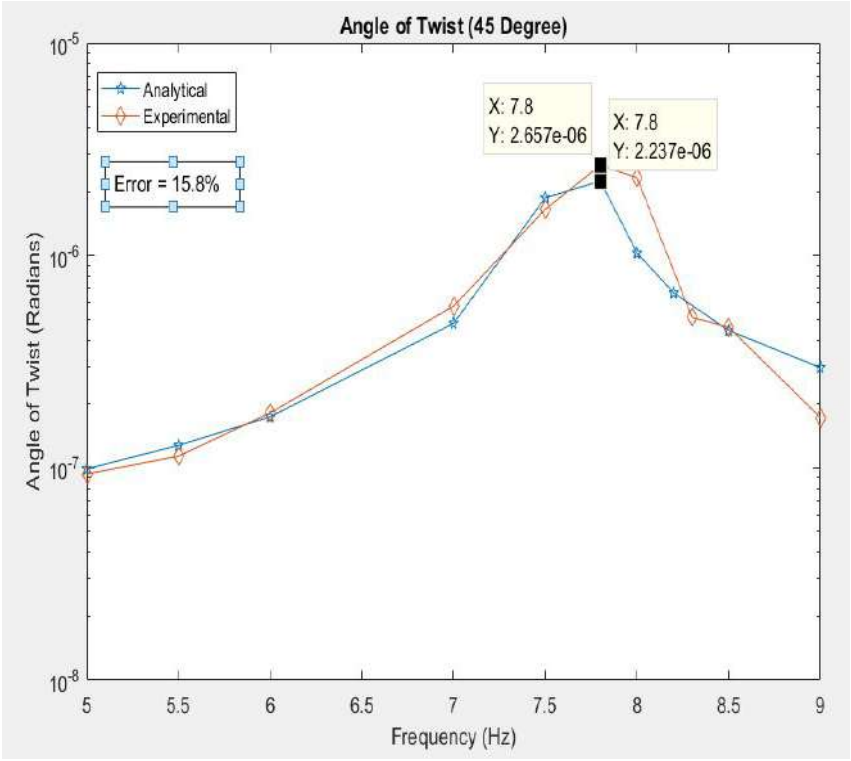

Figure 5.44: Response of SDOF building model with Material irregularity in θ Direction along $\alpha = 45$ degree

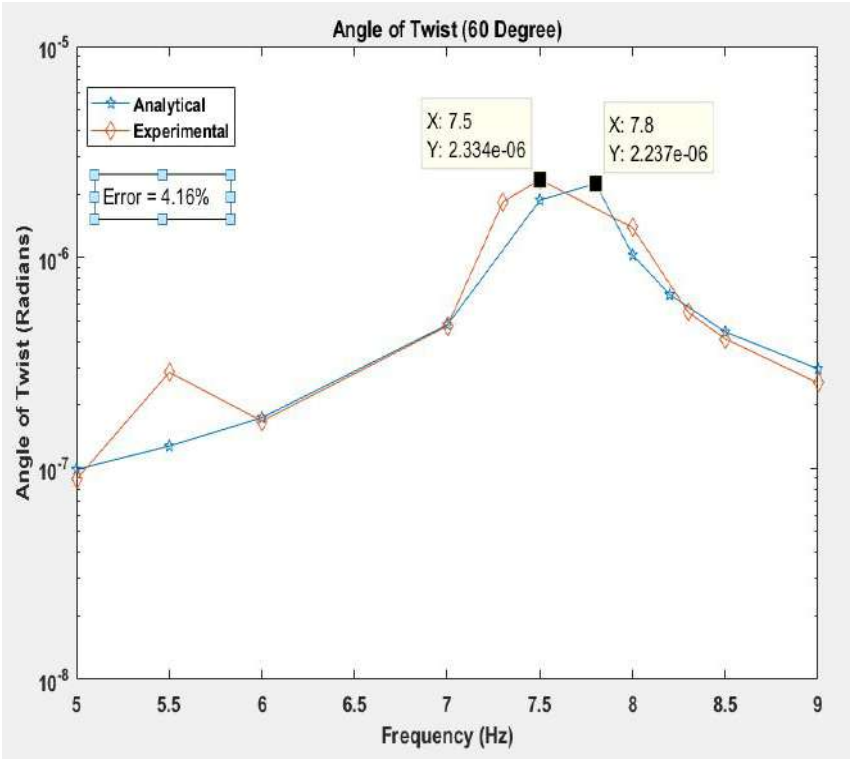

Figure 5.45: Response of SDOF building model with Material irregularity in θ Direction along $\alpha = 60$ degree

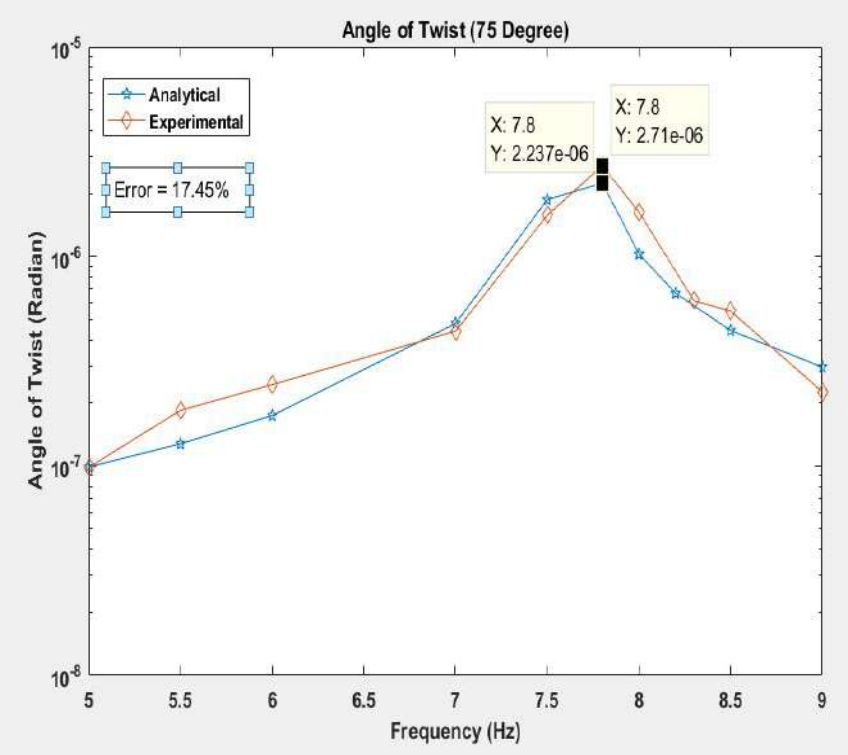

Figure 5.46: Response of SDOF building model with Material irregularity in θ Direction along $\alpha = 75$ degree

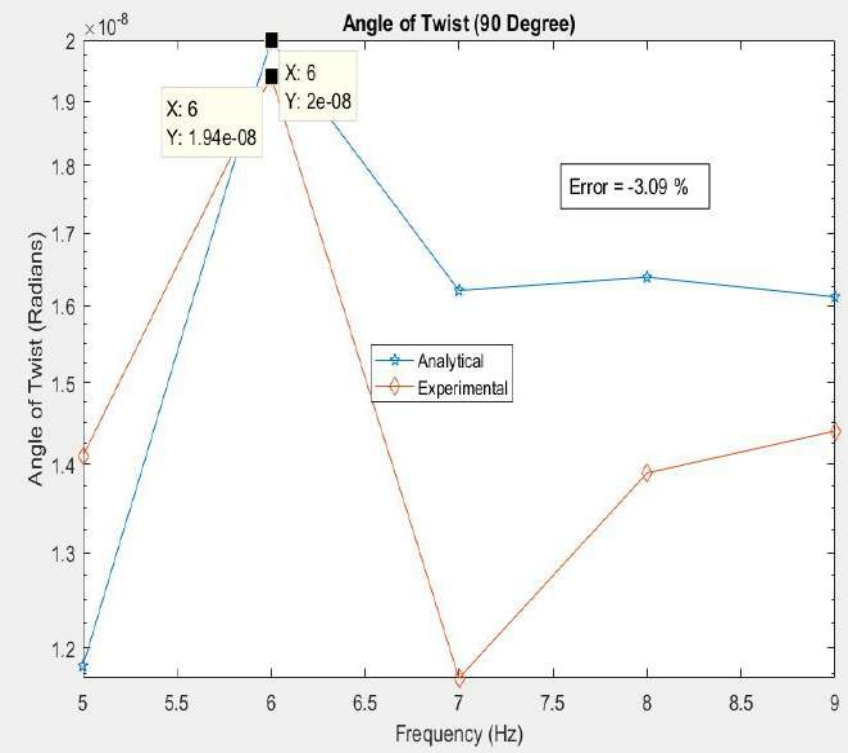

Figure 5.47: Response of SDOF building model with Material irregularity in θ Direction along $\alpha = 90$ degree

Table 5.8: Response for building model with Material Irregularity in X Direction

Angle of Incident (Degree)	Analytical Frequency (Hz)	X analytical (m)	Experimental Frequency (Hz)	X experimental (m)	Error %
0	7.8	0.0106	7.8	0.00939	-12.89
15	7.8	0.0106	7.5	0.0174	3.92
30	7.8	0.0106	7.8	0.0226	53.03
45	7.8	0.0106	7.8	0.01909	44.47
60	7.8	0.0106	7.5	0.0092	-15.21
75	7.8	0.0106	7.8	0.023	53.95
90	6	4.49×10^{-6}	8	1.385×10^{-6}	69.1

Table 5.9: Response for building model with Material Irregularity in Y Direction

Angle of Incident (Degree)	Analytical Frequency (Hz)	Y analytical (m)	Experimental Frequency (Hz)	Y experimental (m)	Error %
0	7.8	1.707×10^{-6}	7.8	1.336×10^{-6}	-27.7
15	7.8	1.707×10^{-6}	7.5	2.137×10^{-6}	22.88
30	7.8	1.707×10^{-6}	7.8	1.059×10^{-6}	-61.18
45	7.8	1.707×10^{-6}	7.5	1.598×10^{-6}	-6.82
60	7.8	1.707×10^{-6}	7.5	1.336×10^{-6}	27.76
75	7.8	1.707×10^{-6}	7.8	1.254×10^{-6}	-36.12
90	6	2.053×10^{-8}	8	3.39×10^{8}	-39.44

Table 5.10: Response for building model with Material Irregularity in θ Direction

Angle of Incident (Degree)	Analytical Frequency (Hz)	θ analytical (radians)	Experimental Frequency (Hz)	θ experimental (radians)	Error %
0	7.8	2.237×10^{-6}	7.8	2.334×10^{-6}	-4.16
15	7.8	2.237×10^{-6}	7.8	2.33×10^{-6}	3.99
30	7.8	2.237×10^{-6}	7.8	2.72×10^{-6}	17.57
45	7.8	2.237×10^{-6}	7.8	2.657×10^{-6}	15.8
60	7.8	2.237×10^{-6}	7.5	2.334×10^{-6}	4.16
75	7..8	2.237×10^{-6}	7.8	2.71×10^{-6}	17.4
90	6	2×10^{-8}	8	1.94×10^{-8}	-3.09

5.5.2 One Storey Building Model Frame with T Planar Geometry

As explained in the Chapter 3 [3.4] Mass matrix, Stiffness Matrix has been formulated below and by using Eigen value analysis, Natural Frequency of the system has been found below.

mass matrix in Kg can be written as below

$$M = \begin{bmatrix} 1.963 & 0 & 0 \\ 0 & 1.963 & 0 \\ 0 & 0 & 0.02878 \end{bmatrix}$$

Stiffness matrix in N/m is generated as below.

$$K = \begin{bmatrix} 3853.86 & 0 & 125.235 \\ 0 & 267629.16 & 0 \\ 125.235 & 0 & 6355.712 \end{bmatrix}$$

Natural Frequency in Hz can be obtained by Eigen value analysis.

$$\omega_n = \begin{bmatrix} 7.049 \\ 58.76 \\ 74.79 \end{bmatrix}$$

5.5.2.1 Experimental Setup of the One Storey Building Model Frame with T Planar Geometry

Similar to the above setup the T Shape Planar Asymmetry building frame is mounted on the electric motor driven shake table in which By varying the speed of the motor the frequency of the harmonic base motion could be varied , also the mounting device is capable of swiveling about the vertical axis, which would permit us to mount the frame at different angles relative to the axis of the base motion. Figure 5.48 shows experimental setup for one storey building frame.

Figure 5.48: Experimental Setup of Building model having planar irregularity T-Shape

5.5.2.2 Studies with Fixed Angle of Incidence of Base Motion ($\alpha = 0$)

The base motion test is run on the frame at different values of frequency making sure that readings at resonant frequencies are not missed , for a given motion frequency the frame is allowed to oscillate for a few seconds.With the help of labview software we were able to tranform the acceleration measured from accelerometer to displacement from which we were able to capture the responses in X,Y and θ, we have applied integration to the acceleration response but it has to be made sure to apply filter before applying the integration as mentioned in the literature review by Slifka D.L [5], and then the measured value was compared theoretically from the Equation give in Chapter [3.5] .

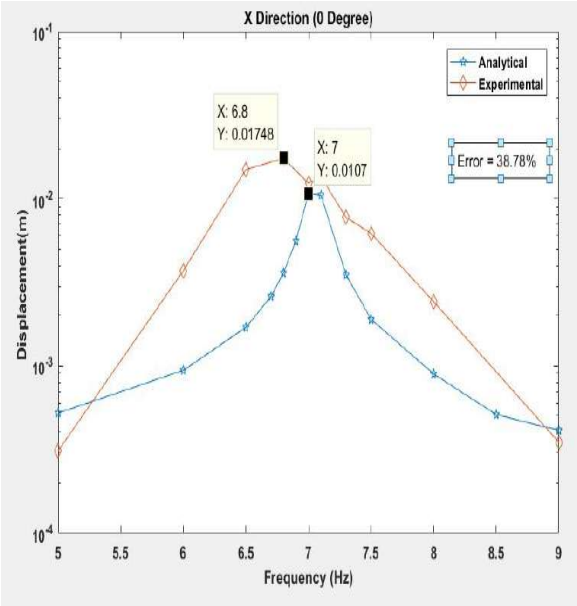

(a) Response of SDOF model with Planar Asymmetry T-Shape in X Direction

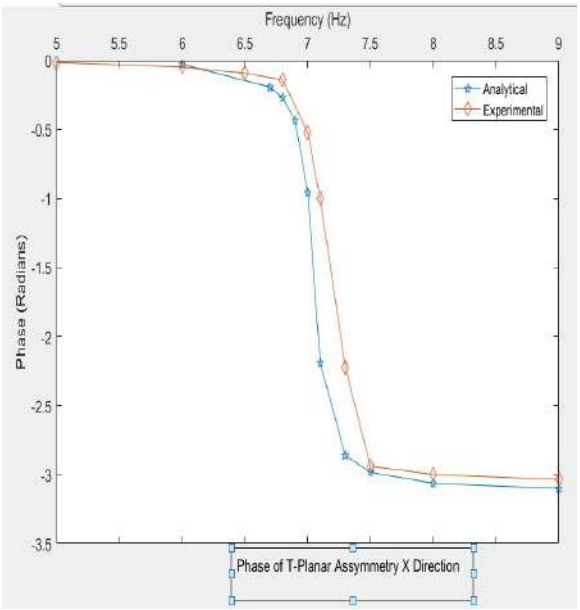

(b) Phase spectra of SDOF model with Planar Asymmetry T-Shape in X Direction

Figure 5.49: Comparison of Amplitude Spectra and Phase Spectra in X- Direction

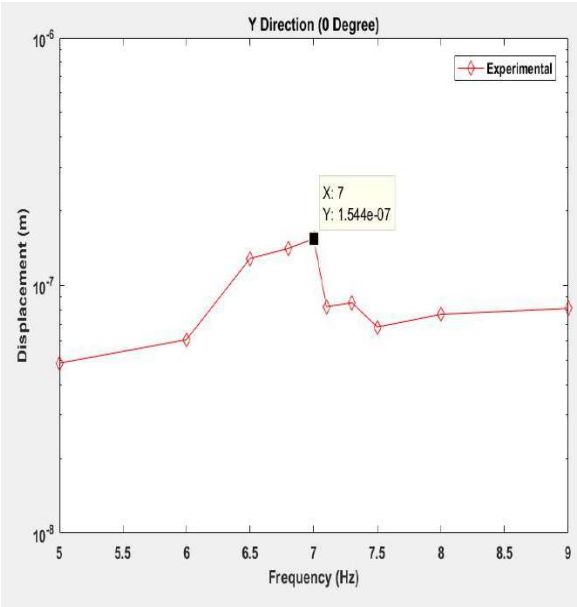

(a) Response of SDOF model with Planar Asymmetry T-Shape in Y Direction

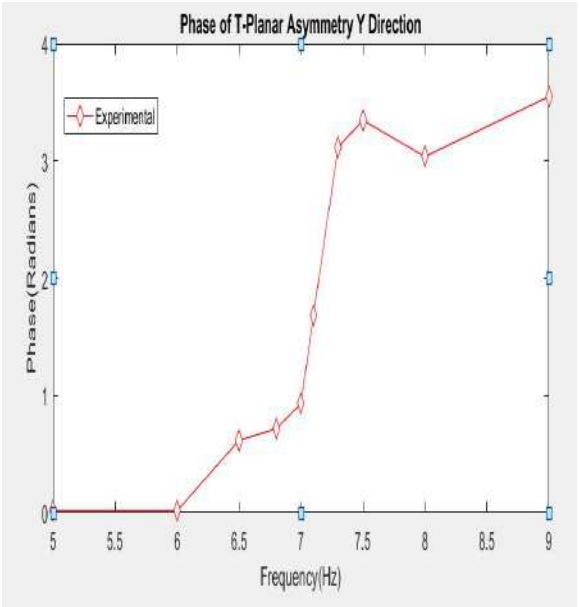

(b) Phase spectra of SDOF model with Planar Asymmetry T-Shape in Y Direction

Figure 5.50: Comparison of Amplitude Spectra and Phase Spectra in θ- Direction

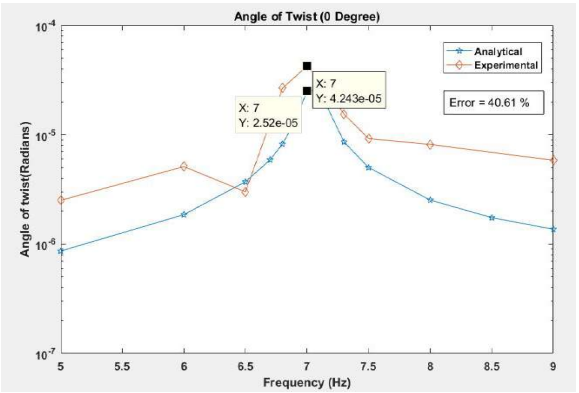

(a) Response of SDOF model with Planar Asymmetry T-Shape in θ Direction

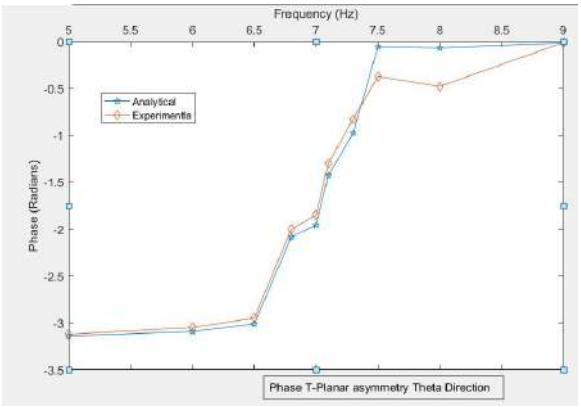

(b) Phase spectra of SDOF model with Planar Asymmetry T-Shape in θ Direction

Figure 5.51: Comparison of Amplitude Spectra and Phase Spectra in θ- Direction

5.5.2.3 Studies with Varying Angle of Incidence of Base Motion

Here we hold the motor RPM fixed and vary angle of incidence of the base motion by mounting the frame on the table at a desired angle in the range of 0 to $\pi/2$.
Response in X Y and θ directions are captured in labVIEW and determined analytically which are shown in the graphs below.

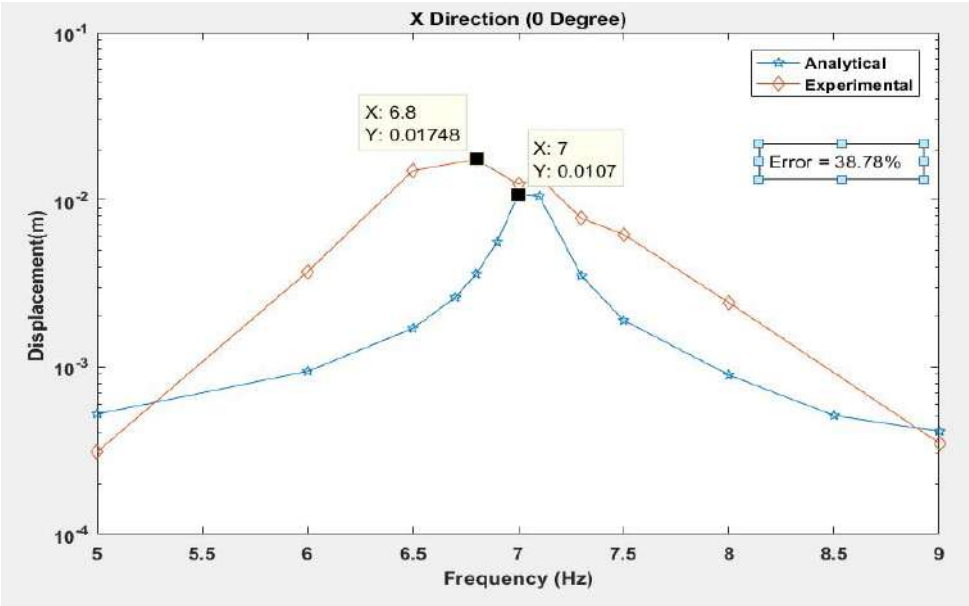

Figure 5.52: Response of SDOF building model with Planar irregularity T-Shape in X Direction along $\alpha = 0$ degree

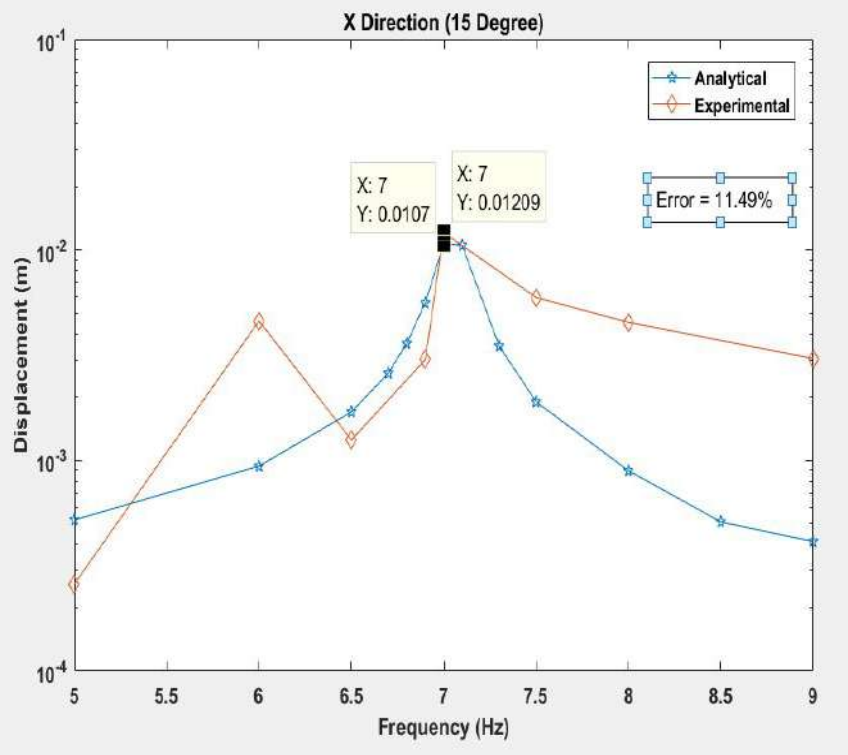

Figure 5.53: Response of SDOF building model with Planar irregularity T-Shape in X Direction along $\alpha = 15$ degree

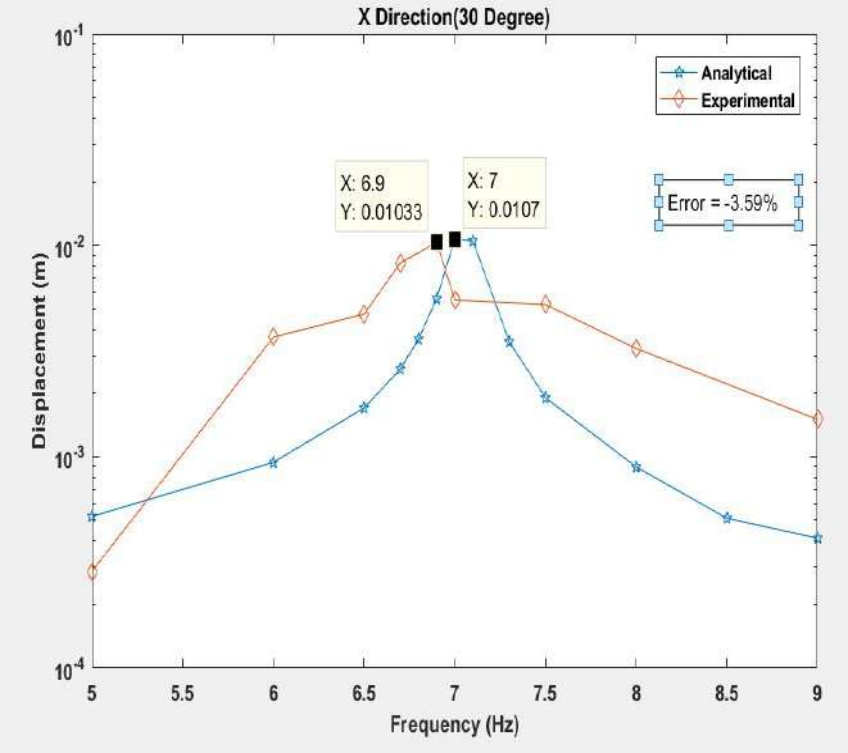

Figure 5.54: Response of SDOF building model with Planar irregularity T-Shape in X Direction along $\alpha = 30$ degree

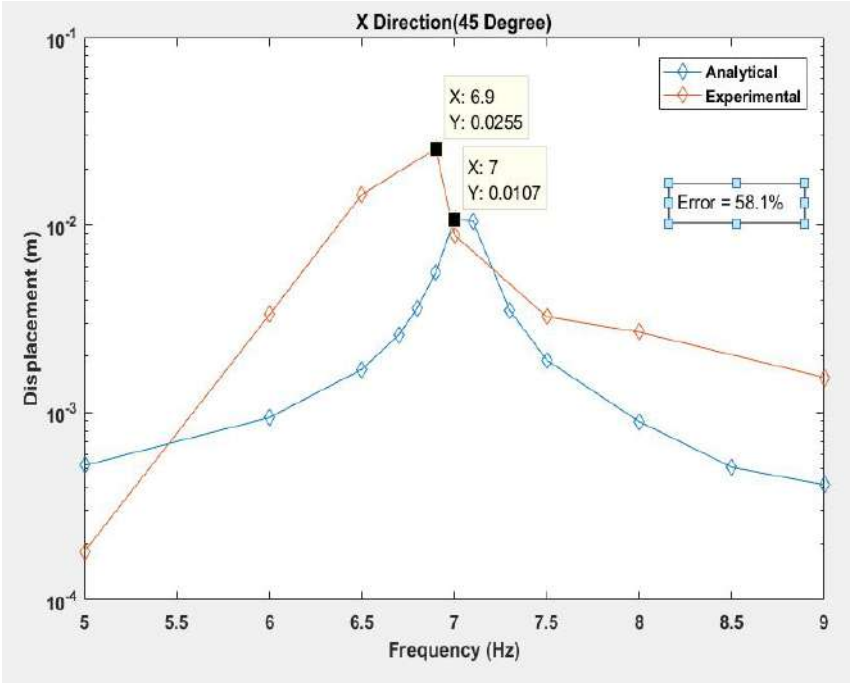

Figure 5.55: Response of SDOF building model with Planar irregularity T-Shape in X Direction along $\alpha = 45$ degree

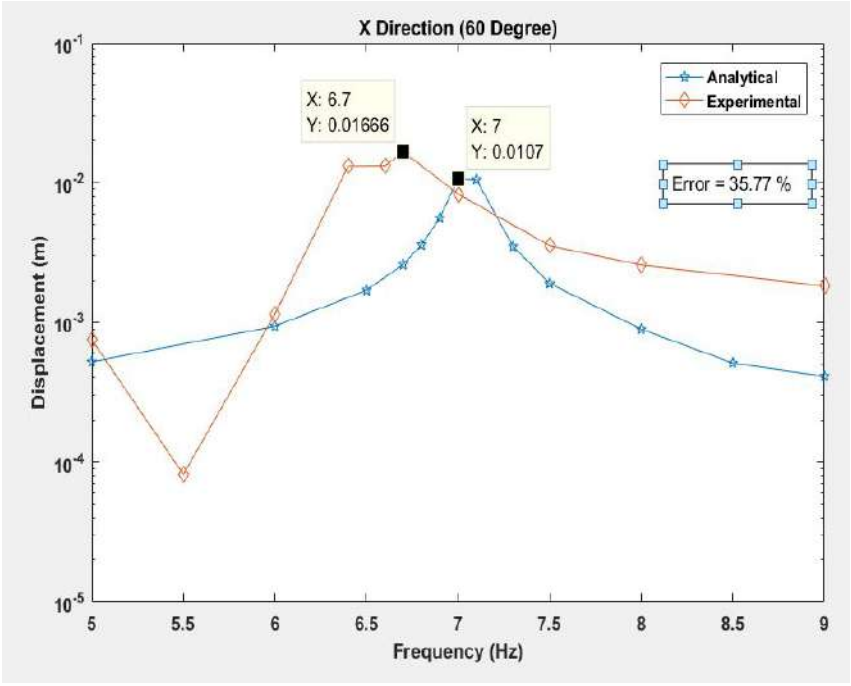

Figure 5.56: Response of SDOF building model with Planar irregularity T-Shape in X Direction along $\alpha = 60$ degree

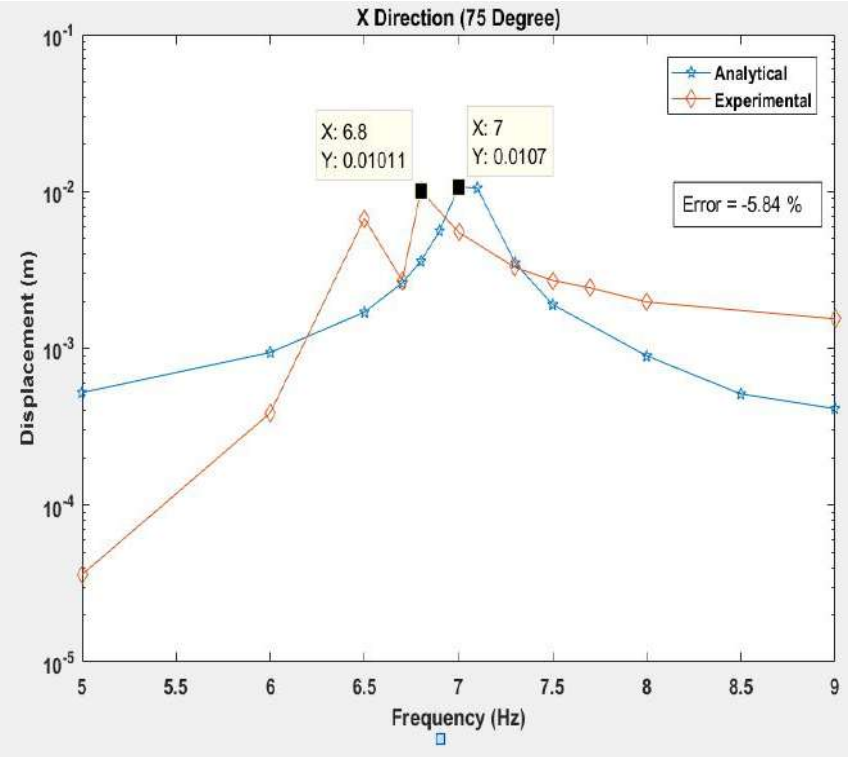

Figure 5.57: Response of SDOF building model with Planar irregularity T-Shape in X Direction along $\alpha = 75$ degree

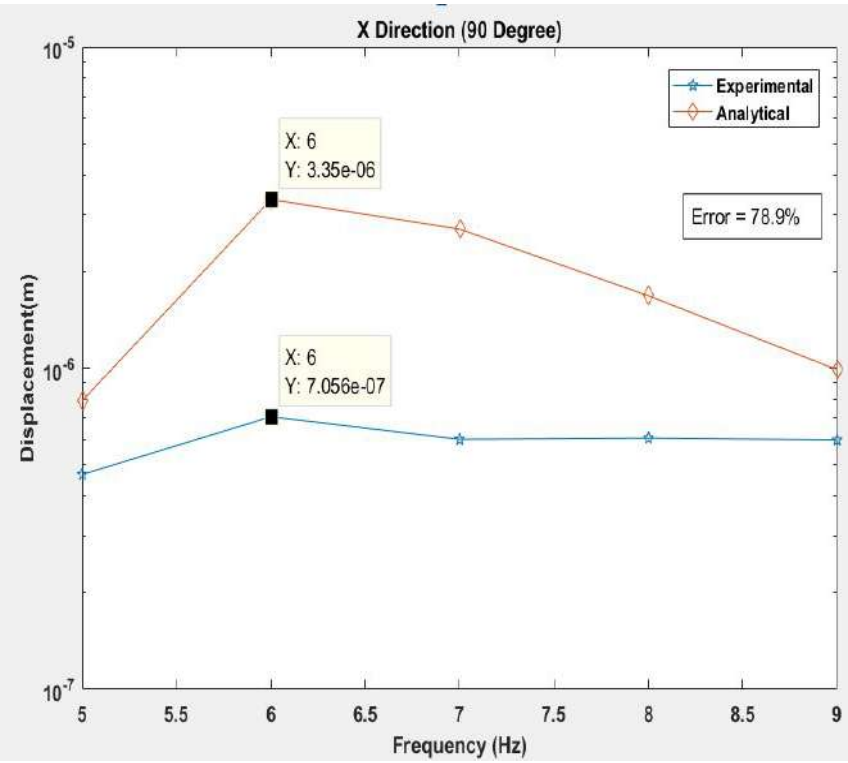

Figure 5.58: Response of SDOF building model with Planar irregularity T-Shape in X Direction along $\alpha = 90$ degree

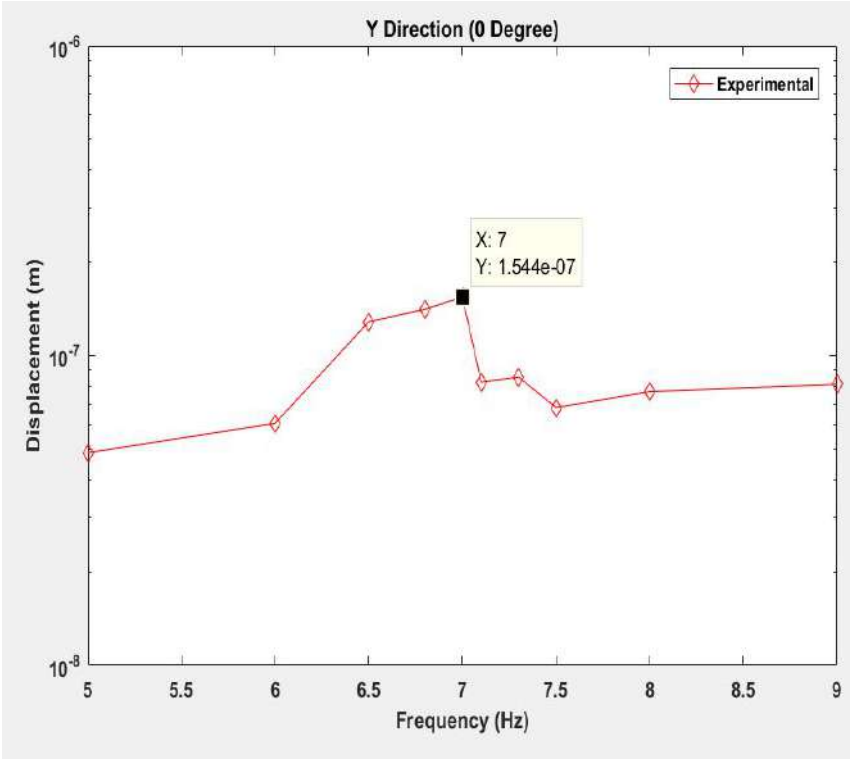

Figure 5.59: Response of SDOF building model with Planar irregularity T-Shape in Y Direction along $\alpha = 0$ degree

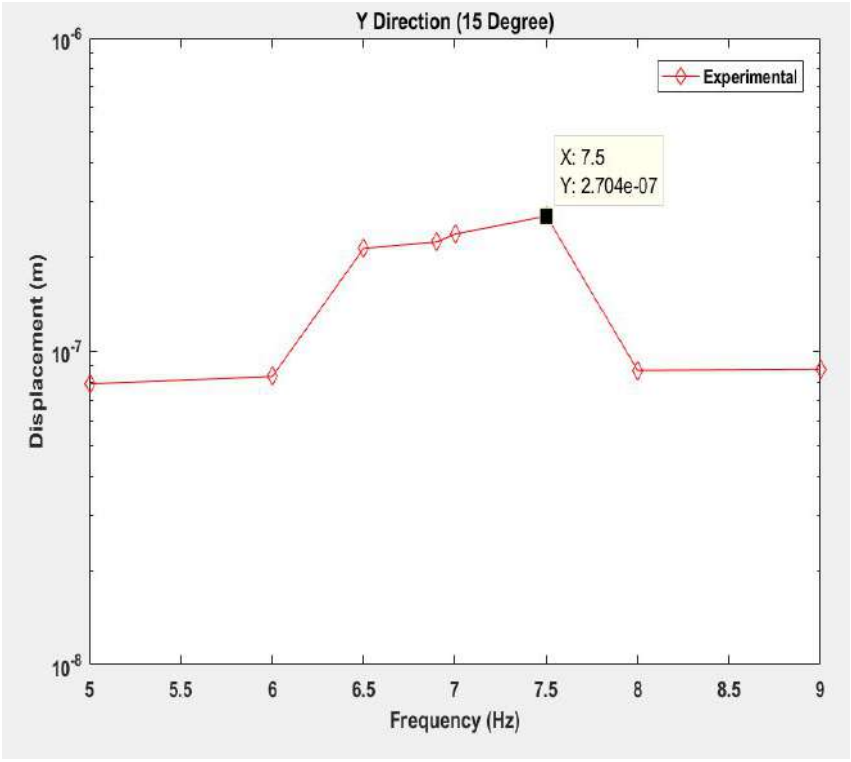

Figure 5.60: Response of SDOF building model with Planar irregularity T-Shape in Y Direction along $\alpha = 15$ degree

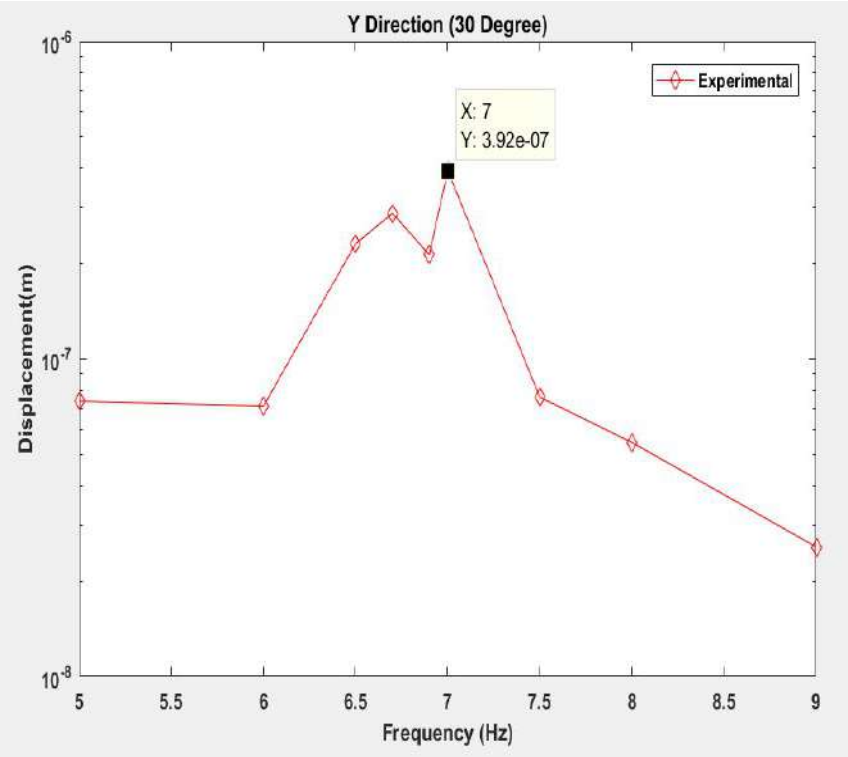

Figure 5.61: Response of SDOF building model with Planar irregularity T-Shape in Y Direction along $\alpha = 30$ degree

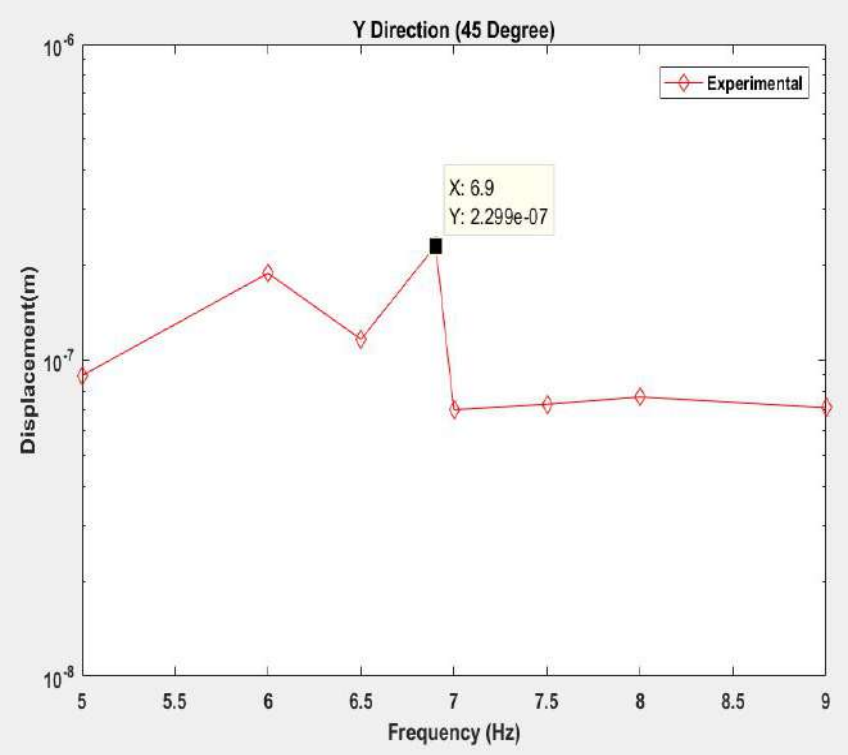

Figure 5.62: Response of SDOF building model with Planar irregularity T-Shape in Y Direction along $\alpha = 45$ degree

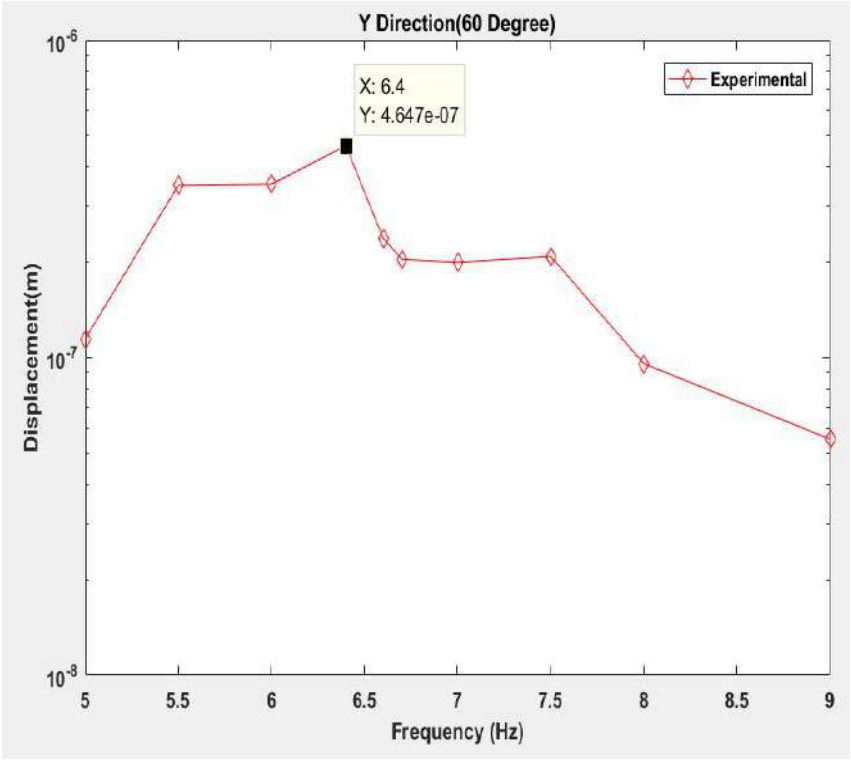

Figure 5.63: Response of SDOF building model with Planar irregularity T-Shape in Y Direction along $\alpha = 60$ degree

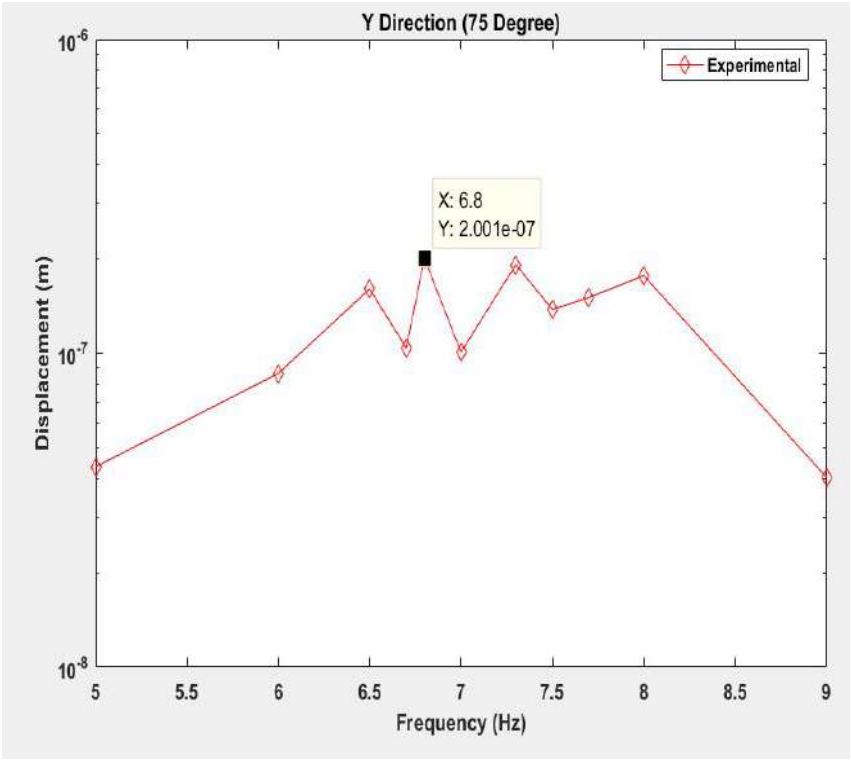

Figure 5.64: Response of SDOF building model with Planar irregularity T-Shape in Y Direction along $\alpha = 75$ degree

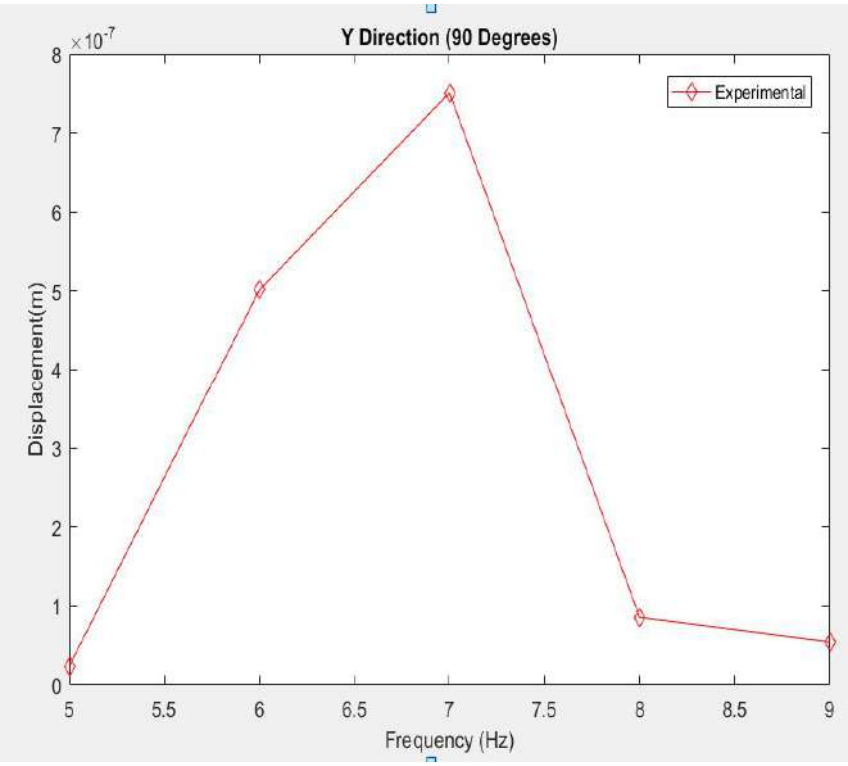

Figure 5.65: Response of SDOF building model with Planar irregularity T-Shape in Y Direction along $\alpha = 90$ degree

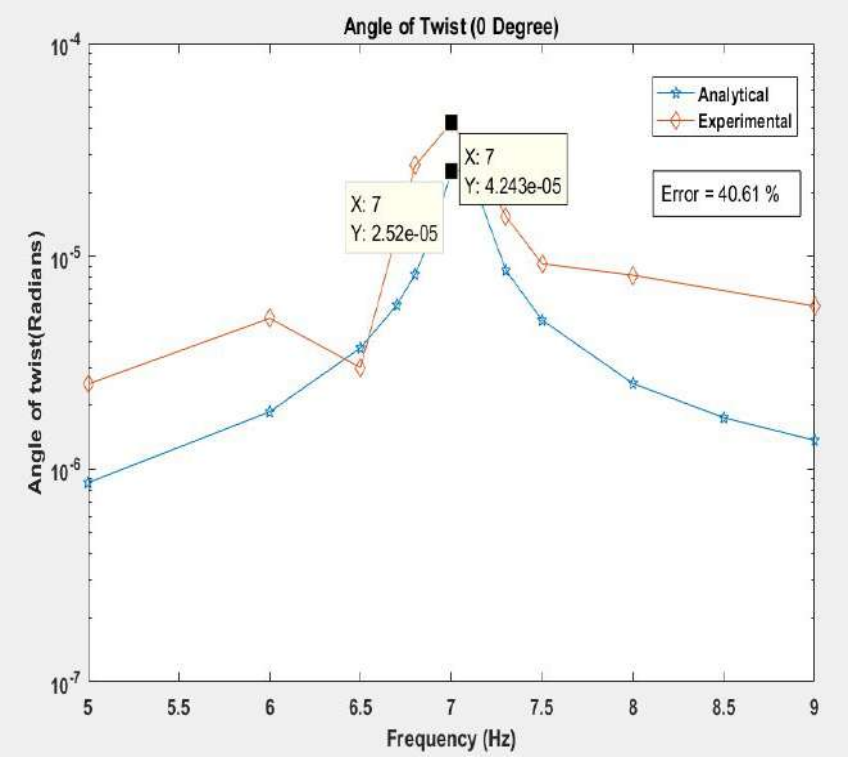

Figure 5.66: Response of SDOF building model with Planar irregularity T-Shape in θ Direction along $\alpha = 0$ degree

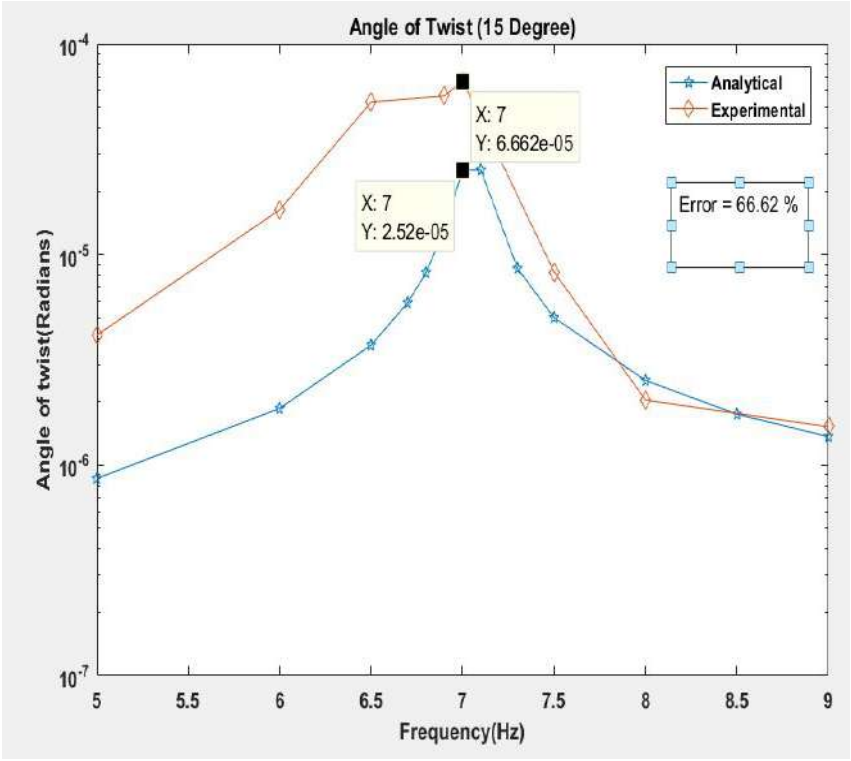

Figure 5.67: Response of SDOF building model with Planar irregularity T-Shape in θ Direction along $\alpha = 15$ degree

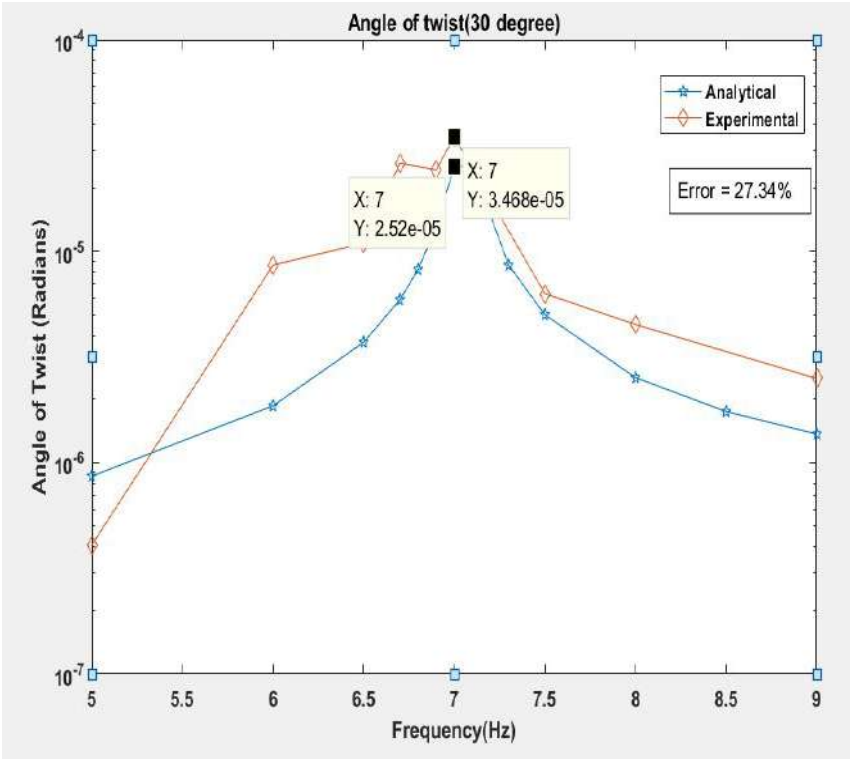

Figure 5.68: Response of SDOF building model with Planar irregularity T-Shape in θ Direction along $\alpha = 30$ degree

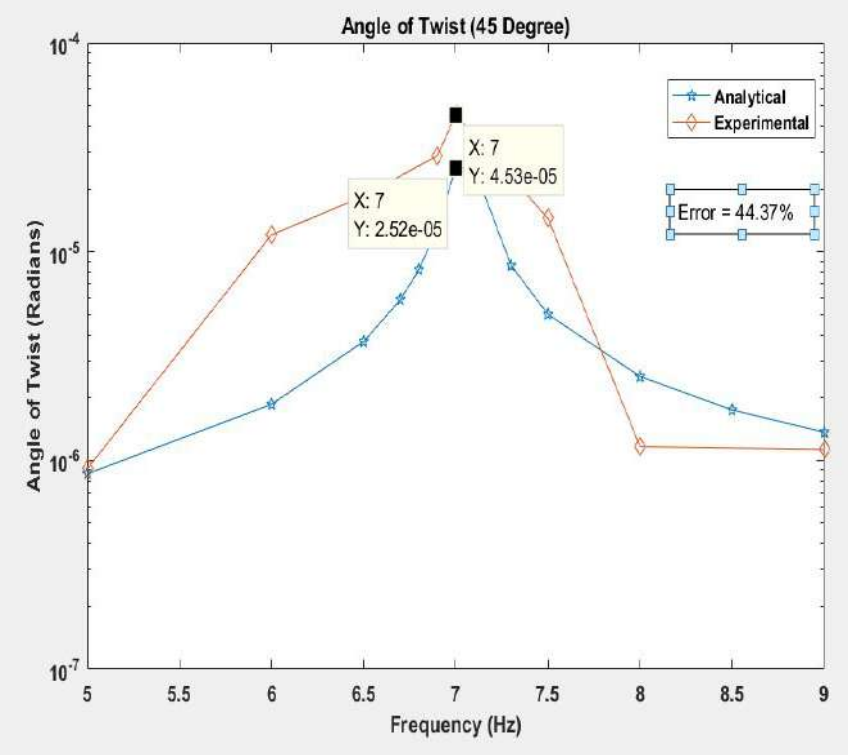

Figure 5.69: Response of SDOF building model with Planar irregularity T-Shape in θ Direction along $\alpha = 45$ degree

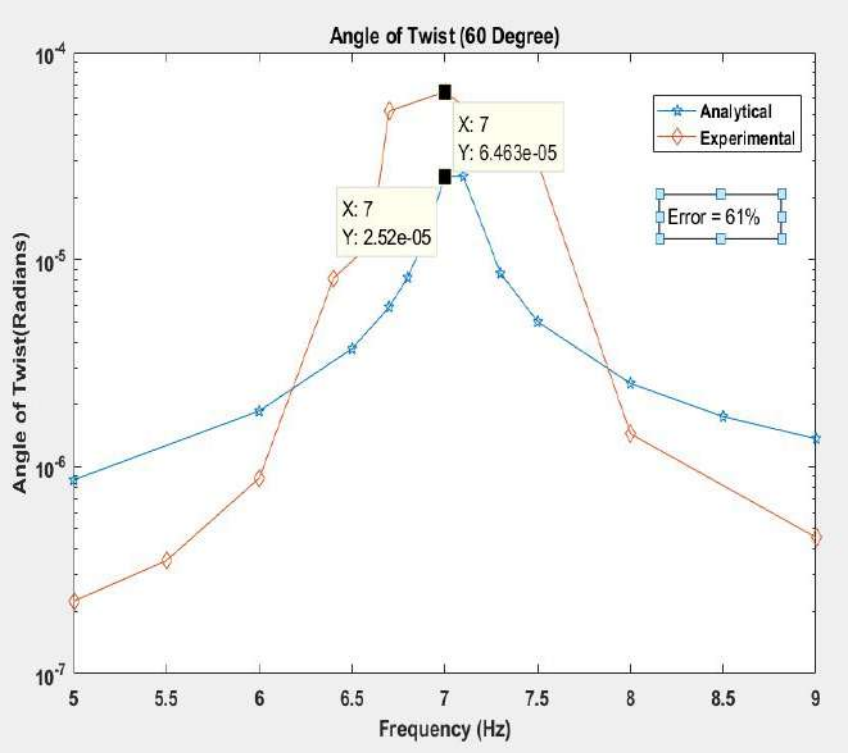

Figure 5.70: Response of SDOF building model with Planar irregularity T-Shape in θ Direction along $\alpha = 60$ degree

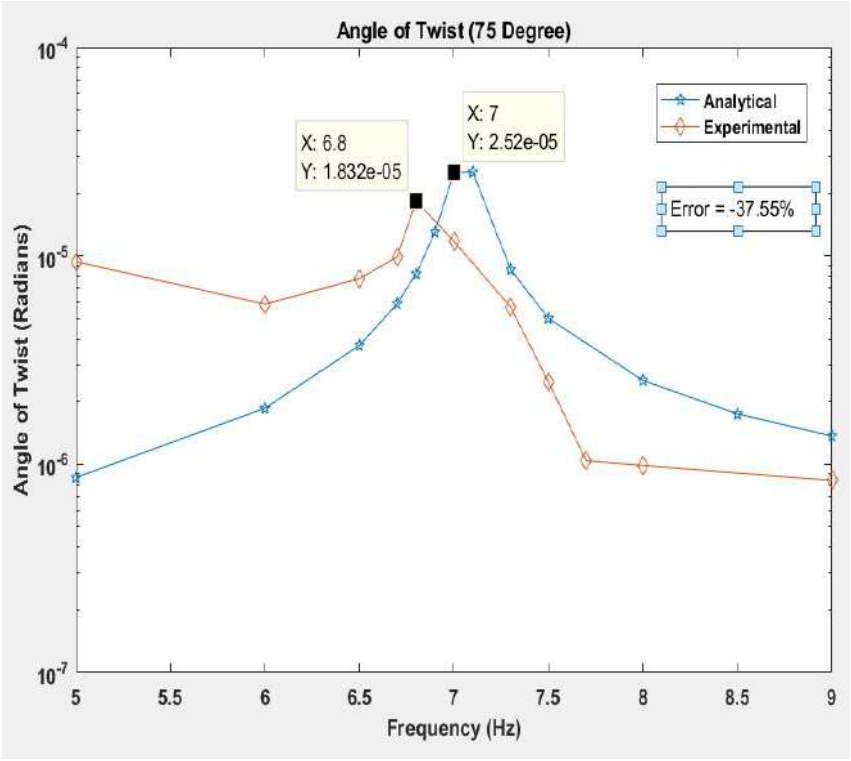

Figure 5.71: Response of SDOF building model with Planar irregularity T-Shape in θ Direction along $\alpha = 75$ degree

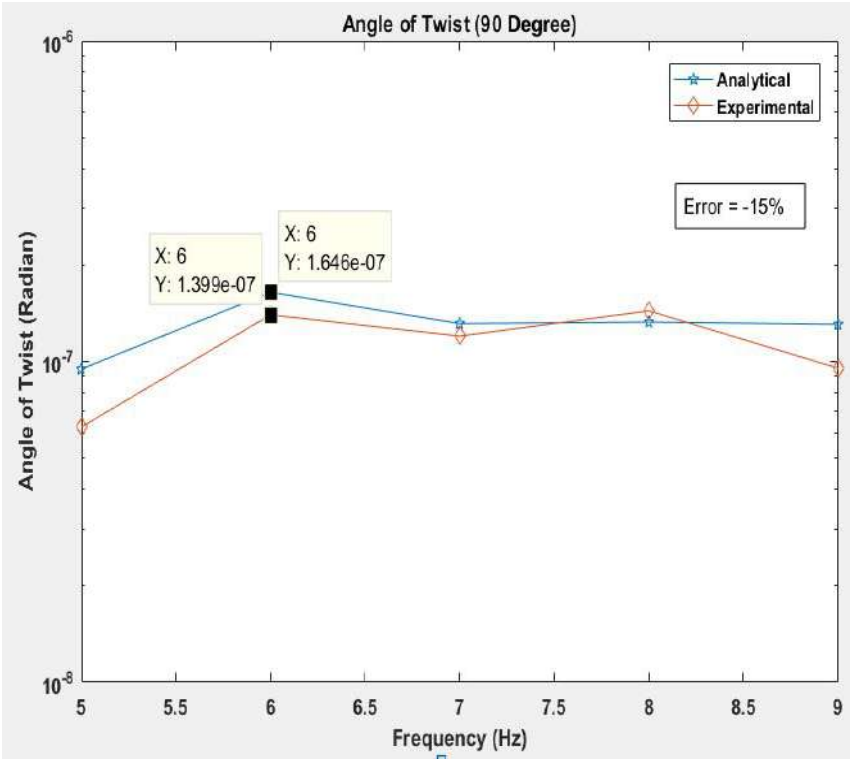

Figure 5.72: Response of SDOF building model with Planar irregularity T-Shape in θ Direction along $\alpha = 90$ degree

Table 5.11: Response for building model with Planar Irregularity of T-Shape in X Direction

Angle of Incident (Degree)	Analytical Frequency (Hz)	X analytical (m)	Experimental Frequency (Hz)	X experimental (m)	Error (%)
0	7	0.0107	6.8	0.0174	38.78
15	7	0.0107	7	0.012	11.49
30	7	0.0107	6.9	0.01033	-3.59
45	7	0.0107	6.9	0.0255	58.10
60	7	0.0107	6.7	0.016	35.72
75	7	0.0107	6.8	0.0101	-5.84
90	6	7.056×10^{-7}	6	3.35×10^{-6}	78.90

Table 5.12: Response for building model with Planar Irregularity of T-Shape in Y Direction

Angle of Incident (Degree)	Experimental Frequency (Hz)	Y experimental (m)
0	7	1.554×10^{-7}
15	7.5	2.704×10^{-7}
30	7	3.92×10^{-7}
45	6.9	2.299×10^{-7}
60	6.4	4.647×10^{-7}
75	6.8	2.001×10^{-7}
90	7	7.82×10^{-7}

Table 5.13: Response for building model with Planar Irregularity of T-Shape in θ Direction

Angle of Incident (Degree)	Analytical Frequency (Hz)	θ analytical (radians)	Experimental Frequency (Hz)	θ experimental (radians)	Error (%)
0	7	2.52×10^{-5}	7	4.243×10^{-5}	40.61
15	7	2.52×10^{-5}	7	6.66×10^{-5}	66.62
30	7	2.52×10^{-5}	7	3.468×10^{-5}	27.34
45	7	2.52×10^{-5}	7	4.53×10^{-5}	44.37
60	7	2.52×10^{-5}	7	6.46×10^{-5}	61
75	7	2.52×10^{-5}	6.8	1.832×10^{-5}	-37.55
90	6	1.646×10^{-7}	6	1.399×10^{-5}	-15

5.5.3 One Storey Building Model Frame with L Planar Geometry

As explained in Chapter 3 mass matrix , stiffness matrix and natural frequency are evaluated.

mass matrix in Kg can be written as below

$$M = \begin{bmatrix} 2.131 & 0 & 0 \\ 0 & 2.131 & 0 \\ 0 & 0 & 0.0338 \end{bmatrix}$$

Stiffness matrix in N/m is generated as below.

$$K = \begin{bmatrix} 3211.51 & 0 & 75.43 \\ 0 & 223024.31 & 4333.362 \\ 75.43 & 4333.362 & 5440.445 \end{bmatrix}$$

Natural Frequency in Hz can be obtained by Eigen value analysis.

$$\omega_n = \begin{bmatrix} 6.171 \\ 50.41 \\ 65.81 \end{bmatrix}$$

5.5.3.1 Experimental Setup of the One Storey Building Model Frame with L Planar Geometry

Similar to the above setup the L Shape Planar Asymmetry building frame is mounted on the electric motor driven shake table in which By varying the speed of the motor the frequency of the harmonic base motion could be varied , also the mounting device is capable of swiveling about the vertical axis, which would permit us to mount the frame at different angles relative to the axis of the base motion. Figure 5.73 shows experimental setup for one storey building frame.

Figure 5.73: Experimental setup for one storey asymmetric building frame

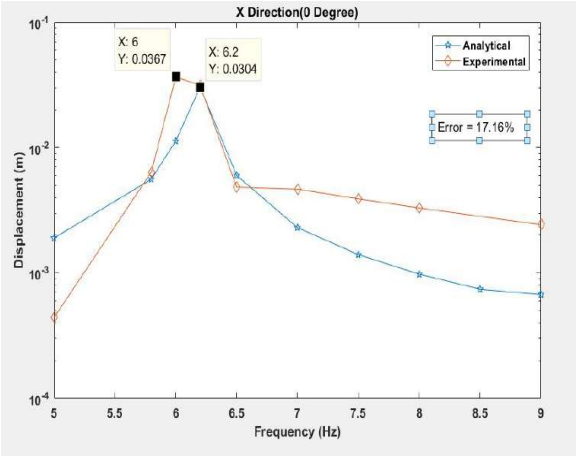

(a) Response of SDOF building model with Planar irregularity L-Shape in X Direction along $\alpha = 0$ degree

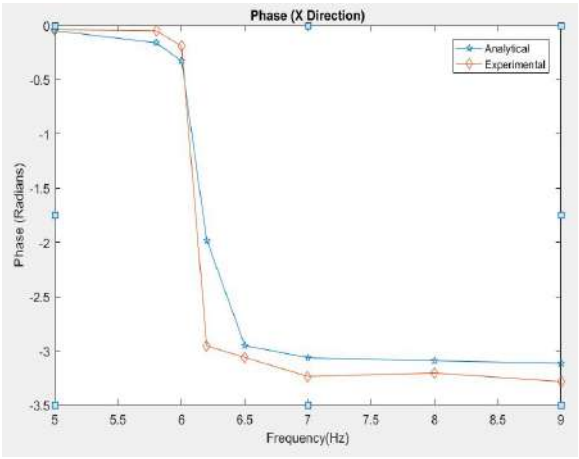

(b) Phase spectra of SDOF building model with Planar irregularity L-Shape in X Direction along $\alpha = 0$ degree

Figure 5.74: Comparison of Amplitude Spectra and Phase Spectra in X- Direction

5.5.3.2 Studies with Fixed Angle of Incidence of Base Motion($\alpha = 0$)

The base motion test is run on the frame at different values of frequency making sure that readings at resonant frequencies are not missed , for a given motion frequency the frame is allowed to oscillate for a few seconds.

With the help of labview software we were able to transform the acceleration measured from accelerometer to displacement from which we were able to capture the responses in X,Y and θ, we have applied integration to the acceleration response but it has to be made sure to apply filter before applying the integration as mentioned in the literature review by Slifka D.L [5], and then the measured value was compared theoretically from the Equation give in Chapter [3.5] Dynamic Response Solution of Asymmetric Structural System .

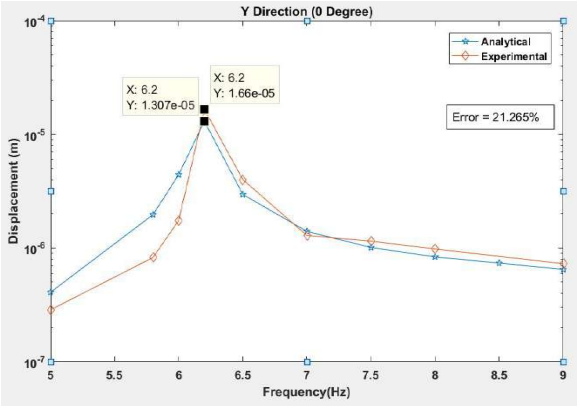

(a) Response of SDOF building model with Planar irregularity L-Shape in Y Direction along $\alpha = 0$ degree

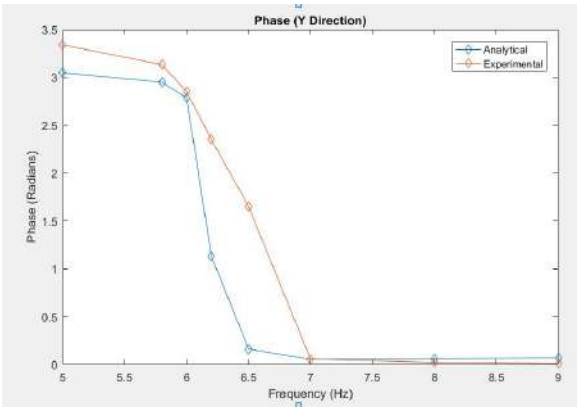

(b) Phase spectra of SDOF building model with Planar irregularity L-Shape in Y Direction along $\alpha = 0$ degree

Figure 5.75: Comparison of Amplitude Spectra and Phase Spectra in θ- Direction

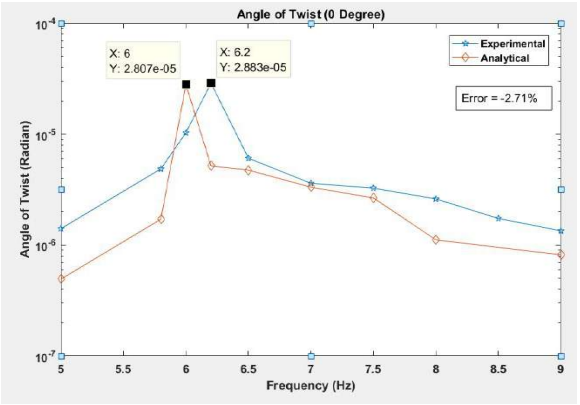

(a) Response of SDOF building model with Planar irregularity L-Shape in θ Direction along $\alpha = 0$ degree

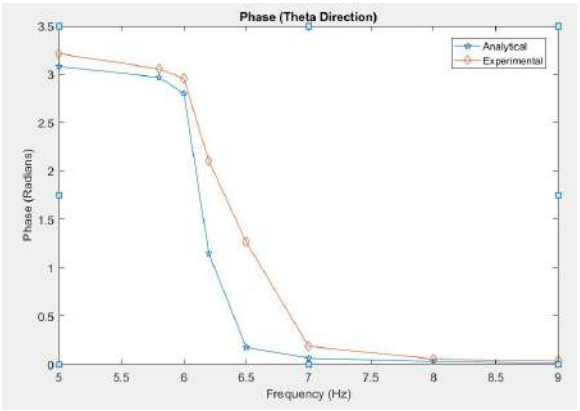

(b) Phase spectra of SDOF building model with Planar irregularity L-Shape in *theta* Direction along $\alpha = 0$ degree

Figure 5.76: Comparison of Amplitude Spectra and Phase Spectra in θ- Direction

5.5.3.3 Studies with Varying Angle of Incidence of Base Motion

Here we hold the motor RPM fixed and vary angle of incidence of the base motion by mounting the frame on the table at a desired angle in the range of 0 to $\pi/2$.

Responses are captured using LabVIEW software in X,Y,θ directions and comparison is

done with analytical results.

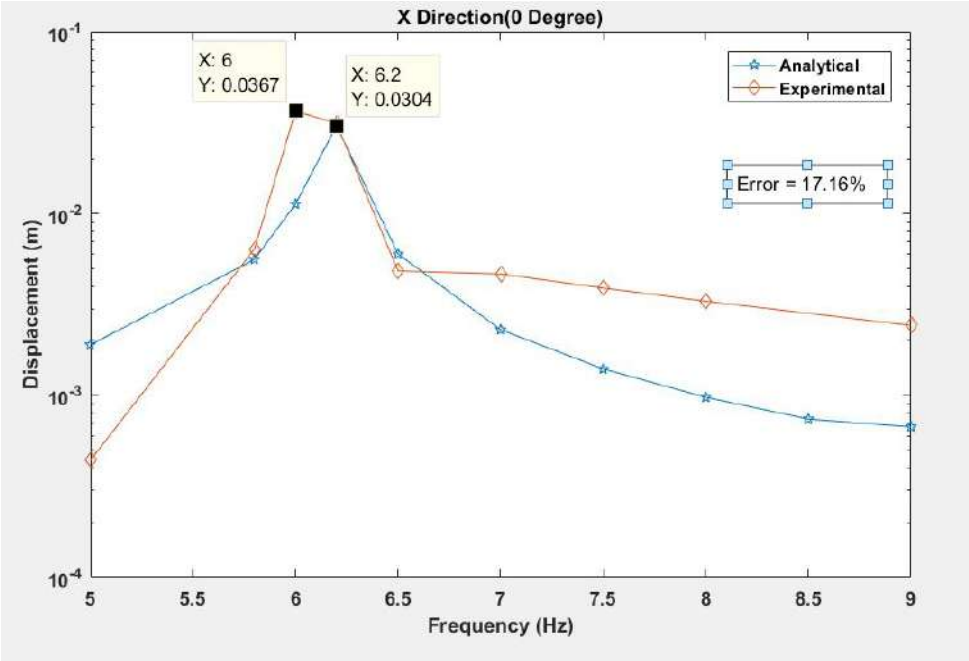

Figure 5.77: Response of SDOF building model with Planar irregularity L-Shape in X Direction along $\alpha = 0$ degree

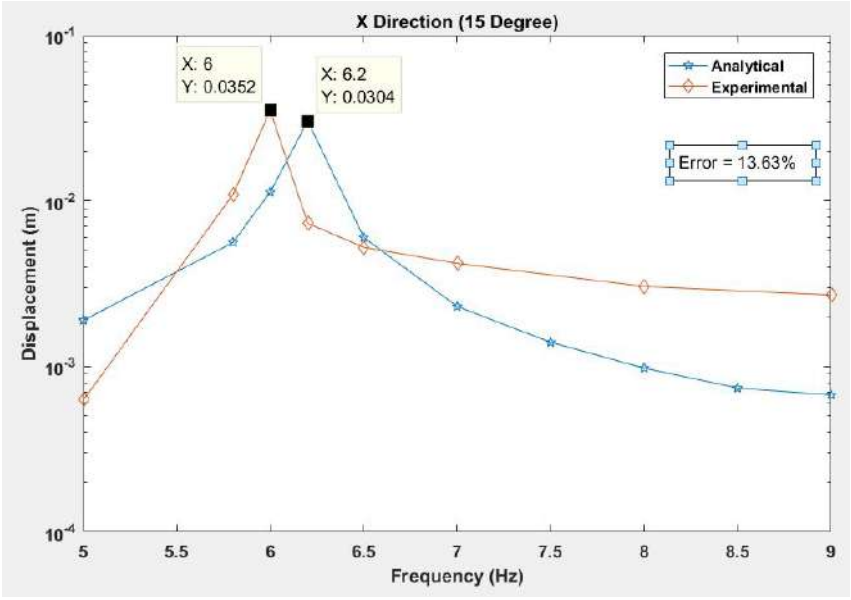

Figure 5.78: Response of SDOF building model with Planar irregularity L-Shape in X Direction along $\alpha = 15$ degree

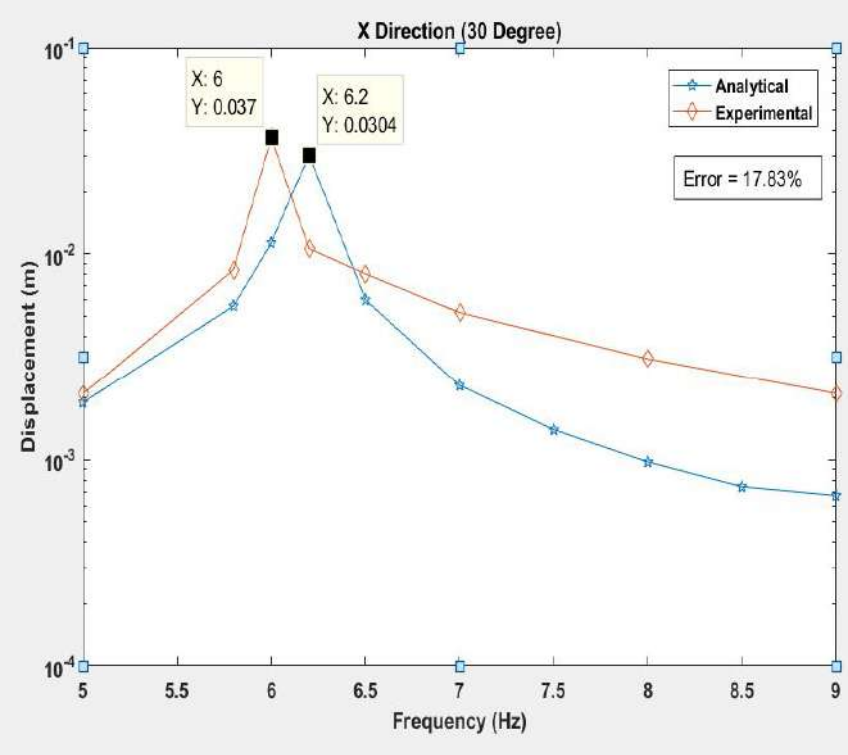

Figure 5.79: Response of SDOF building model with Planar irregularity L-Shape in X Direction along $\alpha = 30$ degree

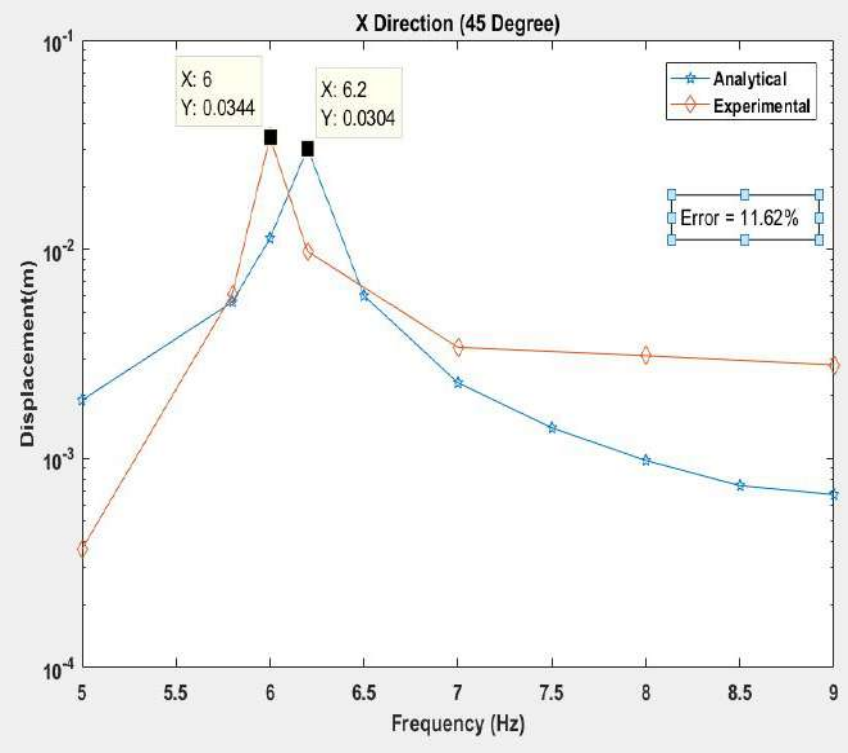

Figure 5.80: Response of SDOF building model with Planar irregularity L-Shape in X Direction along $\alpha = 45$ degree

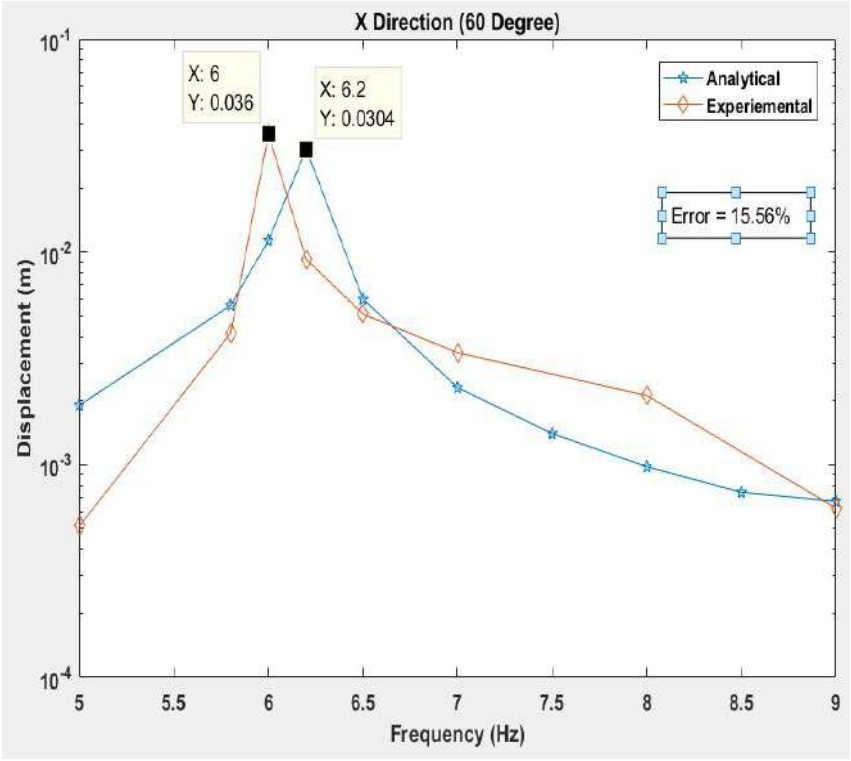

Figure 5.81: Response of SDOF building model with Planar irregularity L-Shape in X Direction along $\alpha = 60$ degree

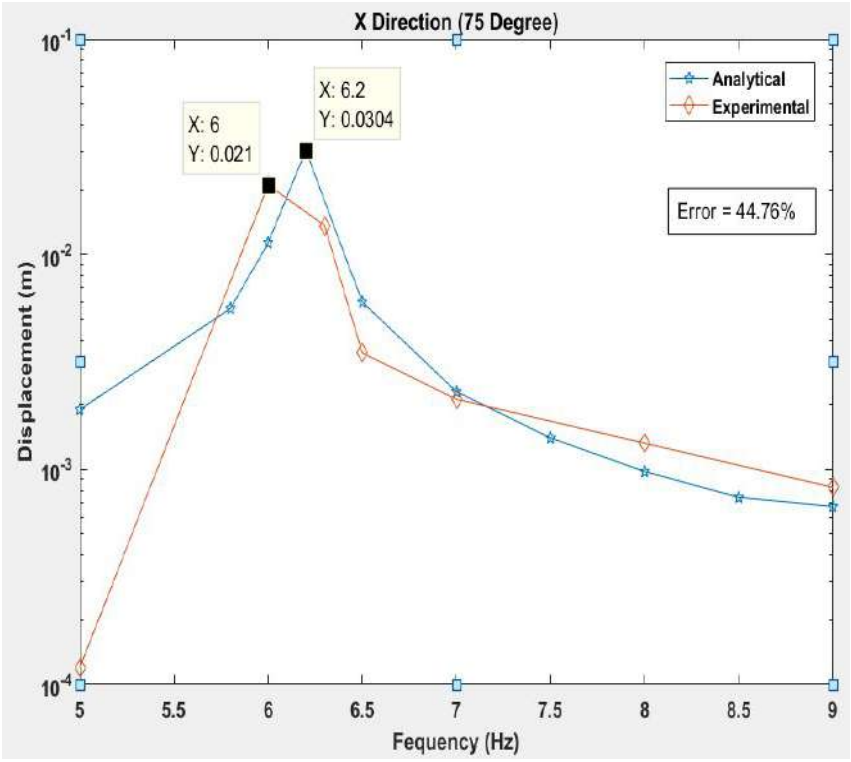

Figure 5.82: Response of SDOF building model with Planar irregularity L-Shape in X Direction along $\alpha = 75$ degree

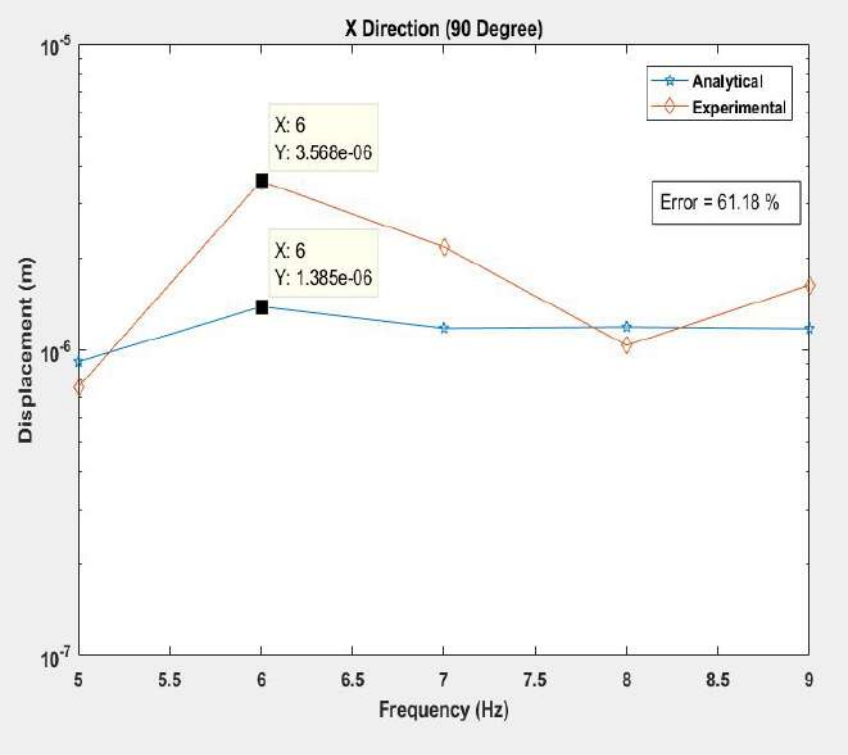

Figure 5.83: Response of SDOF building model with Planar irregularity L-Shape in X Direction along $\alpha = 90$ degree

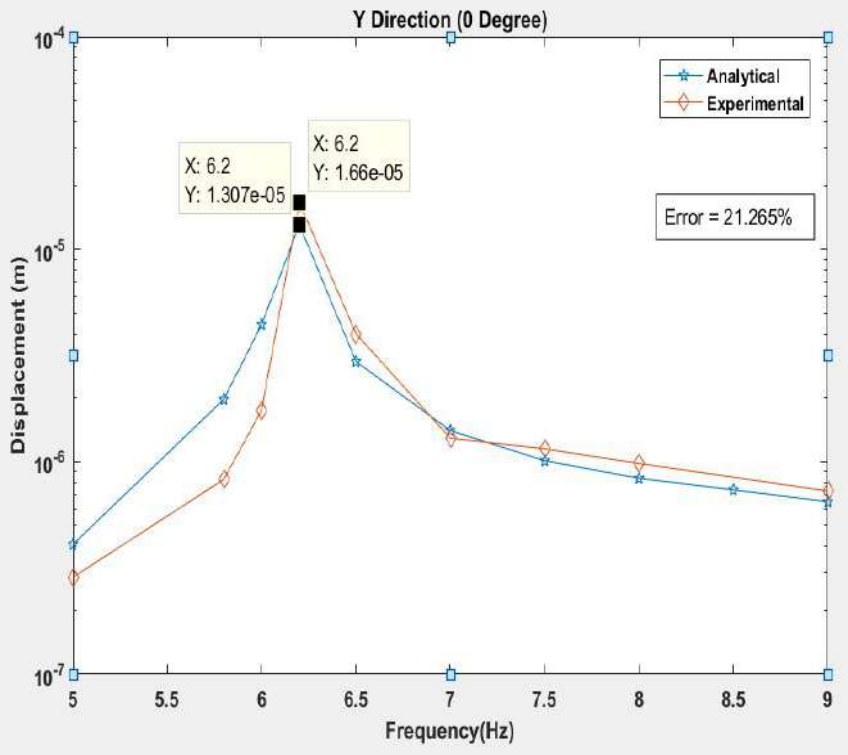

Figure 5.84: Response of SDOF building model with Planar irregularity L-Shape in Y Direction along $\alpha = 0$ degree

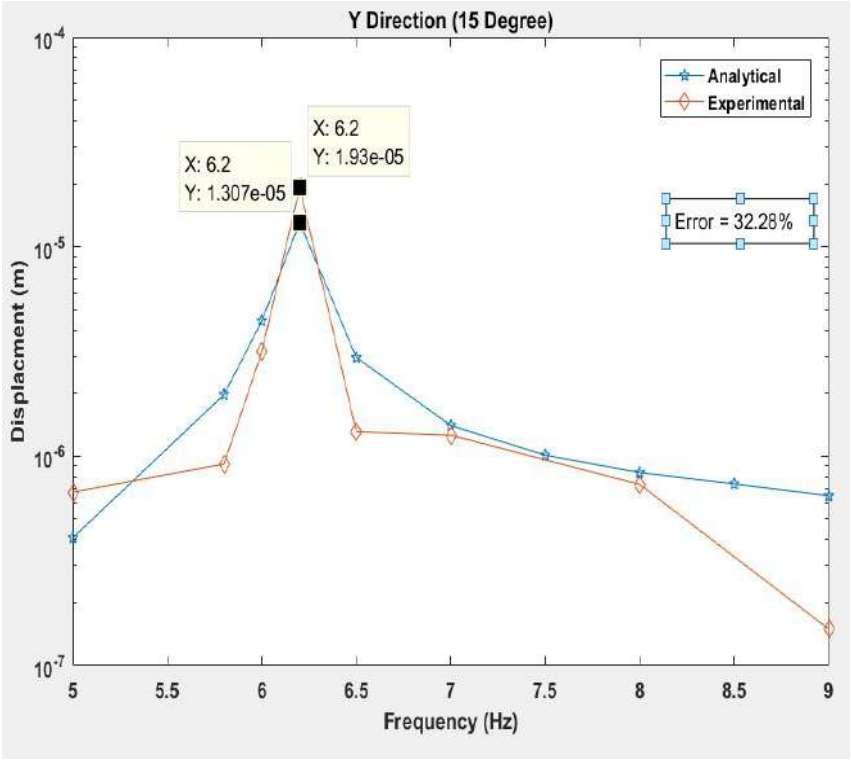

Figure 5.85: Response of SDOF building model with Planar irregularity L-Shape in Y Direction along $\alpha = 15$ degree

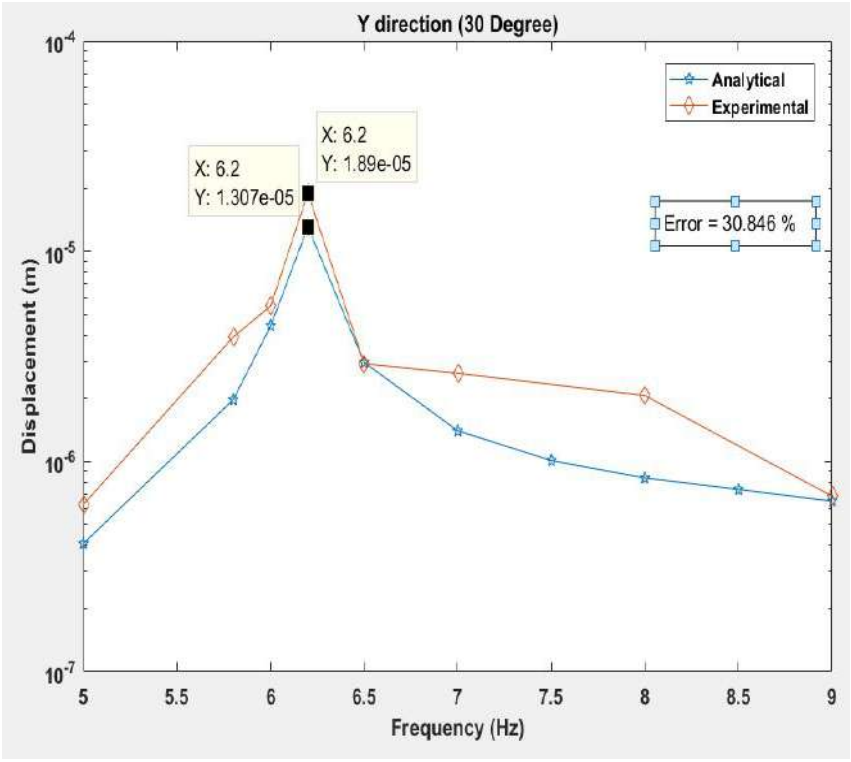

Figure 5.86: Response of SDOF building model with Planar irregularity L-Shape in Y Direction along $\alpha = 30$ degree

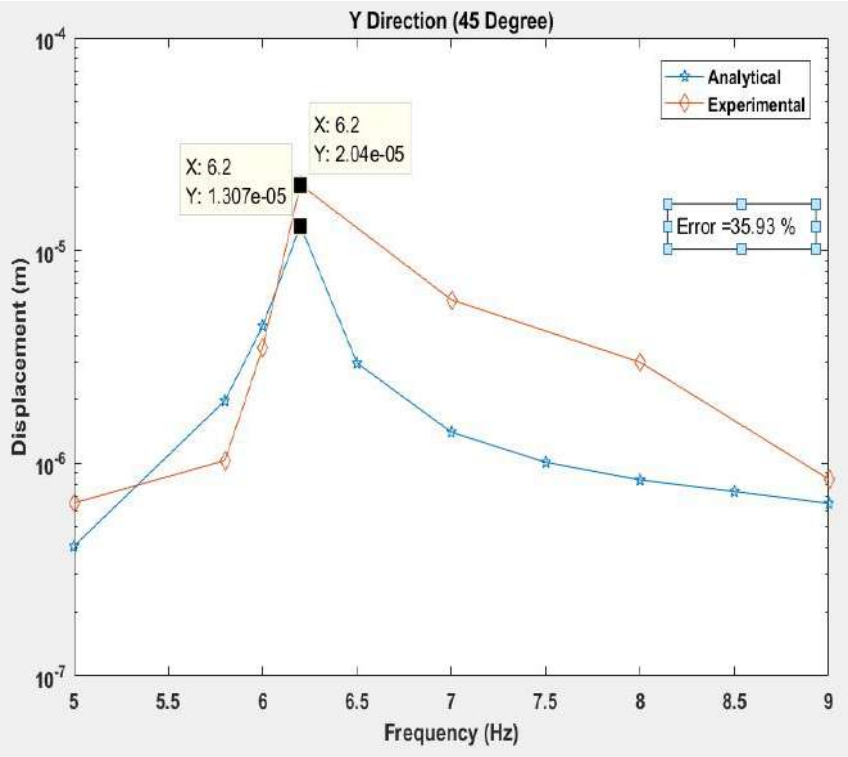

Figure 5.87: Response of SDOF building model with Planar irregularity L-Shape in Y Direction along $\alpha = 45$ degree

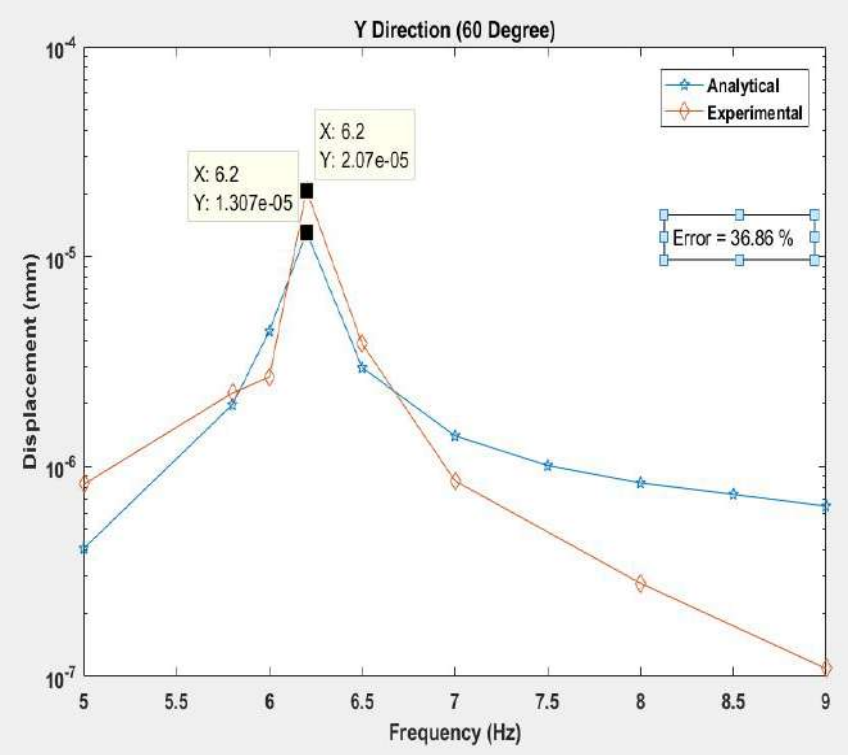

Figure 5.88: Response of SDOF building model with Planar irregularity L-Shape in Y Direction along $\alpha = 60$ degree

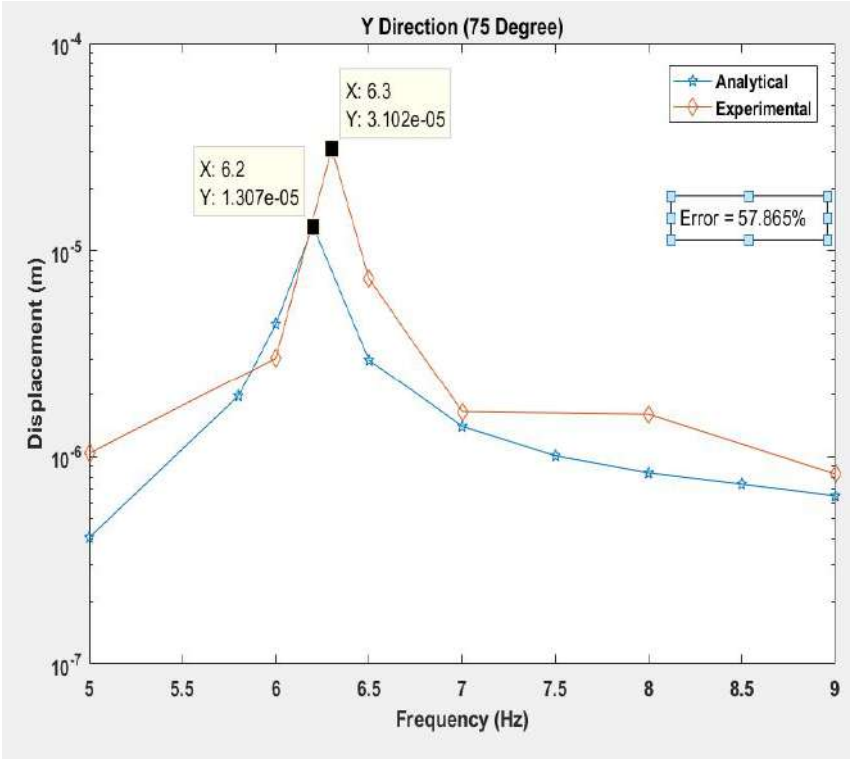

Figure 5.89: Response of SDOF building model with Planar irregularity L-Shape in Y Direction along $\alpha = 75$ degree

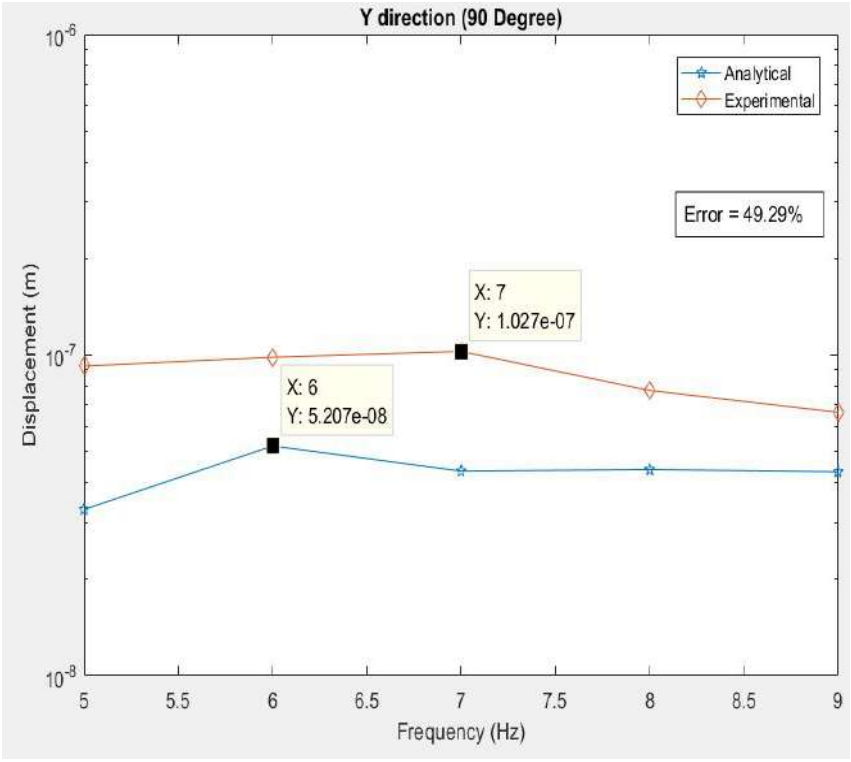

Figure 5.90: Response of SDOF building model with Planar irregularity L-Shape in Y Direction along $\alpha = 90$ degree

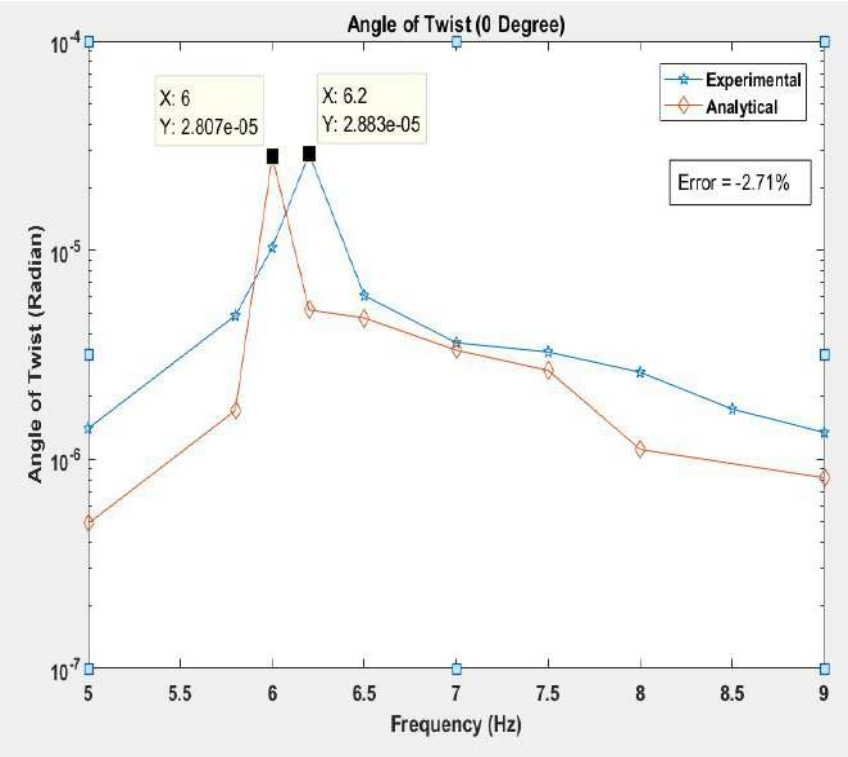

Figure 5.91: Response of SDOF building model with Planar irregularity L-Shape in θ Direction along $\alpha = 0$ degree

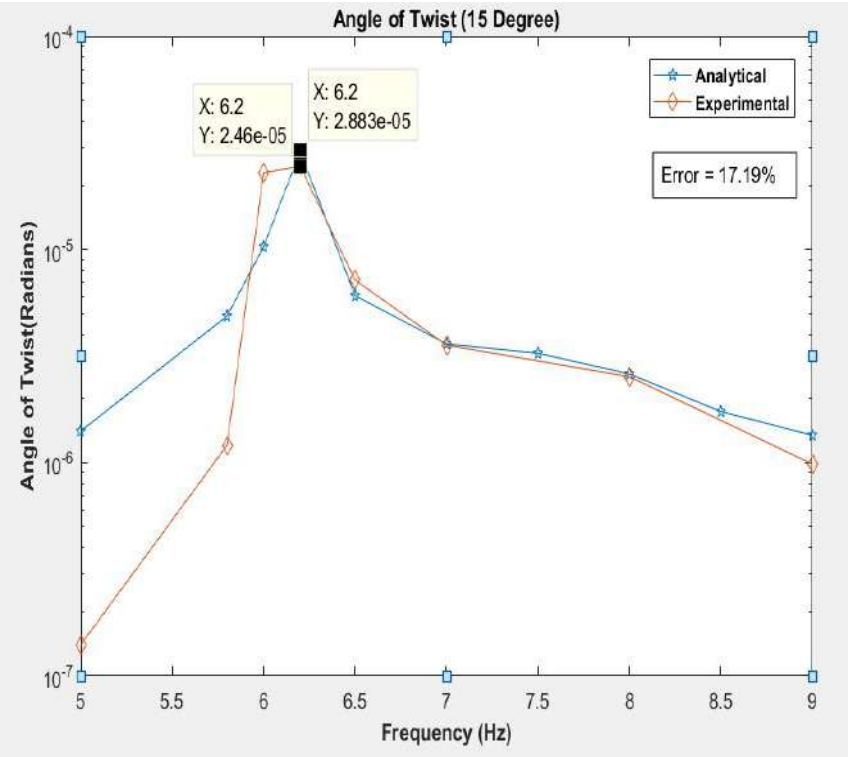

Figure 5.92: Response of SDOF building model with Planar irregularity L-Shape in θ Direction along $\alpha = 15$ degree

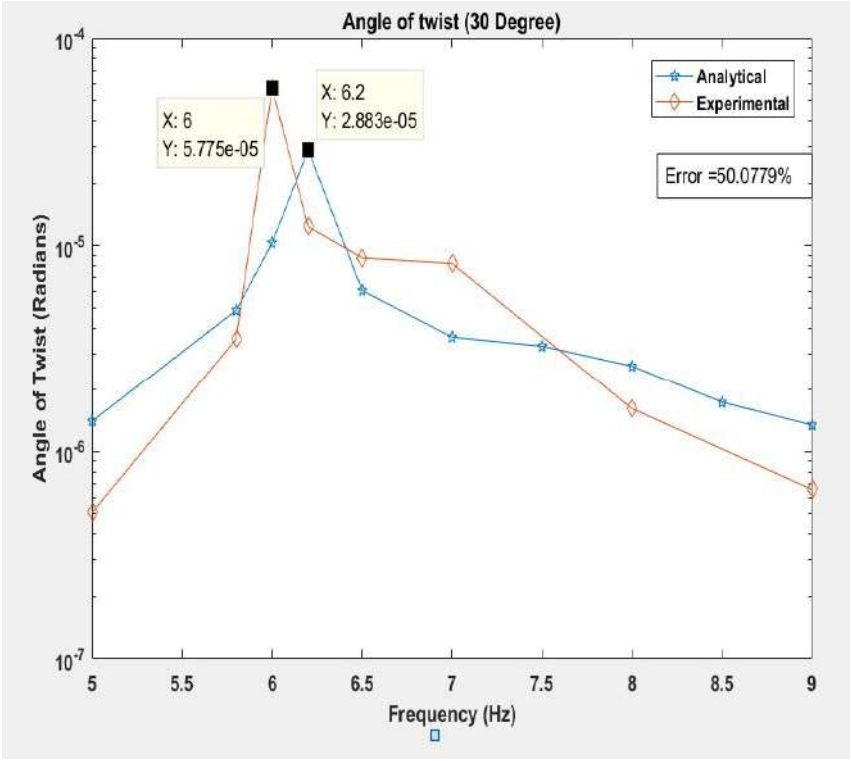

Figure 5.93: Response of SDOF building model with Planar irregularity L-Shape in θ Direction along $\alpha = 30$ degree

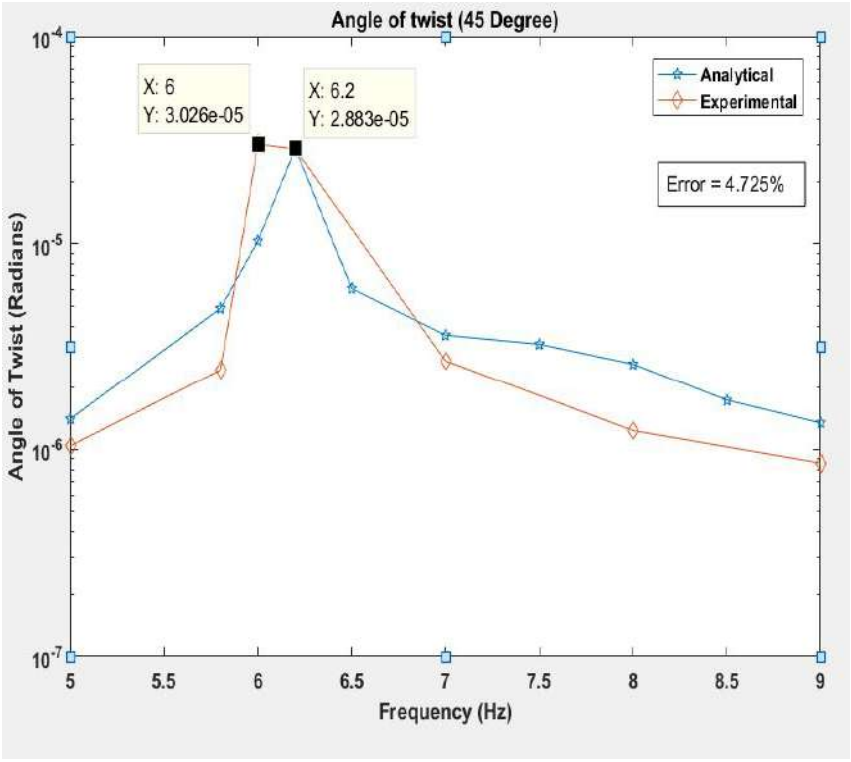

Figure 5.94: Response of SDOF building model with Planar irregularity L-Shape in θ Direction along $\alpha = 45$ degree

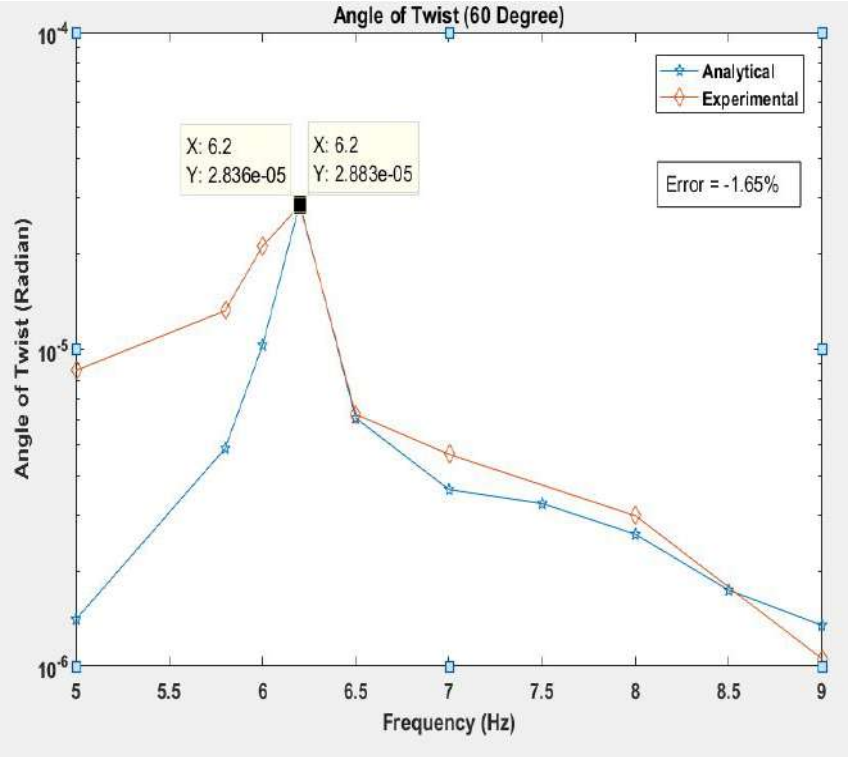

Figure 5.95: Response of SDOF building model with Planar irregularity L-Shape in θ Direction along $\alpha = 60$ degree

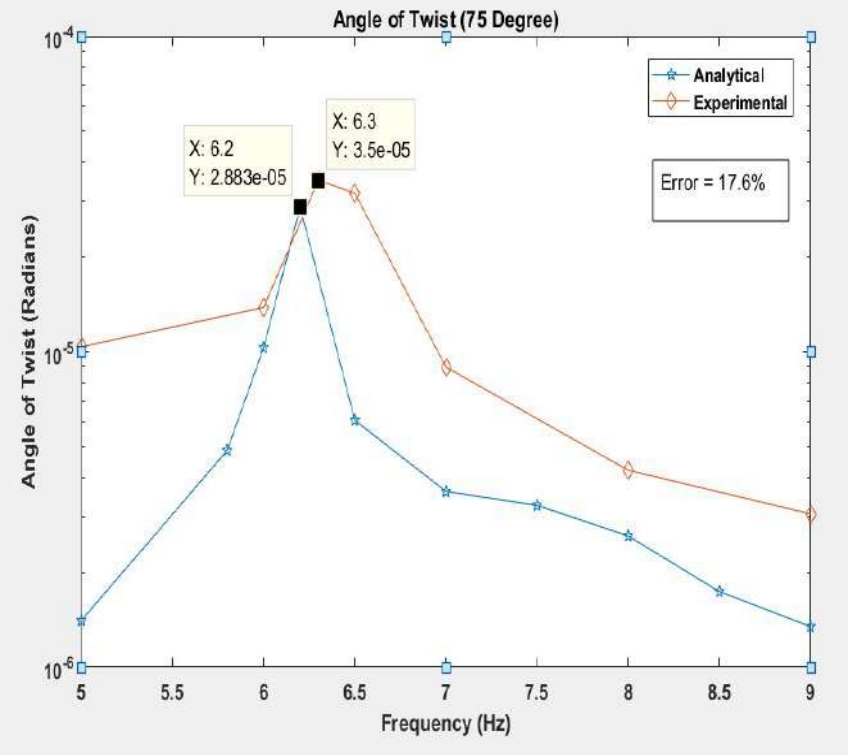

Figure 5.96: Response of SDOF building model with Planar irregularity L-Shape in θ Direction along $\alpha = 75$ degree

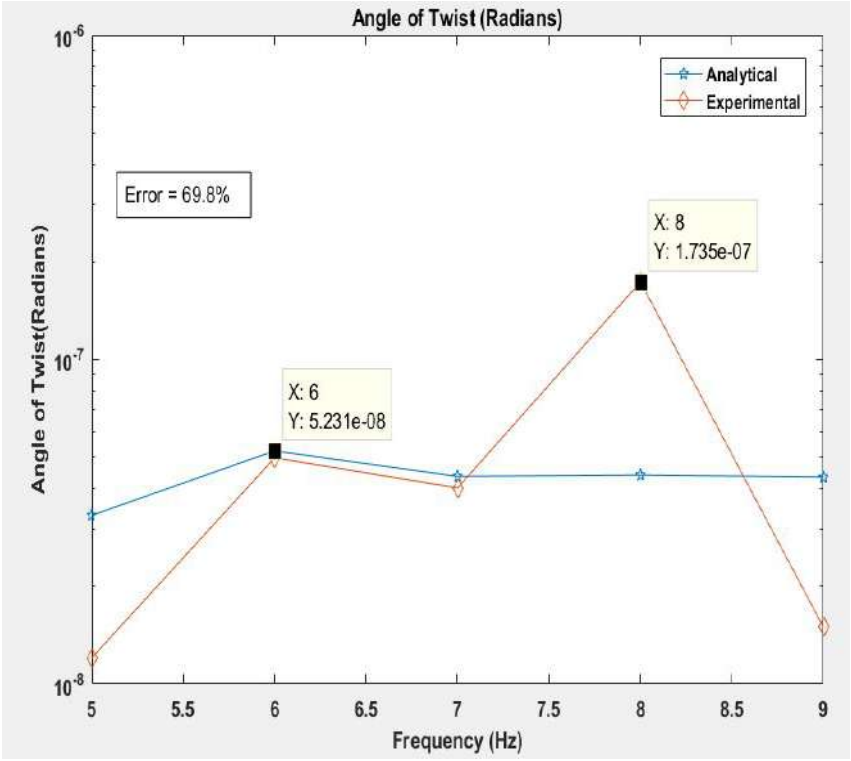

Figure 5.97: Response of SDOF building model with Planar irregularity L-Shape in θ Direction along $\alpha = 90$ degree

Table 5.14: Response for building model with Planar Irregularity of L-Shape in X Direction

Angle of Incident (Degree)	Analytical Frequency (Hz)	X analytical (m)	Experimental Frequency (Hz)	X experimental (m)	Error (%)
0	6.2	0.0304	6	0.0367	17.16
15	6.2	0.0304	6	0.0352	13.63
30	6.2	0.0304	6	0.0226	53.03
45	6.2	0.0304	6	0.037	17.83
60	6.2	0.0304	6	0.036	11.62
75	6.2	0.0304	6	0.021	44.76
90	7	1.38×10^{-6}	8	3.57×10^{-6}	61.18

Table 5.15: Response for building model with Planar Irregularity of L-Shape in Y Direction

Angle of Incident (Degree)	Analytical Frequency (Hz)	Y analytical (m)	Experimental Frequency (Hz)	Y experimental (m)	Error (%)
0	6.2	1.307×10^{-5}	6.2	1.66×10^{-5}	21.26
15	6.2	1.307×10^{-5}	6.2	1.93×10^{-5}	32.28
30	6.2	1.307×10^{-5}	6.2	1.89×10^{-5}	30.85
45	6.2	1.307×10^{-5}	6.2	2.04×10^{-5}	35.93
60	6.2	1.307×10^{-5}	6.2	2.07×10^{-5}	36.86
75	6.2	1.307×10^{-5}	6.2	3.102×10^{-5}	57.86
90	6	5.207×10^{-8}	7	1.027×10^{-7}	49.29

Table 5.16: Response for building model with Planar Irregularity of L-Shape in θ Direction

Angle of Incident (Degree)	Analytical Frequency (Hz)	θ analytical (radians)	Experimental Frequency (Hz)	θ experimental (radians)	Error (%)
0	6.2	2.883×10^{-5}	6	2.807×10^{-5}	-2.71
15	6.2	2.883×10^{-5}	6.2	2.46×10^{-5}	17.19
30	6.2	2.883×10^{-5}	6	5.775×10^{-5}	50.08
45	6.2	2.883×10^{-5}	6	3.026×10^{-5}	4.72
60	6.2	2.883×10^{-5}	6.2	2.836×10^{-5}	-1.65
75	6.2	2.883×10^{-5}	6.3	3.5×10^{-5}	17.60
90	6	5.231×10^{-8}	8	1.735×10^{-7}	69.80

5.6 Summary

In this chapter, dynamic properties of SDOF building model are evaluated through experimentation. Stiffness and natural frequency are found to have good agreement with the corresponding analytical values. Coefficient of Damping (ζ) has been found for Single Storey bare SDOF system and SDOF building model with planar and material irregularity by giving free vibration and ζ is obtained through Logarithmic Decrement Method.

when the building frame with planar and material asymmetry reaches Resonance there is a shift in phase for X,Y and θ directions which is clearly visible in the Amplitude spectra and phase spectra graphs obtained from both analytically and experimentally. As we rotate the building frame fromα 0 to $\pi/2$ there is no influence on response of the building frame with planar such as L and T Shape irregularity and material irregularity in X,Y and θ direction can be observed but as we move from α=75degree to $\pi/2$ there is decrease in response is observed .

Chapter 6

Characterization of Passive Damper Devices

6.1 Introduction

Dynamic load produces vibration in the structure which causes the damage or collapse of the structure. A large amount of energy is imparted into structure during these vibrations. To reduce these vibrations it becomes important for the structure to absorb or dissipate energy. A widely considered strategy consists of incorporating external elements to the structure to control its dynamic response. The branch of Structural Engineering that deals with such concepts is called Structural Control.

The function of seismic passive energy dissipation system is to reduce structural response due to earthquake, wind and other dynamic loads. Passive control system develops control forces at the point of attachment of the system. The power needed to generate these forces is provided by the motion of the points of attachment during dynamic excitation. Passive energy dissipation systems encompass a range of materials and devices for enhancing damping, stiffness and strength, and can be used both for natural hazard mitigation and for rehabilitation of aging or deficient structures.

6.2 Fundamentals of Energy Dissipating Devices

6.2.1 Characterization and applicability of Dampers

This chapter considers the mechanical properties and mathematical modelling of dampers and makes some general comments on their structural applicability.The concept of replacing the complicated and often nonlinear behavior of dampers by equivalent linear stiffness and viscous characteristics has enormous benefits for the preliminary analysis and design of damper added structures.

6.2.2 Viscous Fluid Damper

Viscous dampers are known as effective energy dissipation devices improving structural response to earthquakes. Fluid viscous dampers are fluid-filled cylinders with two chambers that are separated by a moving piston with directional orifices, and an accumulator chamber. As the head moves longitudinally within the shaft, viscous fluid flows from one chamber to the other. The force in the damper is a result of the pressure differential between chambers, which is a function of the orifices in the piston head and the velocity of the piston head. The damping force developed by the viscous damper depends on the physical properties of the fluid used in the damper. The most common type of viscous fluid damper and its parts are shown in Figure 6.1. It can be seen that by simply moving the piston rod back and forth, fluid is orificed through the piston head orifices, generating damping force. It dissipates energy through movement of the piston in the highly viscous fluid. If the fluid is purely viscous (for instance, Newtonian), then the output force of the damper is directly proportional to the velocity of the piston.
The force in the fluid viscous damper can be expressed as :-

$$P(t) = C_d|\dot{u}^{\alpha}|sgn(\dot{u}) \tag{6.1}$$

Where, C_d is the damping coefficient for the damper, α is the velocity exponent for the damper that ranges from 0.1 to 2,$\dot{u}$ is the relative velocity between each end of the device, and sgn is the signum function that, defines the sign of the relative velocity term. A value of $\alpha = 1.0$ represents the linear viscous damper. Structural dampers usually have α values ranging from 0.3 - 1.0.

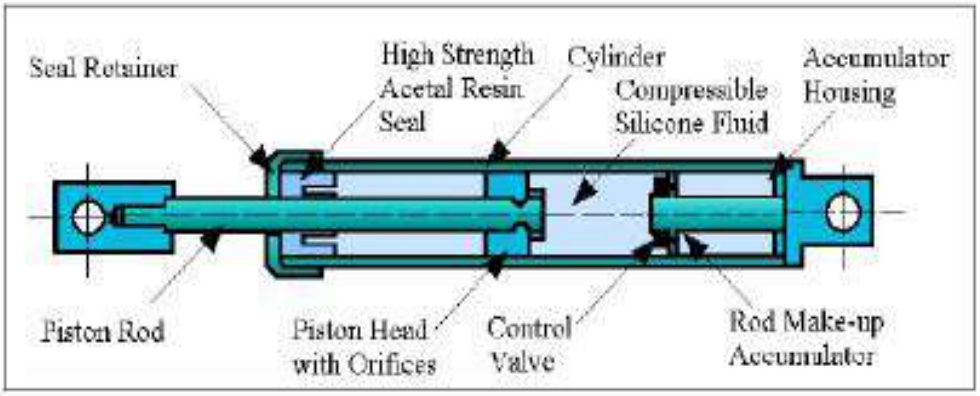

Figure 6.1: Fluid Viscous Damper

6.2.3 Metallic Yielding and Friction Devices

These are hysteric devices since their energy dissipation depends primarily on relative displacements within the device. and their energy dissipation is not sensitive to the relative velocity.Thus they can be modelled with force-displacement hysteric relationships that are well known to structural engineers.

Some typical models that have been used to represent the nonlinear force-displacement relationships are the simple elasto-plastic model,the bi linear model and the polynomial model,which are illustrated in the figure below.The cyclic hysteric characteristic of these models is based on their skeleton curve, which is the name given to the monotonic force-deflection curve obtained by increasing the force acting on the structure from 0 to the desired force or displacement.

The area obtained within one cycle of the hysteric curve is the energy dissipated per cycle. The equivalent viscous damping is obtained by setting the area within the hysteric loop equal to the area within a viscous damper cycle. This is done for each of these characteristic force-displacement shapes in the following discussion .

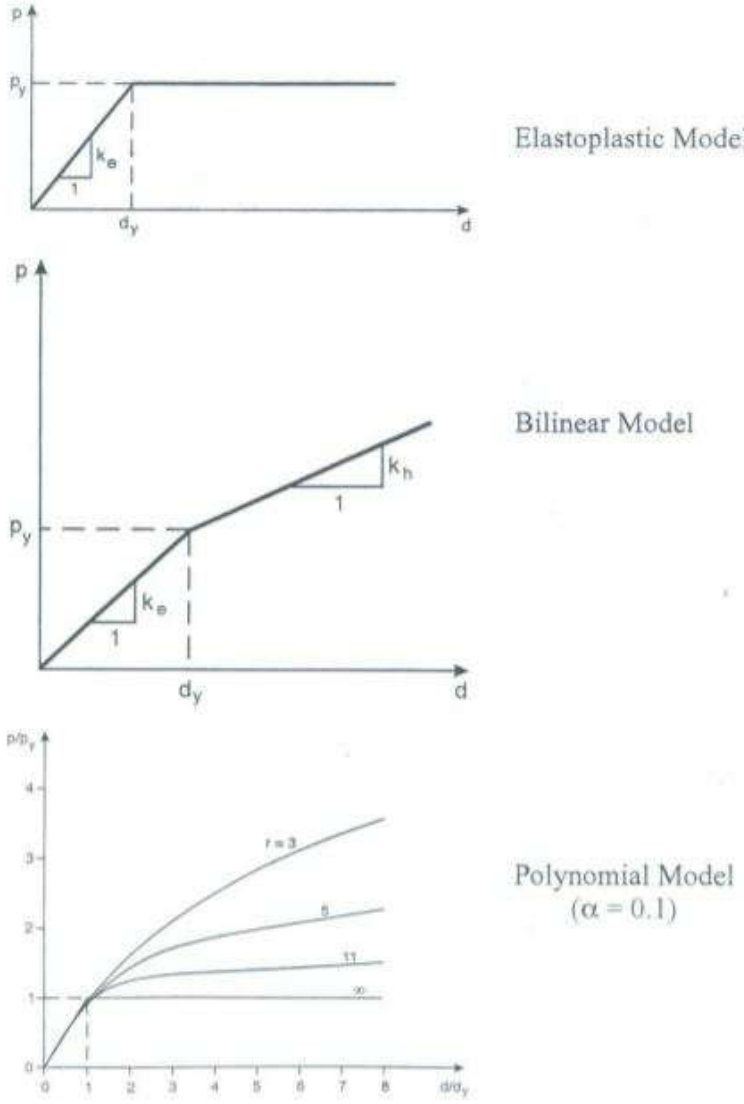

Figure 6.2: Nonlinear force-displacement models

Elasto-plastic Form The initial elastic stiffness (see the elasto-plastic model in above figure 6.2) is determined from experimental yield force and yield displacement data as

$$K_e = p_y/d_y \tag{6.2}$$

Whenever the device displacement exceeds d_y, the force is equal to p_y.The energy dissipated per cycle (E) is equal to the within the hysteric loop between (p_y,d_o) and ($-p_y$,$-d_o$) which is

$$E = 4p_y(d_o - d_y), d_o \geq d_y \tag{6.3}$$

Bi-linear Form As in the elasto-plastic case, the initial elastic stiffness is given by equation 6.2. The second slope, typically called the strain-hardening slope, is defined as having

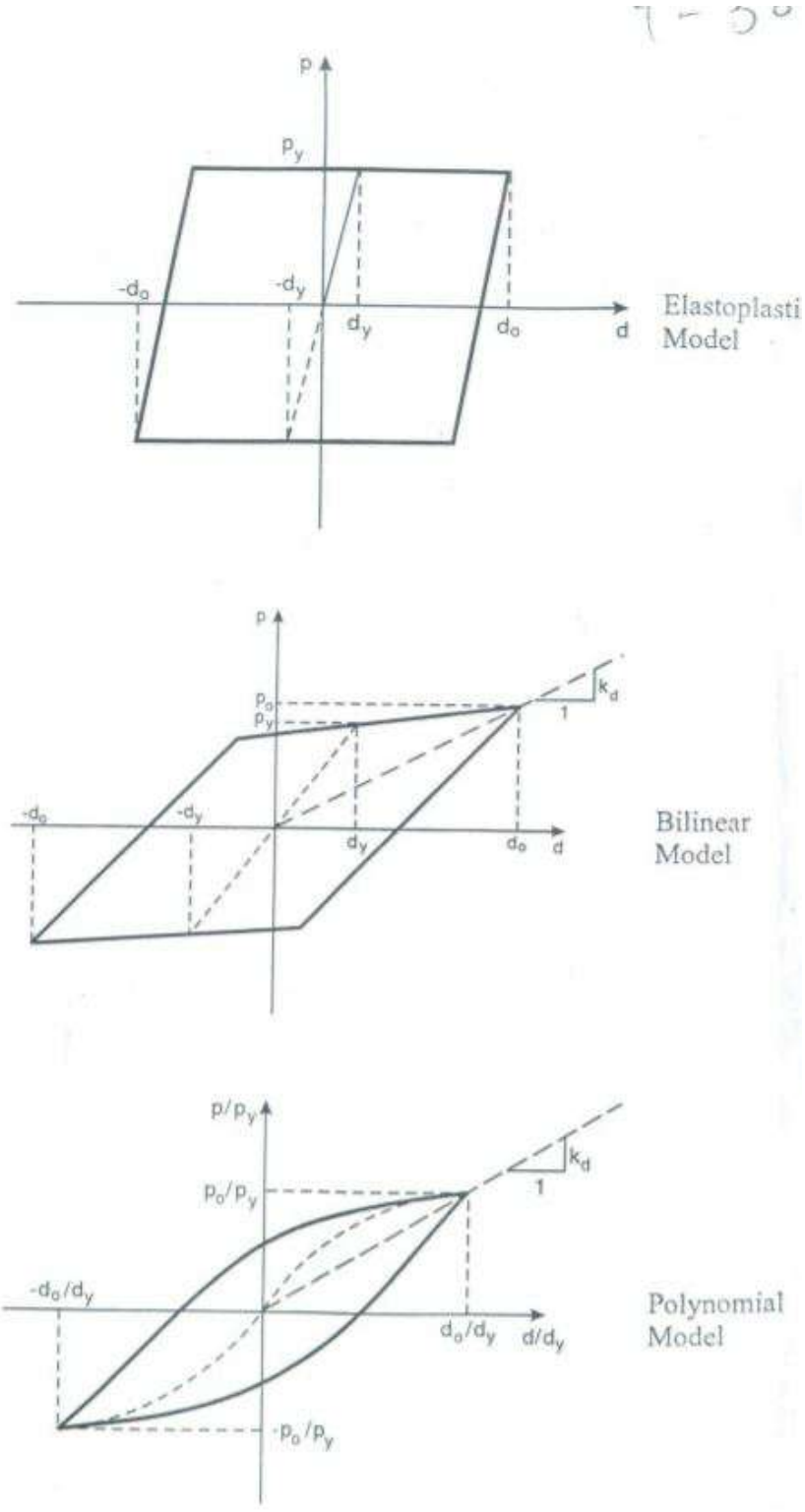

Figure 6.3: Cyclic nonlinear force-displacement models

a stiffness of K_h. It should be noted that the strain-hardening stiffness affects both the cyclic energy dissipated and the device restoring force.The bi-linear energy dissipation

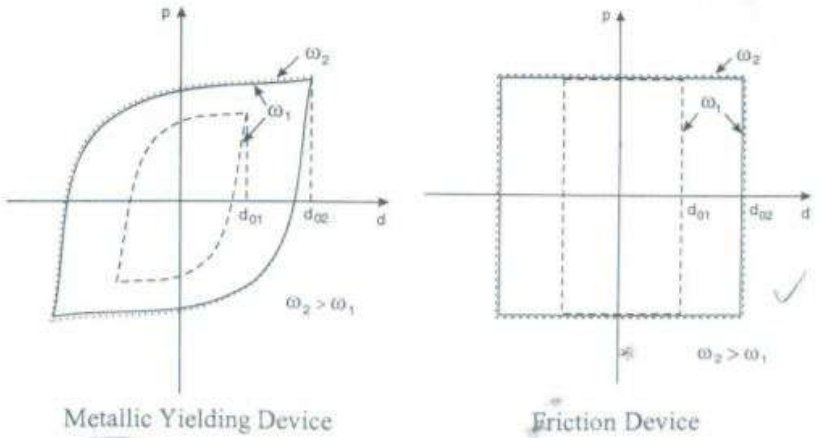

Figure 6.4: Typical cyclic hysteric shapes of metallic yielding device and friction device

relationship is given by:-

$$E = 4d_y(d_o - d_y)(K_e - K_h, d_o \geq d_y \tag{6.4}$$

This means that the restoring force increases as the displacement exceeds d_y,and the energy dissipated per cycle decreases as the hardening stiffness increases.

Polynomial model The force Displacement relationship (see the polynomial model in figure 6.2) in this case is

$$d/d_y = p/p_y + \alpha(p/p_y)^r \tag{6.5}$$

where d is the displacement of the device, d_y is the characteristic displacement , p is the load applied to the device,p_y is the characteristic load , α is a positive constant coefficient ,and r is an odd positive integer greater than 1. The area within a cyclic hysteric loop between (p_o,d_o) and ($-p_o$,$-d_o$) is

$$E = 4d_y py[(r-1)/(r+1)](p_o/p_y)^(r+1) \tag{6.6}$$

The coefficients, d_y, p_y, α and r are determined from the experimental test data of the specific device to be used. Figure 6.4 shows typical cyclic hysteric shapes of a metallic yielding device and a friction device; these shapes are based on the mechanical properties of the devices and on experimental data.It is note that a bi-linear or a polynomial model

can be used to approximate the hysteric behaviour of a metallic yielding device. For a friction damper, the elasto-plastic model with d_y=0 is quite adequate.Figure 6.4 also indicates that, for both metallic yielding and friction devices, the hysteric loops at the same maximum device displacement remain essentially unchanged at various excitation frequencies,thus demonstrating their rate-independent property.

6.2.4 Equivalent Viscous Damping and stiffness

Consider a simple one-story elastic structure with velocity-proportional viscous damping.The well-known equation of motion is

$$m\ddot{x} + c\dot{x} + kx = -m\ddot{x}_g \tag{6.7}$$

where $\ddot{x}$,$\dot{x}$ and x are the horizontal structural acceleration,velocity and displacement relative to the foundation; $\ddot{x}_g$ is the horizontal acceleration of the foundation caused by the earthquake;and m, c and k are the mass, viscous damping coefficients and stiffness of the structure.The $c\ddot{x}$ and kx terms are illustrated in the following figure 6.5.The structural reactive force can be defined as $c\dot{x}$ + kx.Note that the maximum force P_{max},does not occur at the same time as the maximum displacement,x_{max}.

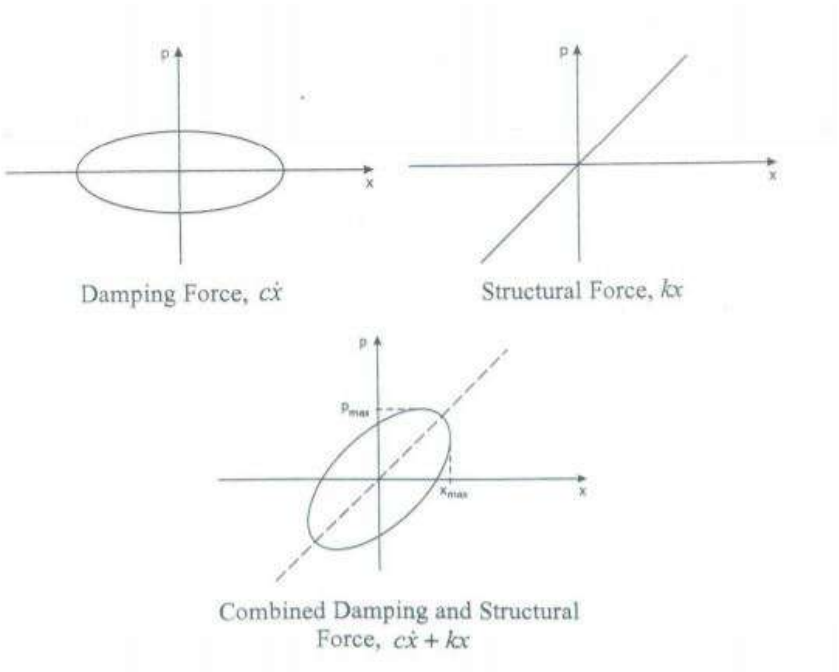

Figure 6.5: Damping and structural restoring forces.

The energy dissipated per cycle is equal to the area of the ellipse described by

$$E = (2\pi c x_o^2)/T \tag{6.8}$$

6.2.5 Energy dissipated in Viscous Damping

Consider the steady-state motion of an SDOF system due to p(t)=$p_o$sinωt.The energy dissipated by viscous damping in one cycle of harmonic vibration is

$$\begin{aligned} E_D = \int f_d du = \int_0^{2\pi/\omega} (c\dot{u})\dot{u}dt = \int_0^{2\pi/\omega} c\dot{u}^2 dt \\ = c\int_0^{2\pi/\omega} [\omega u_o cos(\omega t - \phi)]^2 dt = \pi c\omega u_o^2 = 2\pi\zeta\omega/\omega_n k u_o^2 \end{aligned} \tag{6.9}$$

In steady-state vibration, the energy input to the system due to the applied force is dissipated in viscous damping. The external force p(t) inputs energy to the system, which for each cycle of vibration is

$$\begin{aligned} E_I = \int p(t)du = \int_0^{2\pi/\omega} p(t)\dot{(u)}dt \\ = \int_0^{2\pi/\omega} [p_o sin\omega t][\omega u_o cos(\omega t - \phi)]dt = \pi p_o u_o sin\phi \end{aligned} \tag{6.10}$$

Over each cycle of harmonic vibration the changes in potential energy and kinetic energy are zero

$$\begin{aligned} E_s = \int f_s du = \int_0^{2\pi/\omega} (ku)\dot{u}dt = \int_0^{2\pi/\omega} k[u_o sin(\omega t - \phi)][\omega u_o cos(\omega t - \phi)]dt = 0 \\ E_k = \int f_1 du = \int_0^{2\pi/\omega} (m\ddot{u})\dot{(u)}dt = \int_0^{2\pi/\omega} m[-\omega^2 u_o sin(\omega t - \phi)][\omega u_o cos(\omega t - \phi)]dt = 0 \end{aligned} \tag{6.11}$$

For $\omega = \omega_n$,$\phi = 90^o$ and 6.10 gives

$$E_I = \pi p_o u_o \tag{6.12}$$

The input energy varies linearly with the displacement amplitude. In contrast the dissipated energy varies quadratic-ally with the displacement amplitude.

By equating Eq 6.9 and Eq 6.11

$$\pi p_o u_o = \pi c \omega_n u_o^2 \tag{6.13}$$

Solving for u_o leads to

$$u_o = p_o / c\omega_n \tag{6.14}$$

Graphical interpretation for the energy dissipated in viscous damping is solved by deriving an equation relating the damping force f_d to the displacement u:

$$f_D = c\dot{u}(t) = c\omega u_o cos(\omega t - \phi) = c\omega\sqrt{u_o^2 - u_o^2 sin^2(\omega t - \phi)} = c\omega\sqrt{u_o^2 - [u(t)]^2} \tag{6.15}$$

This can be rewritten as

$$(\frac{u}{u_o})^2 + (\frac{f_D}{c\omega u_o})^2 = 1 \tag{6.16}$$

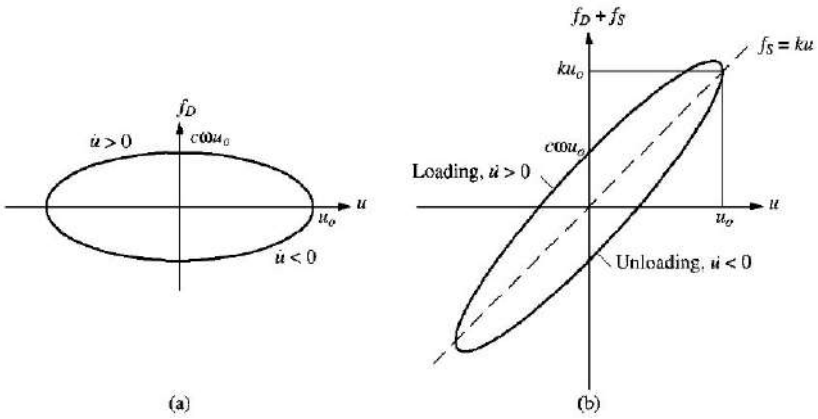

Figure 6.6: Damping and structural restoring forces.

Which is the equation of ellipse as shown in Fig 6.6 . Thus the area within the hysteresis loop gives the dissipated energy It is of interest to examine the total (elastic plus damping) resisting force that is measured in an experiment:

$$\begin{aligned} f_s + f_D &= ku(t) + c\dot{U}(t) \\ &= ku + c\omega\sqrt{(u_o)^2 - u^2} \end{aligned} \tag{6.17}$$

We mention two measures of damping: damping capacity and the specific damping factor. The specific damping capacity,E_d/E_{So},is that fractional part of the strain energy, E_{So}= $((ku_o^2)/2)$ which is dissipated during each cycle of motion; both E_D and E_{So}, are shown in figure 6.7. The specific damping factor, also known as the loss factor, is defined as

$$\zeta = \frac{E_D}{2\pi E_{So}} \tag{6.18}$$

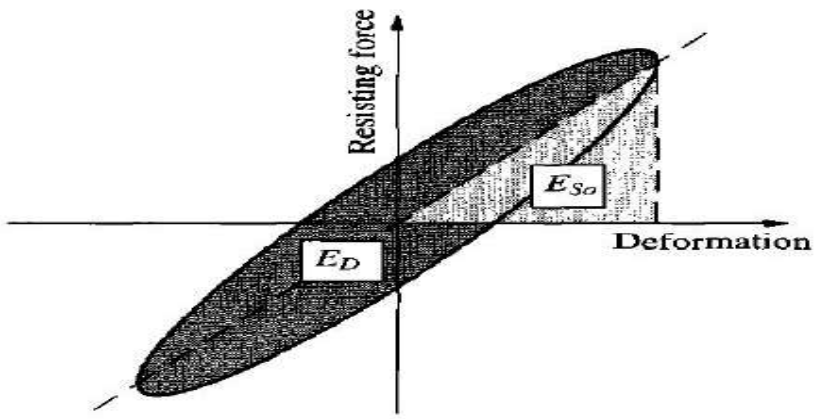

Figure 6.7: Definition of energy loss E_D in a cycle of harmonic vibration and maximum strain energy E_{So}

6.3 Characterization of Pneumatic Damper

Pneumatic Damper was purchased in order to understand the characteristics of it, pneumatic damper consists of two key,through which the damping capacity of the pneumatic damper can be increased.

Figure 6.8: Pneumatic Damper

Cyclic Load was given using Unconfined Compression Testing Machine available in Geotechnical Laboratory in Nirma University,In Unconfined Compression Testing Machine we can change the rate of Loading at 1.25mm/min ,1.5mm/min and 2.5mm/min, For this experiment we have kept the rate at 2.5mm/min and this experiment we have fully tightened the two keys in order to get maximum damping. Readings were taken at 1mm using Dial Gauge.S-Type Load cell was used to measure the Cyclic Loading. The Experimental Setup can be seen in the figure below 6.9.

We have obtained the Load-Displacement curve for 6 cycles,In this we have recorded the readings at each 1 mm displacement of the base of Unconfined Compression Testing Machine. One cycle consists of first displacement of 12 mm in one direction i.e the piston moves inwards and then 24 mm cycle in opposite direction i.e the piston moves outwards and then again 12 mm in which the piston moves inwards.The load displacement curve can be seen below, which is obtained for 6 Cycles.

Figure 6.9: Experimental Setup for applying Cyclic Load on Pneumatic Damper

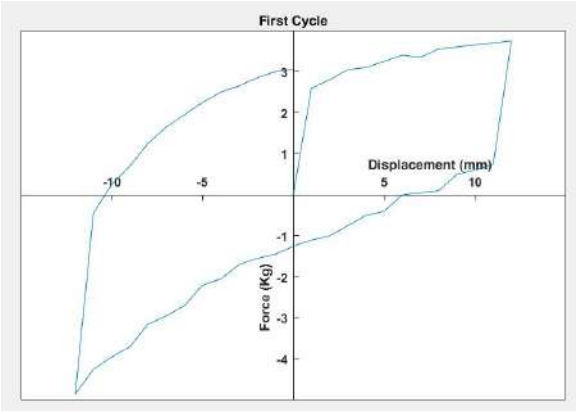

(a) Load Displacement curve of the First Cycle

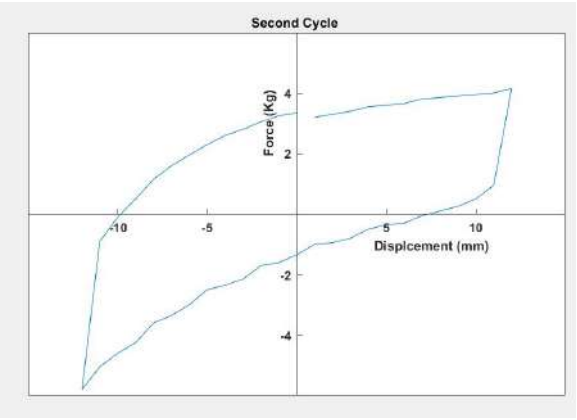

(b) Load Displacement curve of the Second Cycle

Figure 6.10: Load Displacement Curve of First Cycle and Second Cycle

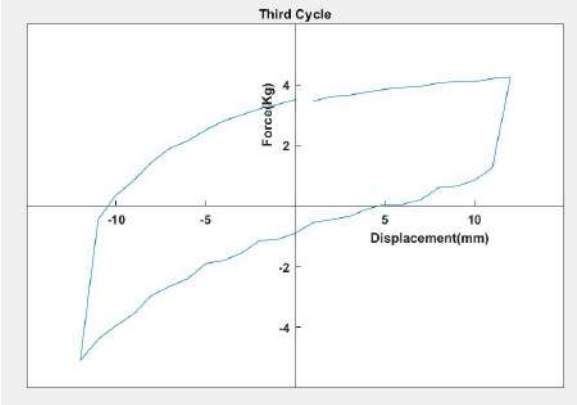

(a) Load Displacement curve of the Third Cycle

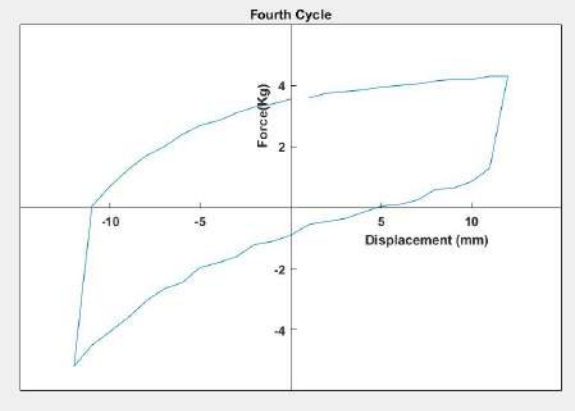

(b) Load Displacement curve of the Fourth Cycle

Figure 6.11: Load Displacement Curve of third Cycle and Fourth Cycle

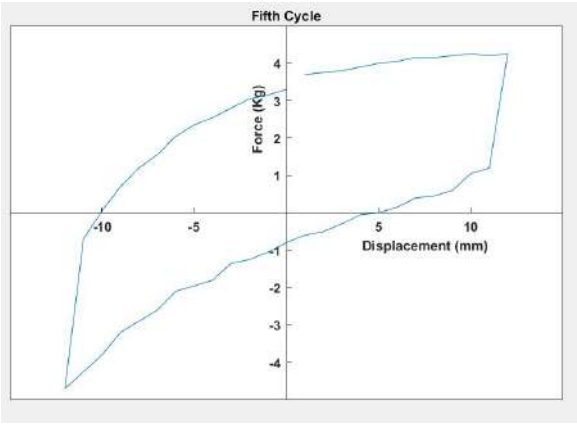

(a) Load Displacement curve of the Fifth Cycle

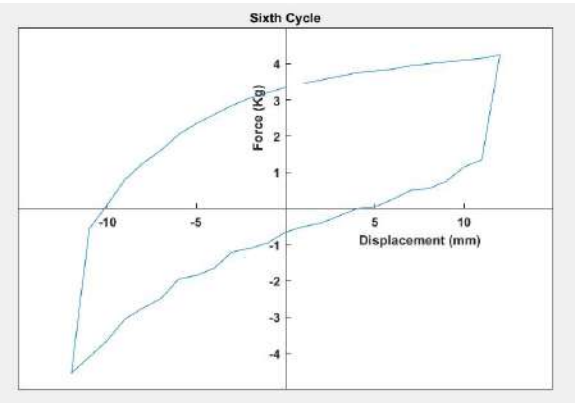

(b) Load Displacement curve of the Sixth Cycle

Figure 6.12: Load Displacement Curve of Fifth Cycle and Sixth Cycle

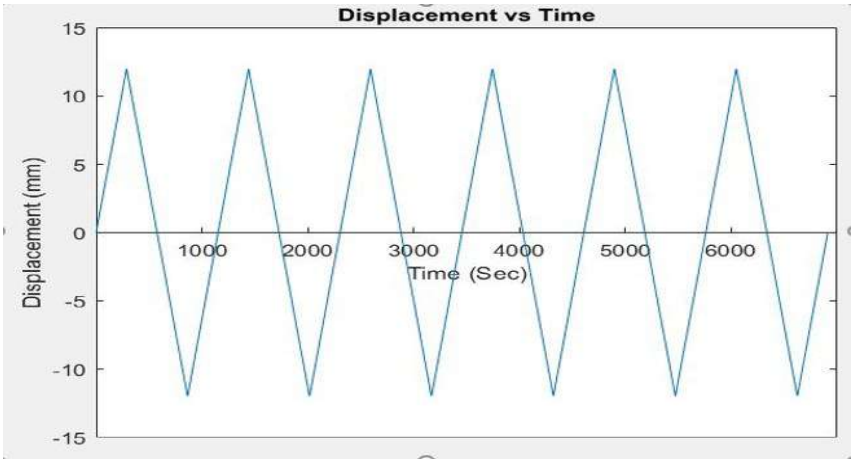

Figure 6.13: Input Displacement vs Time Graph

Table 6.1: Damping Ratio of Pneumatic Damper

Sr.No	$E_d(Kg-mm)$	$P_{max}(Kg)$	$P_{min}(Kg)$	$D_{max}(mm)$	$D_{min}(mm)$	$K_{eff}(Kg/mm)$	ζ
1	88.825	3.75	-4.85	12	-12	0.358	0.274
2	99.4	4.15	-5.8	12	-12	0.414	0.265
3	93.3	4.25	-5.1	12	-12	0.389	0.265
4	97.4	4.3	-5.2	12	-12	0.3958	0.272
5	90.85	4.25	-4.7	12	-12	0.3729	0.269
6	86.85	4.25	-4.55	12	-12	0.367	0.2575

$$K_{eff} = \frac{|P_{max}| - |P_{min}|}{|D_{max}| - |D_{min}|} \tag{6.19}$$

$$\zeta = \frac{1}{4\prod}\frac{E_d}{E_s} = \frac{1}{2\prod}\frac{E_d}{K_{eff}D^2} \tag{6.20}$$

The above Equations has been taken from the Literature of Reza Aghlara and Mahmood Tahir [7] which has also been mentioned in Literature Review.

ζ_{avg} has been found out to be 0.267

6.4 Characterization of Piston Type Damper

Figure 6.14: Piston Damper

Cyclic Load was given using Unconfined Compression Testing Machine available in Geotechnical Laboratory in Nirma University,In Unconfined Compression Testing Machine we can change the rate of Loading at 1.25mm/min ,1.5mm/min and 2.5mm/min, For this experiment we have kept the rate at 2.5mm/min and this experiment. Readings were taken at 1mm using Dial Gauge.S-Type Load cell was used to measure the Cyclic Loading. The Experimental Setup can be seen in the figure below 6.15.

We have obtained the Load-Displacement curve for 6 cycles,In this we have recorded the readings at each 1 mm displacement of the base of Unconfined Compression Testing Machine. One cycle consists of first displacement of 12 mm in one direction i.e the piston moves inwards and then 24 mm cycle in opposite direction i.e the piston moves outwards and then again 12 mm in which the piston moves inwards.The load displacement curve can be seen below, which is obtained for 6 Cycles.

Figure 6.15: Experimental Setup for applying Cyclic Load on Pneumatic Damper

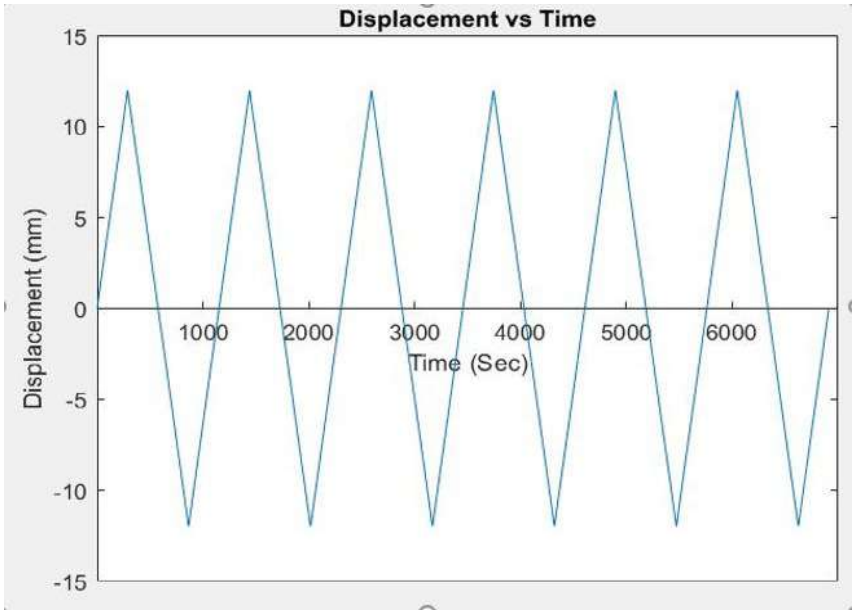

Figure 6.19: Input Displacement vs Time Graph

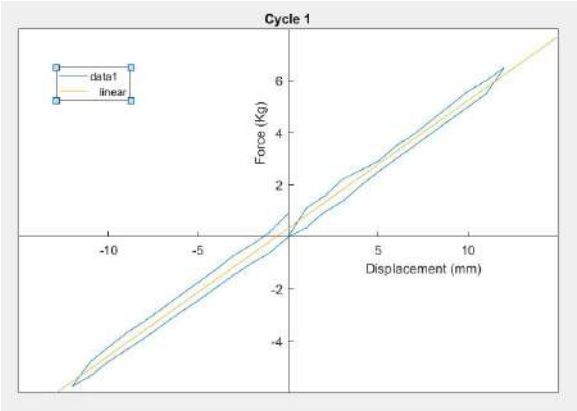

(a) Load Displacement curve of the First Cycle

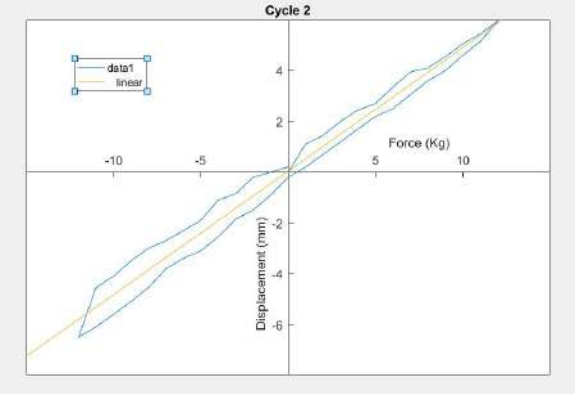

(b) Load Displacement curve of the Second Cycle

Figure 6.16: Load Displacement Curve of First Cycle and Second Cycle

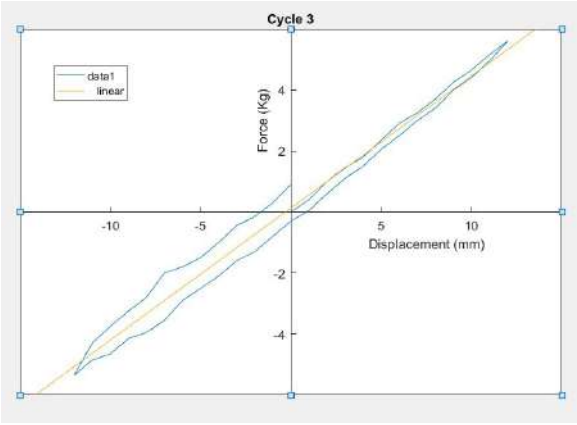

(a) Load Displacement curve of the Third Cycle

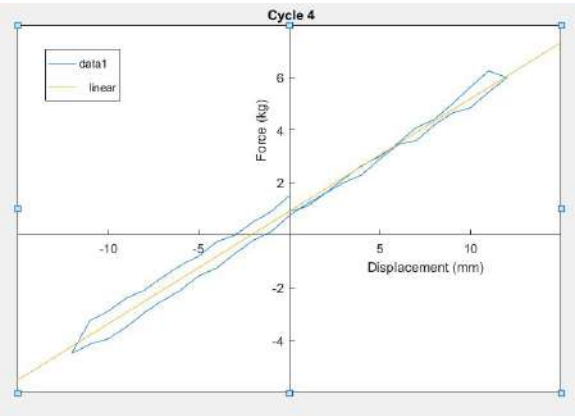

(b) Load Displacement curve of the Fourth Cycle

Figure 6.17: Load Displacement Curve of third Cycle and Fourth Cycle

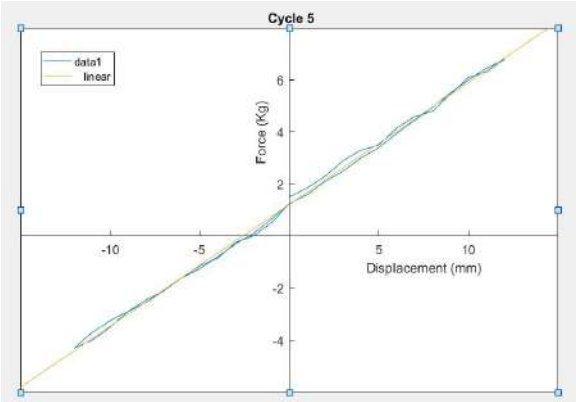

(a) Load Displacement curve of the Fifth Cycle

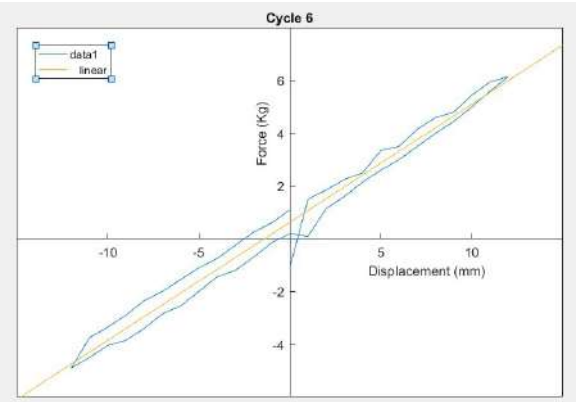

(b) Load Displacement curve of the Sixth Cycle

Figure 6.18: Load Displacement Curve of Fifth Cycle and Sixth Cycle

Table 6.2: Damping Ratio of Piston Type Damper

Cycle	X	Y	Area	ζ	ζ_{avg}
1	11.49	5.174	14.1	.0654	.0646
2	11.89	5.824	21.8	.1002	
3	10.48	4.667	15.75	.1025	
4	11.89	6.005	6.72	.0230	
5	11.89	6.787	1.985	.00782	
6	10.69	5.411	16.115	.0887	

The above calculation of ζ are taken from the theory given above in this chapter.Figure 6.6 and Equation 6.18 shown above in the theory has been used in this calculation.By using curve fit on the above Load vs Displacement curve, co-ordinate X and Y were found out using which E_{so} were found out. Area were found out in MATLAB using Poly-area command and from Equation 6.18, ζ were found out.

6.5 Summary

In the above chapter, an effort has been made to evaluate the damping of Pneumatic Type damper and Piston Type damper.Cyclic Load was given to the Damper and Load vs Displacement was plotted through which ζ was found out.

Chapter 7

Structural Response control of Asymmetric structural system using passive energy dampers

7.1 General

Structural System when subjected to Earthquake excitation's results in excessive damage of the Structure's.In order to reduce the response of structural systems active dampers or passive dampers are generally attached to the structural systems, which helps in dissipation of energy of the structural system.

Pneumatic dampers were attached to the Single storey bare SDOF system and SDOF system having planar and geometrical irregularities. Free and Forced vibrations were given to the Structural system and comparison of the Damping Ratio and Response of the structural systems are done.

7.2 Free Vibration Test

Initial Displacement were given to the structural system and response of the structural system are captured, Using Logarithmic decrement Method, damping were evaluated, We have attached dampers as bracing's , in which at first single pneumatic damper were attached to the structural system and then response were captured after that two pneu-

matic dampers were attached as bracing's to the structural systems and then Dynamic Properties were evaluated.

7.2.1 SDOF System with Single Pneumatic Damper

Below figure 7.1 shows the SDOF System with Single Pneumatic Damper

Figure 7.1: SDOF System with Single Pneumatic Damper

Simple Bare SDOF system having single pneumatic damper was attached to the Shake table using Allen screws and free vibrations were imparted to it. Response were captured in LabVIEW Software, Response obtained from LabVIEW are shown in below figure 7.2.

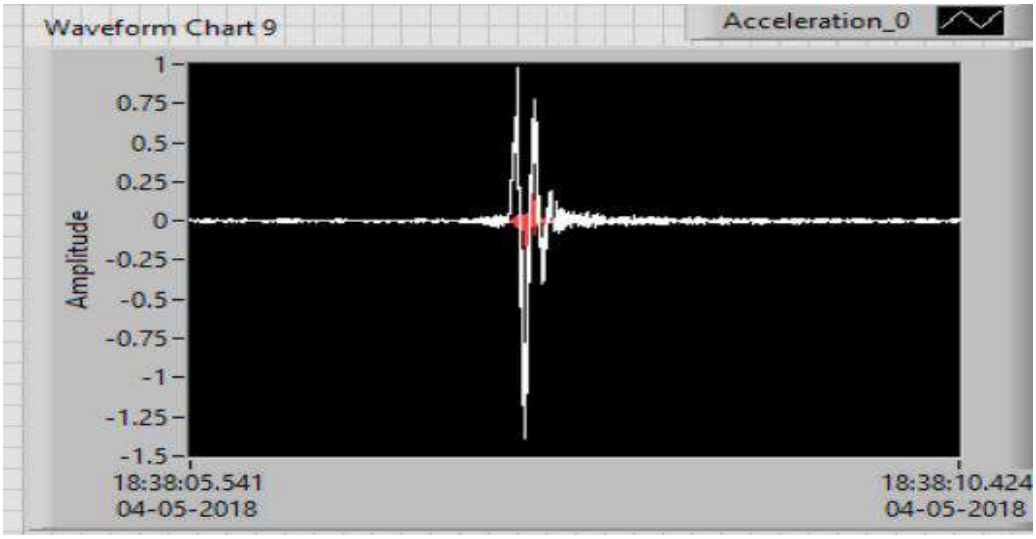

Figure 7.2: Acceleration Response of SDOF system with single pneumatic damper

After capturing Acceleration response of the SDOF system, Splitting of the response and Extraction of the Acceleration response were done in LabVIEW Software which is presented in the below Figure 7.3.

Figure 7.3: Extracted Acceleration Response of SDOF System with single pneumatic damper

Fast Fourier Transformation of the Extracted Response were done in LabVIEW from Power Spectrum Pallet in LabVIEW. Through which we can obtain the Frequency of the SDOF Bare model having Single Pneumatic Damper attached to it. Figure 7.4 below shows the Fast Fourier Transformation of the system,

Coefficient of Damping (ζ) can be calculated with the help of Logarithmic decrement

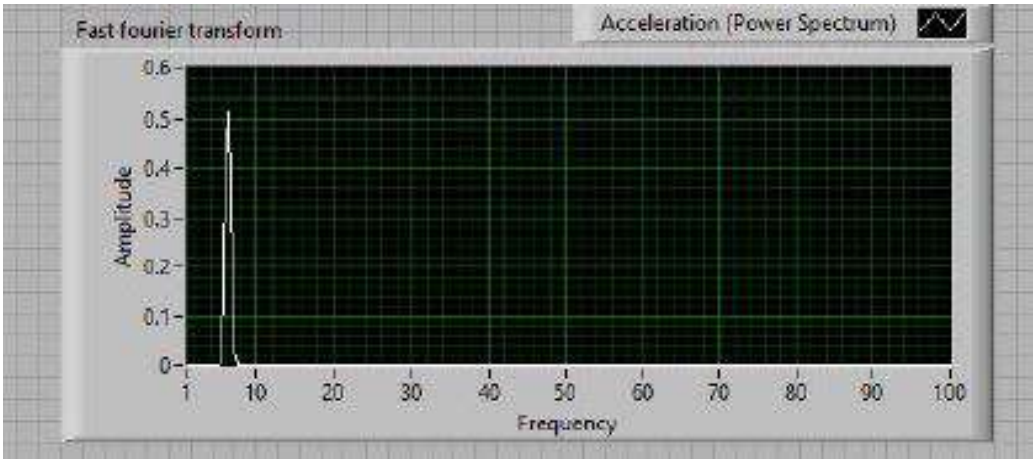

Figure 7.4: Fundamental Frequency Extraction for Bare Regular SDOF Model with single pneumatic damper Through Fast Fourier Transform Techniques

method. There were only two peaks which were captured through which Coefficient of Damping were Calculated, ζ was found out to be as 23.551% and frequency were calculated as 8.49 Hz.

7.2.2 SDOF System with Double Pneumatic Damper

Below figure 7.5 shows the SDOF System with Double Pneumatic Damper

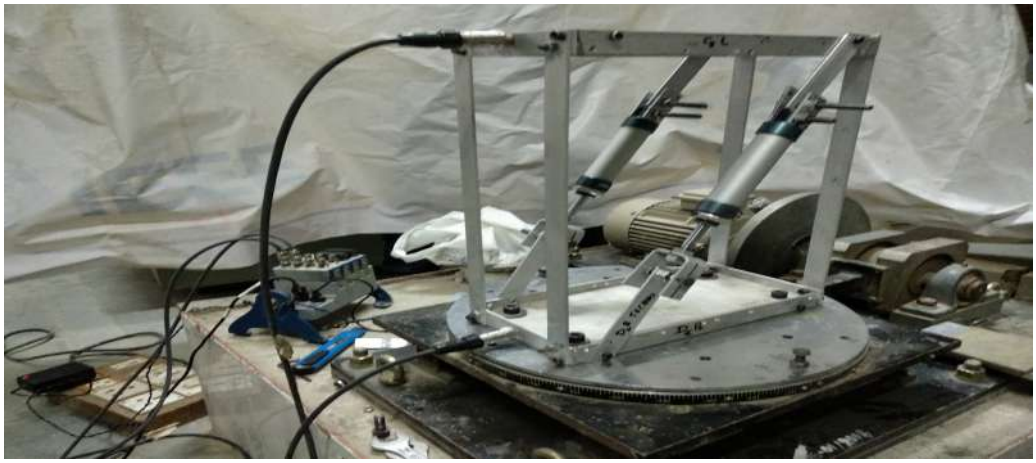

Figure 7.5: SDOF System with Double Pneumatic Damper

Simple Bare SDOF system with double pneumatic damper was attached to the Shake table using Allen screws and free vibrations were imparted to it. Response were captured

in LabVIEW Software, Response obtained from LabVIEW are shown in below figure 7.6.

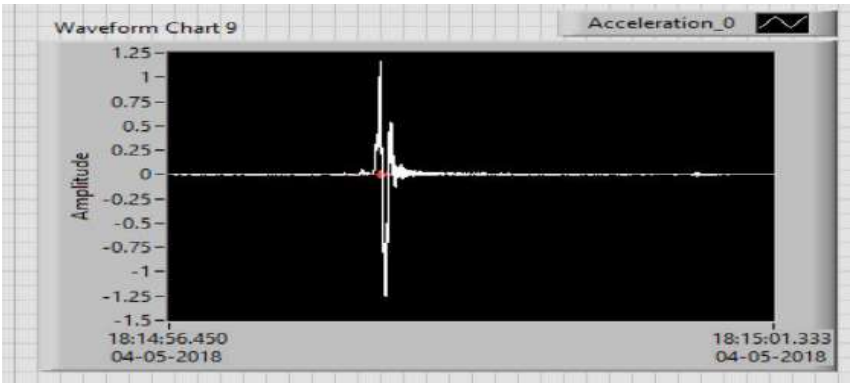

Figure 7.6: Acceleration Response of SDOF system with double pneumatic damper

After capturing Acceleration response of the SDOF system having double pneumatic damper attached to it, Splitting and Extraction of the Acceleration response were done in LabVIEW Software which is presented in the below Figure 7.7.

Figure 7.7: Extracted Acceleration Response of SDOF System with double pneumatic damper

Fast Fourier Transformation of the Extracted Response were done in LabVIEW from Power Spectrum Pallet in LabVIEW. Through which we can obtain the Frequency of the SDOF Bare model having Double Pneumatic Damper attached to it. Figure 7.8 below shows the Fast Fourier Transformation of the system,

Coefficient of Damping (ζ) can be calculated with the help of Logarithmic decrement method. There were only two peaks which were captured through which Coefficient of

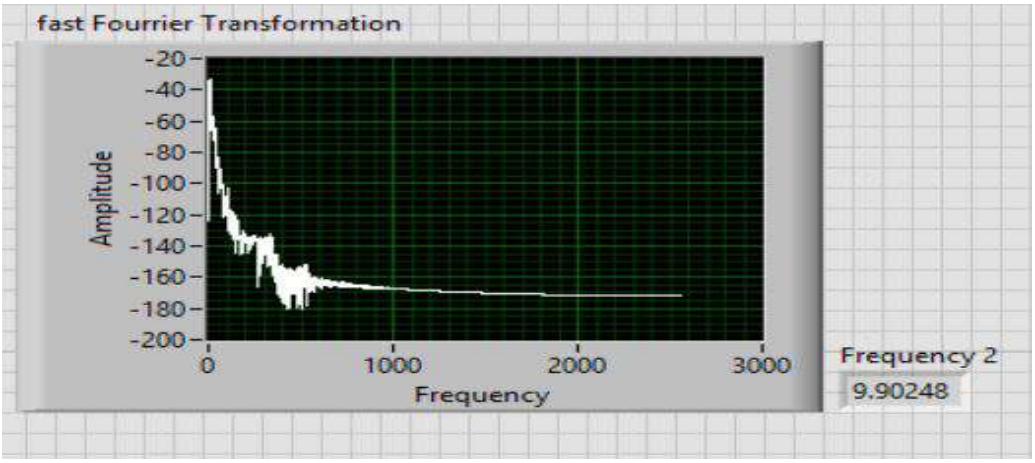

Figure 7.8: Fundamental Frequency Extraction for Bare Regular SDOF Model with double pneumatic damper Through Fast Fourier Transform Techniques

Damping were Calculated, ζ was found out to be as 59.822% and frequency were calculated as 9.9 Hz.

7.2.3 SDOF System with material irregularity with single Pneumatic Damper

Below figure 7.9 shows the SDOF System with material irregularity with Single Pneumatic Damper

Figure 7.9: SDOF System with material irregularity with Single Pneumatic Damper

SDOF system with material irregularity having single pneumatic damper was attached to the Shake table using Allen screws and free vibrations were imparted to it. Response were captured in LabVIEW Software, Response obtained from LabVIEW are shown in below figure 7.10.

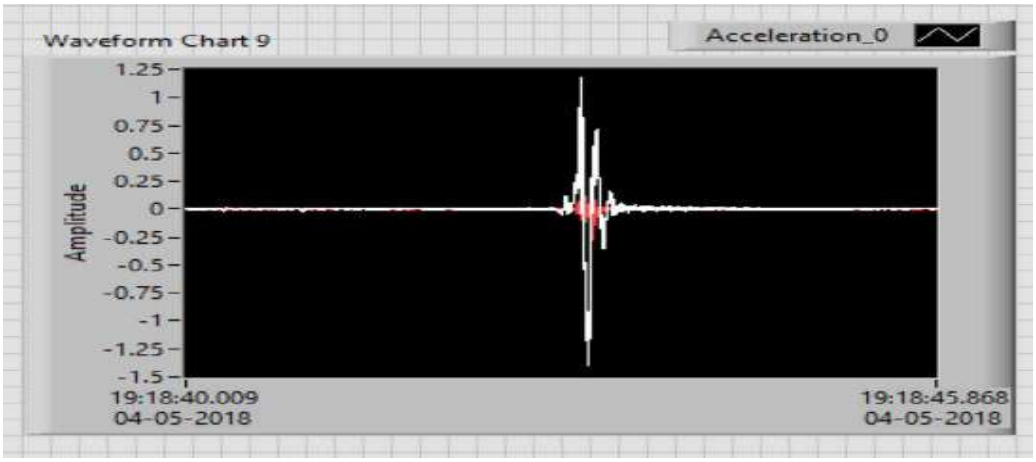

Figure 7.10: Acceleration Response of SDOF system with material Irregularity with single Pneumatic Damper

After capturing Acceleration response of the SDOF system with material irregularity, Splitting of the response and Extraction of the Acceleration response were done in LabVIEW Software which is presented in the below Figure 7.11.

Figure 7.11: Extracted Acceleration Response of SDOF system with material Irregularity with single Pneumatic Damper

Fast Fourier Transformation of the Extracted Response were done in LabVIEW from Power Spectrum Pallet in LabVIEW. Through which we can obtain the Frequency of the SDOF model with material irregularity having Single Pneumatic Damper attached to it. Figure 7.12 below shows the Fast Fourier Transformation of the system,

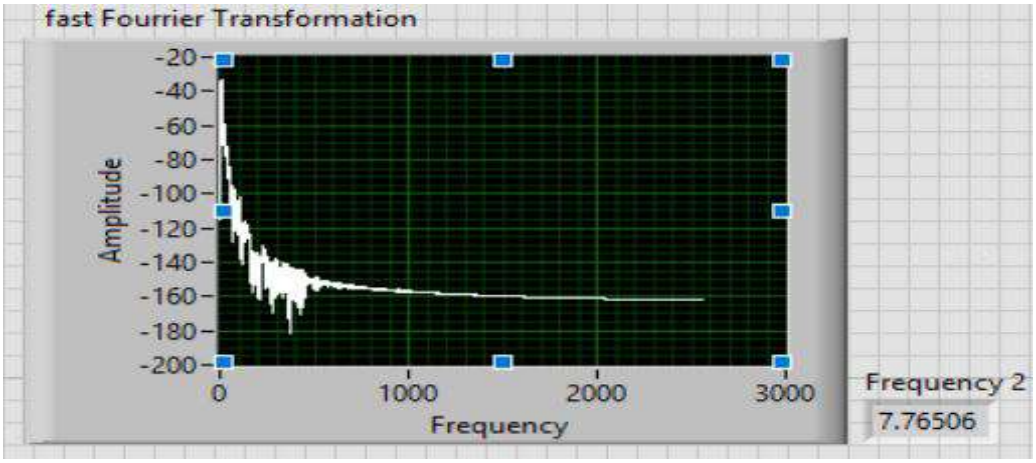

Figure 7.12: Fundamental Frequency Extraction for SDOF Model with material Irregularity with single Pneumatic Damper Through Fast Fourier Transform Techniques

Coefficient of Damping (ζ) can be calculated with the help of Logarithmic decrement method. There were only two peaks which were captured through which Coefficient of Damping were Calculated, ζ was found out to be as 24.058% and frequency were calculated as 7.76 Hz.

7.2.4 SDOF System with material irregularity with Double Pneumatic Damper

Below figure 7.13 shows the SDOF System with material irregularity with Double Pneumatic Damper

SDOF system having material irregularity with double pneumatic damper was attached to the Shake table using Allen screws and free vibrations were imparted to it. Response were captured in LabVIEW Software, Response obtained from LabVIEW are shown in below figure 7.14.

Figure 7.13: SDOF System with material irregularity with Double Pneumatic Damper

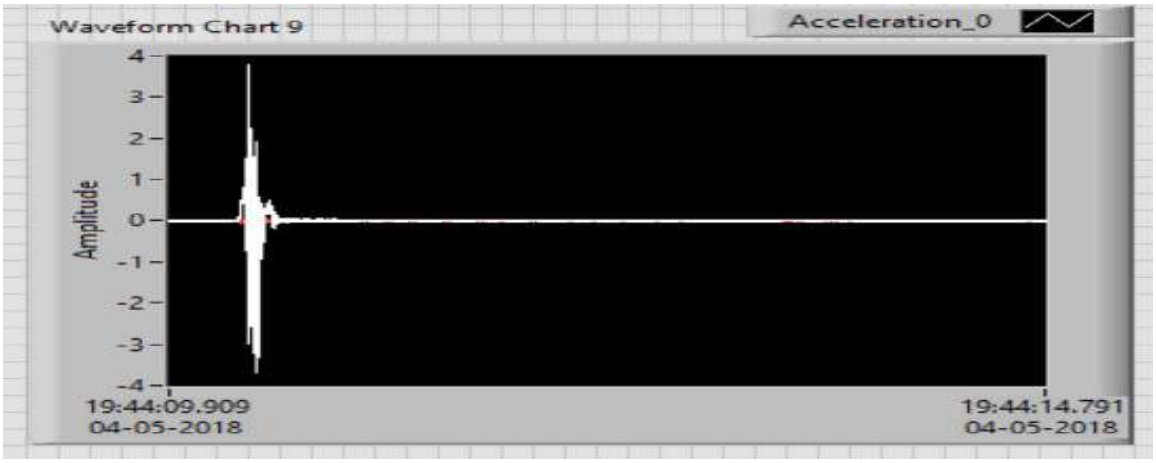

Figure 7.14: Acceleration Response of SDOF system with material Irregularity with Double Pneumatic Damper

After capturing Acceleration response of the SDOF system with material irregularity having double pneumatic damper attached to it, Splitting of the response and Extraction of the Acceleration response were done in LabVIEW Software which is presented in the below Figure 7.15.

Fast Fourier Transformation of the Extracted Response were done in LabVIEW from

Figure 7.15: Extracted Acceleration Response of SDOF system with material Irregularity with Double Pneumatic Damper

Power Spectrum Pallet in LabVIEW. Through which we can obtain the Frequency of the SDOF model with material irregularity having Double Pneumatic Damper attached to it. Figure 7.16 below shows the Fast Fourier Transformation of the system,

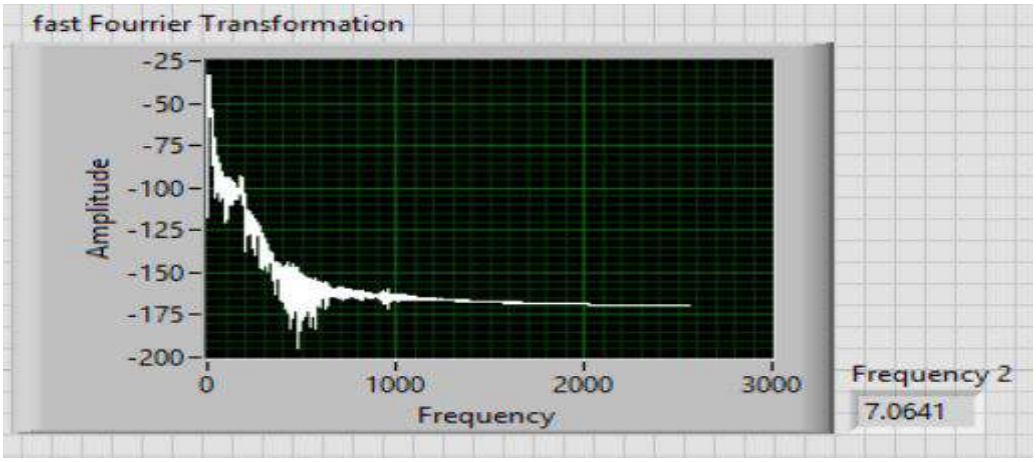

Figure 7.16: Fundamental Frequency Extraction for SDOF Model with material Irregularity with Double Pneumatic Damper Through Fast Fourier Transform Techniques

Coefficient of Damping (ζ) can be calculated with the help of Logarithmic decrement method. There were only two peaks which were captured through which Coefficient of Damping were Calculated, ζ was found out to be as 46.83% and frequency were calculated as 7.06 Hz.

7.2.5 SDOF System with L Planar As-symmetry with Single Pneumatic Damper

Below figure 7.17 shows the SDOF System with Planar Asymmetry L -Shape with Single Pneumatic Damper

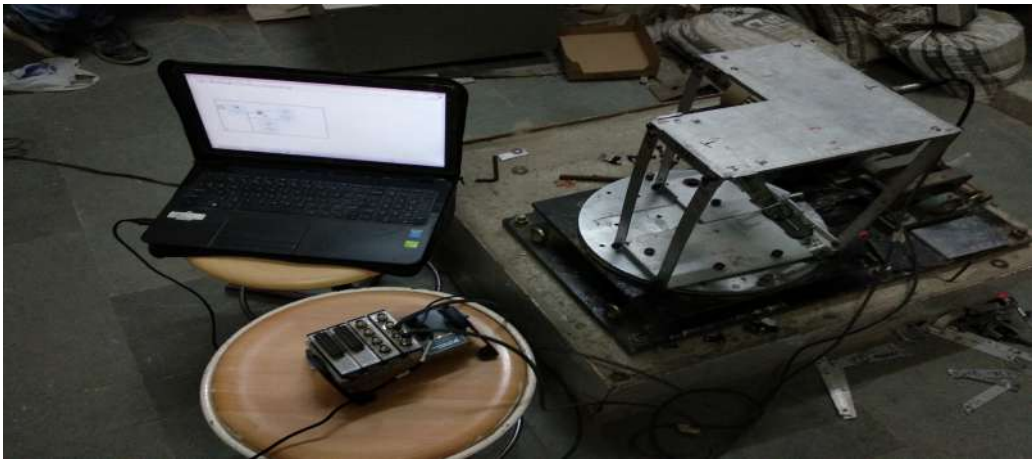

Figure 7.17: SDOF System with Planar Asymmetry L -Shape with Single Pneumatic Damper

SDOF system with Planar Irregularity of L Shape having single pneumatic damper was attached to the Shake table using Allen screws and free vibrations were imparted to it. Response were captured in LabVIEW Software, Response obtained from LabVIEW are shown in below figure 7.18.

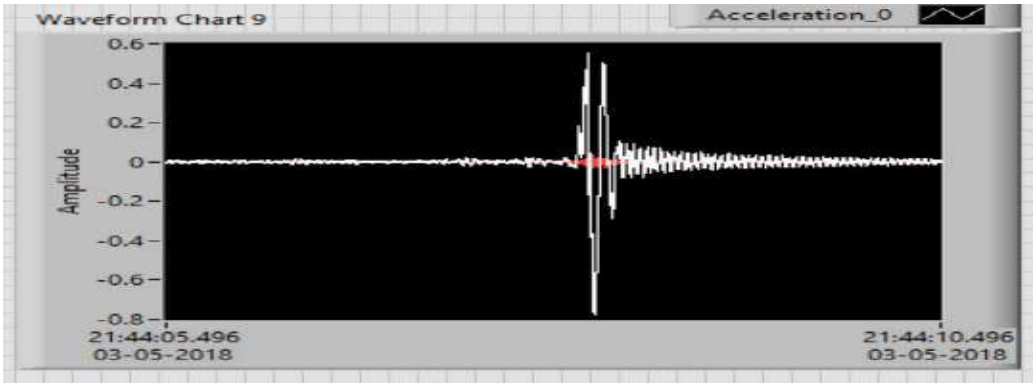

Figure 7.18: Acceleration Response of SDOF system with L Planar Asymmetry with single Pneumatic Damper

After capturing Acceleration response of the SDOF system with Planar irregularity L-Shape, Splitting of the response and Extraction of the Acceleration response were done in LabVIEW Software which is presented in the below Figure 7.19.

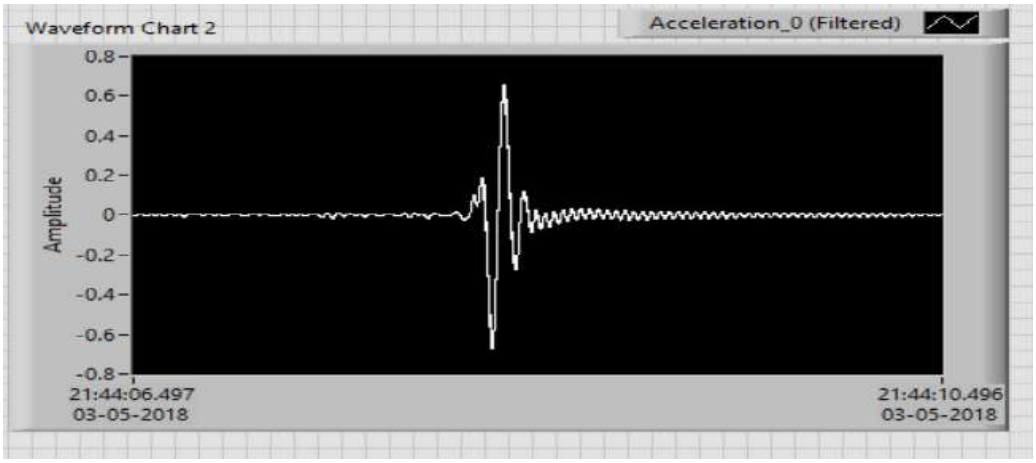

Figure 7.19: Extracted Acceleration Response of SDOF system with L Planar Asymmetry with single Pneumatic Damper

Fast Fourier Transformation of the Extracted Response were done in LabVIEW from Power Spectrum Pallet in LabVIEW. Through which we can obtain the Frequency of the SDOF with Planar irregularity L-shape having Single Pneumatic Damper attached to it. Figure 7.20 below shows the Fast Fourier Transformation of the system,

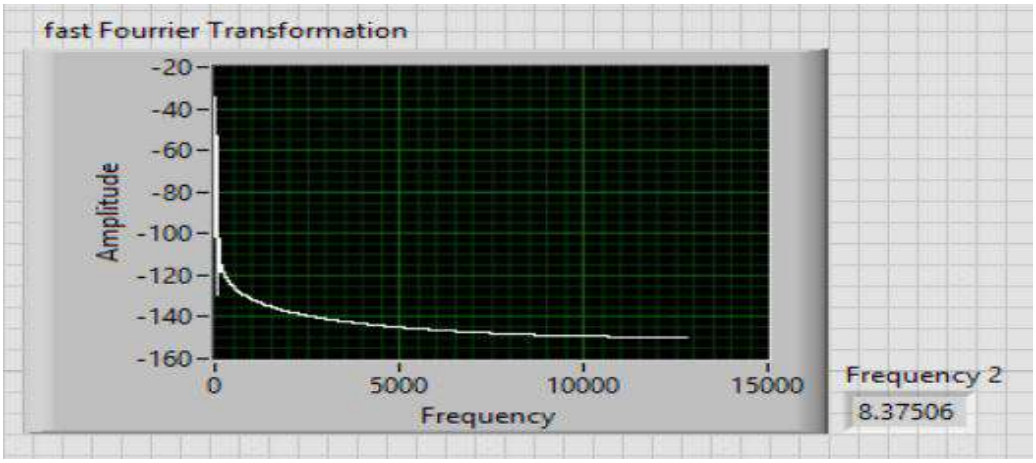

Figure 7.20: Fundamental Frequency Extraction for SDOF Model with L Planar Asymmetry with single Pneumatic Damper Through Fast Fourier Transform Techniques

Coeffcient of Damping (ζ) can be calculated with the help of Logarithmic decrement method. There were only two peaks which were captured through which Coefficient of Damping were Calculated, ζ was found out to be as 21.11% and frequency were calculated as 8.37 Hz.

7.2.6 SDOF System with L Planar As-symmetry with Double Pneumatic Damper

Below figure 7.21 shows the SDOF System with Planar Asymmetry L -Shape with Double Pneumatic Damper

Figure 7.21: SDOF System with Planar Asymmetry L -Shape with Double Pneumatic Damper

SDOF system having Planar asymmetry having double pneumatic damper was attached to the Shake table using Allen screws and free vibrations were imparted to it. Response were captured in LabVIEW Software, Response obtained from LabVIEW are shown in below figure 7.22.

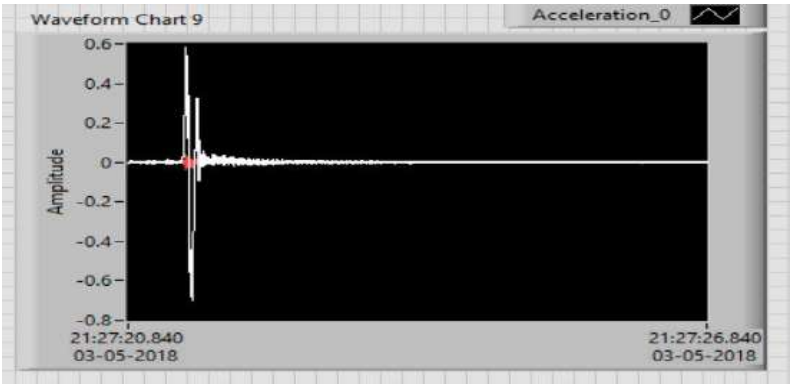

Figure 7.22: Acceleration Response of SDOF system with L Planar asymmetry with Double Pneumatic Damper

After capturing Acceleration response of the SDOF system with planar irregularity L-shape having double pneumatic damper attached to it, Splitting of the Acceleration response and Extraction of the Acceleration response were done in LabVIEW Software which is presented in the below Figure 7.23.

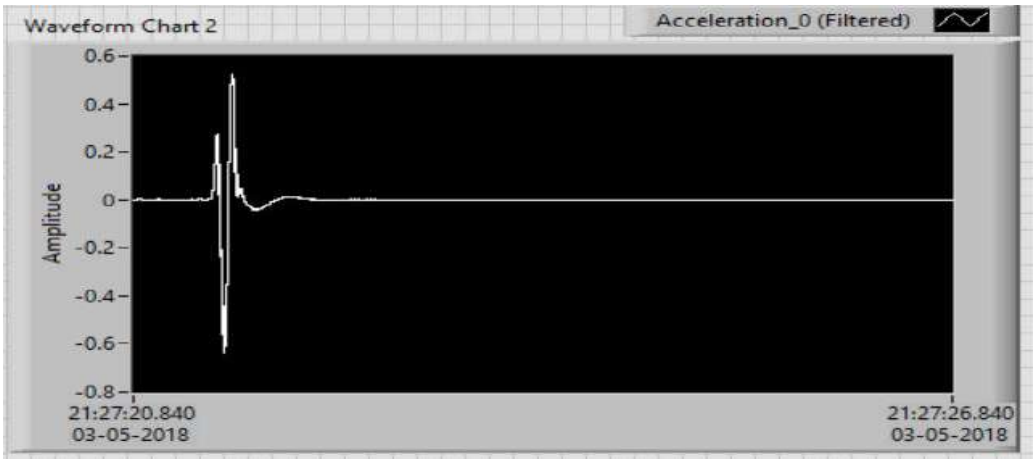

Figure 7.23: Extracted Acceleration Response of SDOF system with L Planar asymmetry with Double Pneumatic Damper

Fast Fourier Transformation of the Extracted Response were done in LabVIEW from Power Spectrum Pallet in LabVIEW. Through which we can obtain the Frequency of the SDOF model with planar irregularity L-shape having Double Pneumatic Damper attached to it. Figure 7.24 below shows the Fast Fourier Transformation of the system,

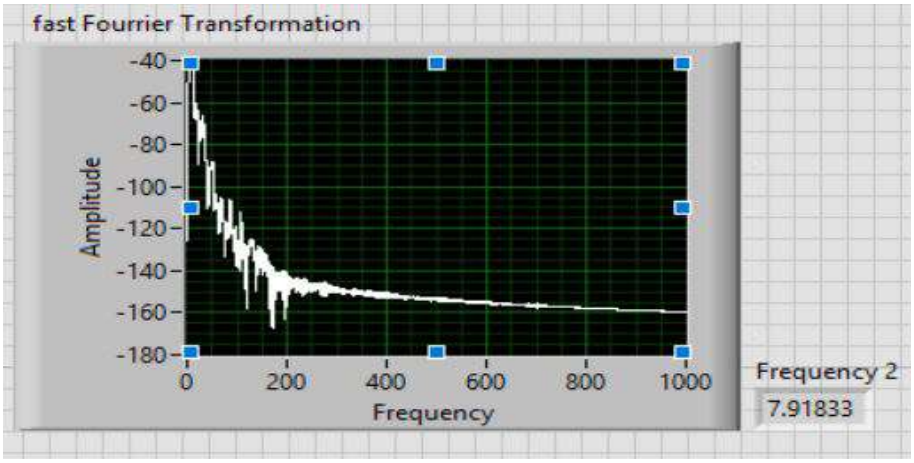

Figure 7.24: Fundamental Frequency Extraction for SDOF Model with L Planar asymmetry with Double Pneumatic Damper Through Fast Fourier Transform Techniques

Coefficient of Damping (ζ) can be calculated with the help of Logarithmic decrement method. There were only two peaks which were captured through which Coefficient of Damping were Calculated, ζ was found out to be as 47.071% and frequency were calculated as 7.92 Hz.

7.2.7 SDOF System with T Planar As-symmetry with Single Pneumatic Damper

Below figure 7.25 shows the SDOF System with Planar Asymmetry L -Shape with Single Pneumatic Damper

SDOF system with Planar asymmetry T-Shape having single pneumatic damper was attached to the Shake table using Allen screws and free vibrations were imparted to it. Response were captured in LabVIEW Software, Response obtained from LabVIEW are shown in below figure 7.26.

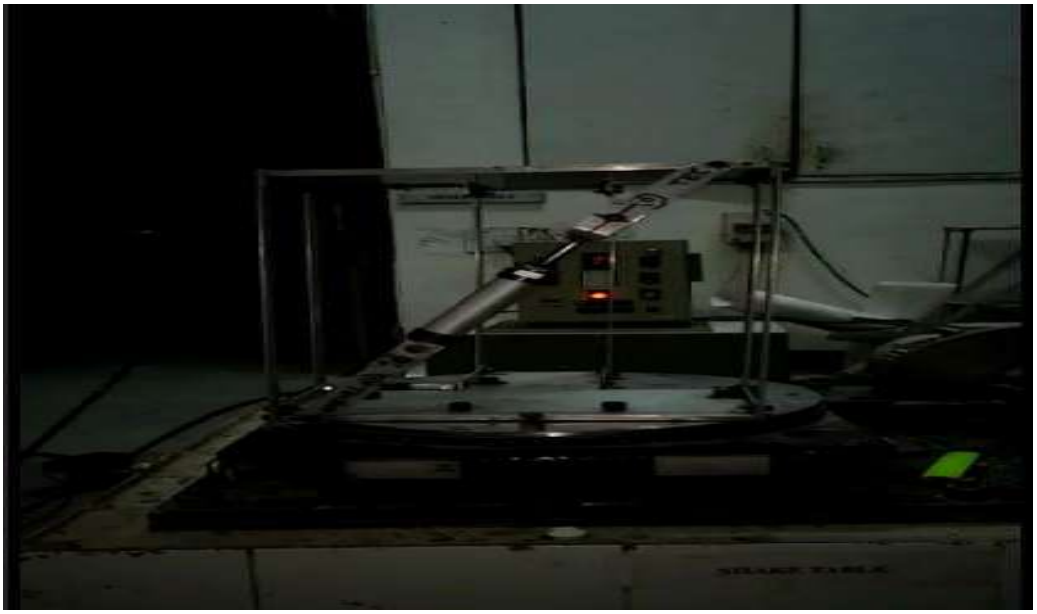

Figure 7.25: SDOF System with Planar Asymmetry L -Shape with Single Pneumatic Damper

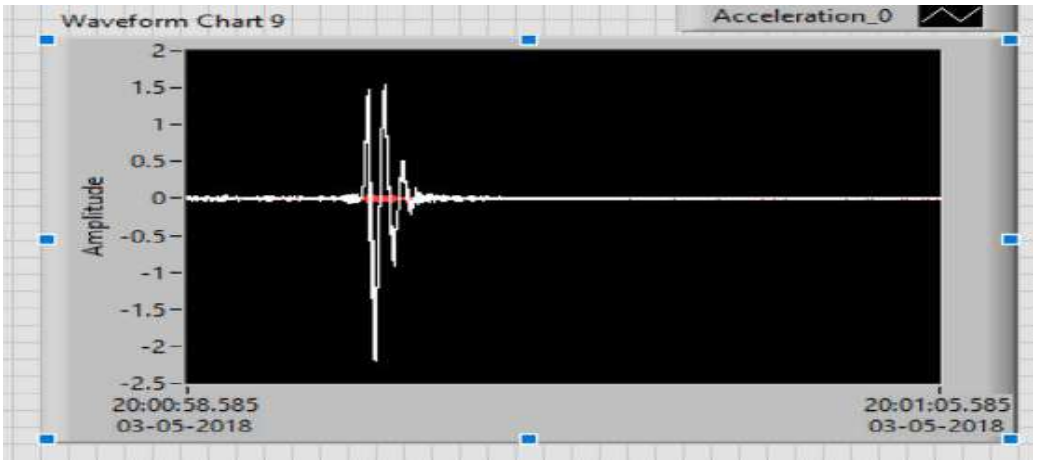

Figure 7.26: Acceleration Response of SDOF system with T Planar Asymmetry with single Pneumatic Damper

After capturing Acceleration response of the SDOF system with Planar asymmetry T-Shape having single Pneumatic Damper, Splitting of the Acceleration response and Extraction of the Acceleration response were done in LabVIEW Software which is presented in the below Figure 7.27.

Fast Fourier Transformation of the Extracted Response were done in LabVIEW from

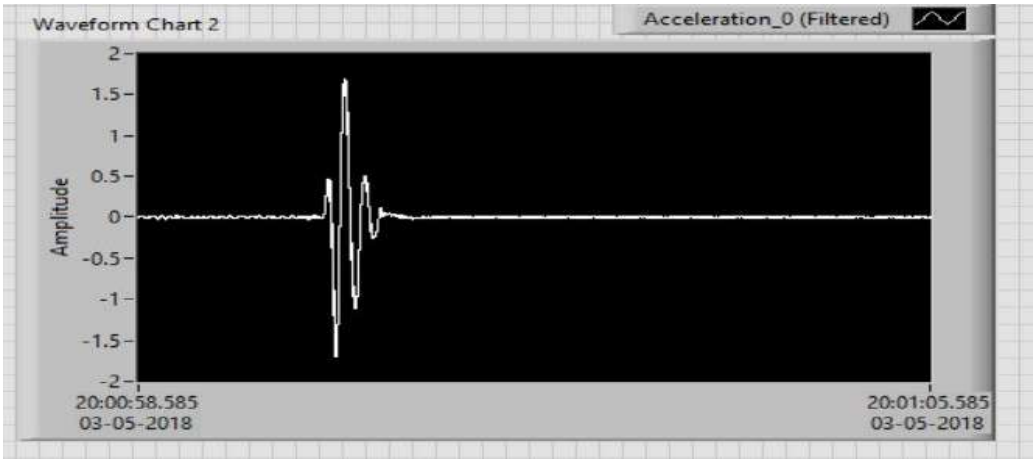

Figure 7.27: Extracted Acceleration Response of SDOF system with T Planar Asymmetry with single Pneumatic Damper

Power Spectrum Pallet in LabVIEW. Through which we can obtain the Frequency of the SDOF model with Planar Irregularity having Single Pneumatic Damper attached to it. Figure 7.28 below shows the Fast Fourier Transformation of the system,

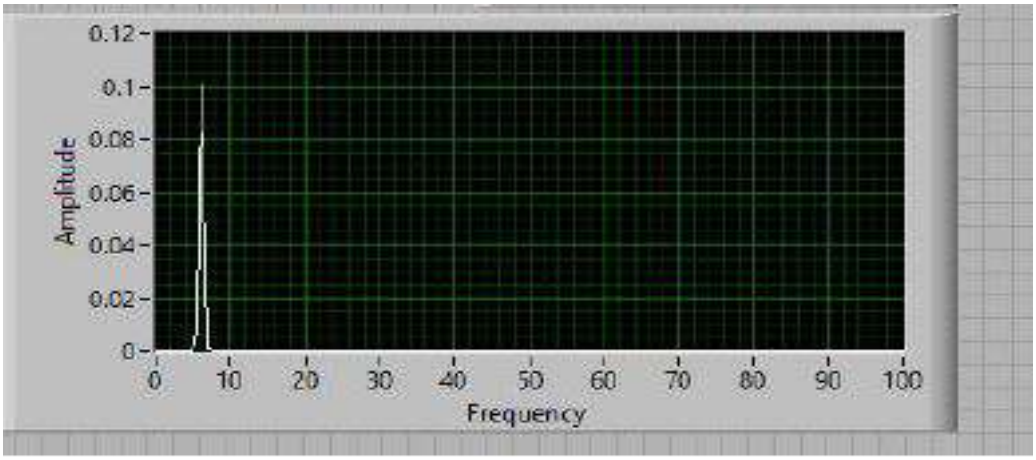

Figure 7.28: Fundamental Frequency Extraction for SDOF Model with T Planar Asymmetry with single Pneumatic Damper Through Fast Fourier Transform Techniques

Coeffcient of Damping (ζ) can be calculated with the help of Logarithmic decrement method. There were only two peaks which were captured through which Coefficient of Damping were Calculated, ζ was found out to be as 24.105% and frequency were calculated as 7.4 Hz.

7.2.8 SDOF System with T Planar Asymmetry with Double Pneumatic Damper

Below figure 7.29 shows the SDOF System with Planar Asymmetry T -Shape with Double Pneumatic Damper.

Figure 7.29: SDOF System with Planar Asymmetry T -Shape with Double Pneumatic Damper

SDOF system with Planar asymmetry T-shape having double pneumatic damper was attached to the Shake table using Allen screws and free vibrations were imparted to it. Response were captured in LabVIEW Software, Response obtained from LabVIEW are shown in below figure 7.30.

Figure 7.30: Acceleration Response of SDOF system with T Planar asymmetry with Double Pneumatic Damper

After capturing Acceleration response of the SDOF system with Planar asymmetry T Shape having double pneumatic damper attached to it, Splitting and Extraction of the Acceleration response were done in LabVIEW Software which is presented in the below Figure 7.31.

Figure 7.31: Extracted Acceleration Response of SDOF system with T Planar asymmetry with Double Pneumatic Damper

Fast Fourier Transformation of the Extracted Response were done in LabVIEW from Power Spectrum Pallet in LabVIEW. Through which we can obtain the Frequency of the SDOF model having T-planar asymmetry having Double Pneumatic Damper attached to it. Figure 7.32 below shows the Fast Fourier Transformation of the system,
Coefficient of Damping (ζ) can be calculated with the help of Logarithmic decrement method. There were only two peaks which were captured through which Coefficient of Damping were Calculated, ζ was found out to be as 41.94% and frequency were calculated as 8.42 Hz.

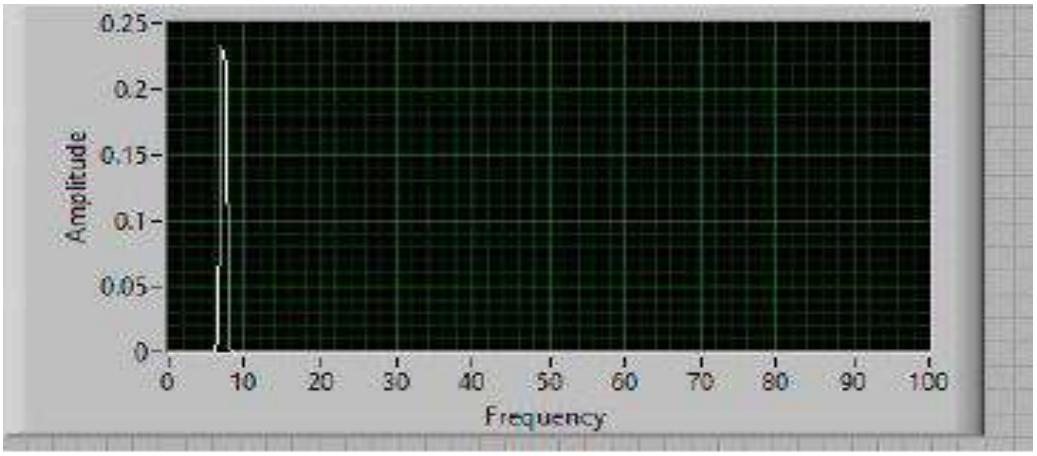

Figure 7.32: Fundamental Frequency Extraction for SDOF Model with T Planar asymmetry with Double Pneumatic Damper Through Fast Fourier Transform Techniques

7.3 Forced Vibration Test

For understanding the dynamic behaviour of SDOF irregular building models, force vibration test is carried out on the building model under harmonic base excitation.Dynamic behaviour of all the SDOF irregular building models at various frequency has been observed.At the condition of resonance,All irregular building model gives maximum acceleration response.

In this section, comparison of Transmissibility plots of each building model having single and double pneumatic damper and also building model without damper has been included for the comparison.

7.3.1 SDOF System with Pneumatic Damper

SDOF system was attached to Shake table using Allen screws and Harmonic excitation's were given to the SDOF system.Comparison of Transmissiblity ratio of SDOF Building model with Single and Double pneumatic damper and also its comparison was done for SDOF Building Model without Pneumatic Damper . Figure 7.34 shows the results of SDOF building model with and without Pneumatic damper.

(a) Experimental setup of SDOF building model with single Pneumatic Damper

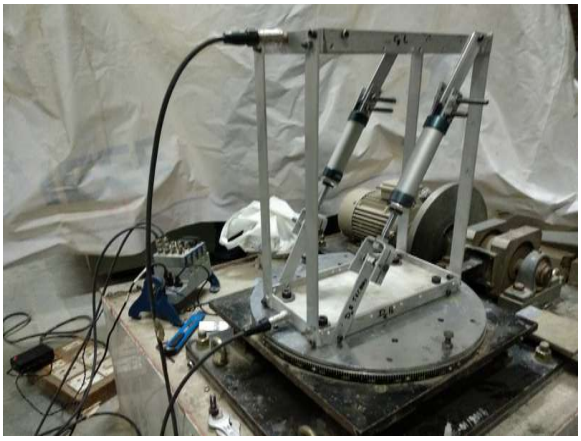

(b) Experimental setup of SDOF building model with double Pneumatic Damper

Figure 7.33: Experimental setup of SDOF system with Pneumatic Damper

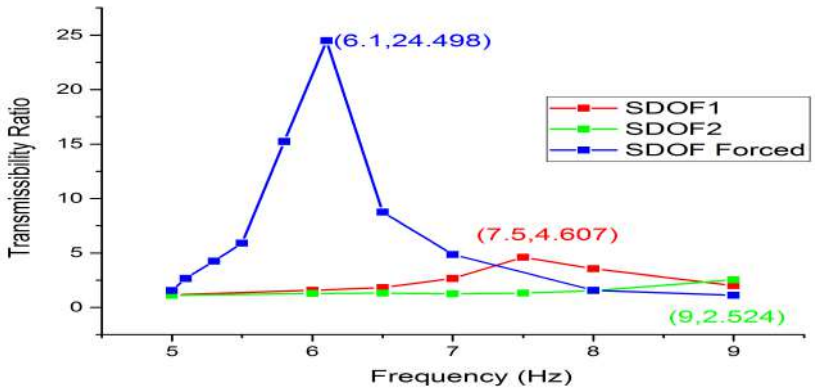

Figure 7.34: Comparison of Transmissiblity Plot

In the above figure "SDOF 1" represents SDOF building model with single Pneumatic Damper, also, SDOF 2 represents SDOF Building Models with Double Pneumatic Damper and SDOF Forced represents SDOF building model without Dampers.

There is decrease in Response of SDOF building model with double Pneumatic Damper compared to Single Pneumatic Damper and also compared to building model without Pneumatic Damper.

7.3.2 SDOF System having material irregularity with Pneumatic Damper

(a) Experimental setup of SDOF building model with material irregularity having single Pneumatic Damper

(b) Experimental setup of SDOF building model with material irregularity having double Pneumatic Damper

Figure 7.35: Experimental setup of SDOF system with material irregularity having Pneumatic Damper

SDOF system with Material irregularity was attached to Shake table using Allen screws and Harmonic excitation's were given to the SDOF system with Material irregularity.

Comparison of Transmissiblity ratio of SDOF Building model having material irregularity with Single and Double pneumatic damper and also its comparison was done for SDOF Building Model with material irregularity without Pneumatic Damper . Figure 7.36 shows the results of SDOF building model having material irregular with and without Pneumatic damper.

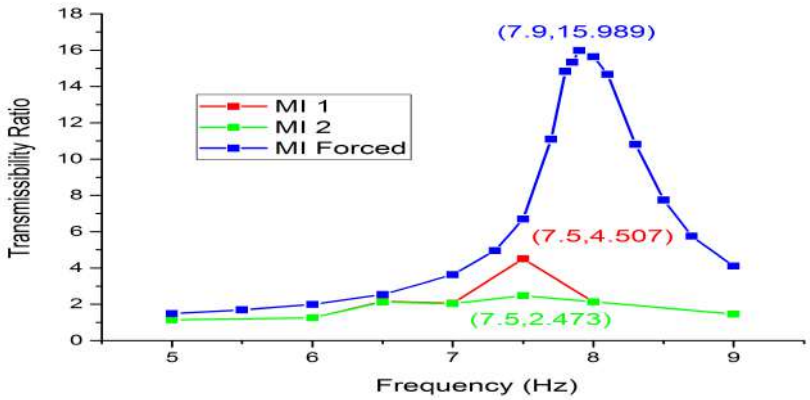

Figure 7.36: Comparison of Transmissibility Plot

In the above figure "MI 1" represents SDOF building model with material irregularity having single Pneumatic Damper, also, MI 2 represents SDOF Building Models with material irregularity with Double Pneumatic Damper and MI Forced represents SDOF building model with material irregularity without Dampers.

There is decrease in Response of SDOF building model with material irregularity with double Pneumatic Damper compared to Single Pneumatic Damper and without Pneumatic Damper.

7.3.3 SDOF System having L-Planar Asymmetry with Pneumatic Damper

SDOF system with Planar Asymmetry L Shape was attached to Shake table using Allen screws and Harmonic excitation's were given to the SDOF system with Planar asymmetry L Shape.

Comparison of Transmissiblity ratio of SDOF Building model having Planar asymmetry L Shape with Single and Double pneumatic damper and also its comparison was done for SDOF Building Model having Planar asymmetry L Shape without Pneumatic Damper . Figure 7.38 shows the results of SDOF building model having Planar asymmetry L Shape with and without Pneumatic damper.

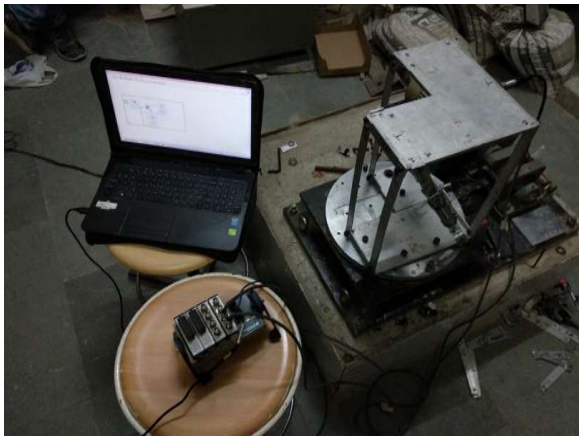

(a) Experimental setup of SDOF building model with Planar Asymmetry L Shape having single Pneumatic Damper

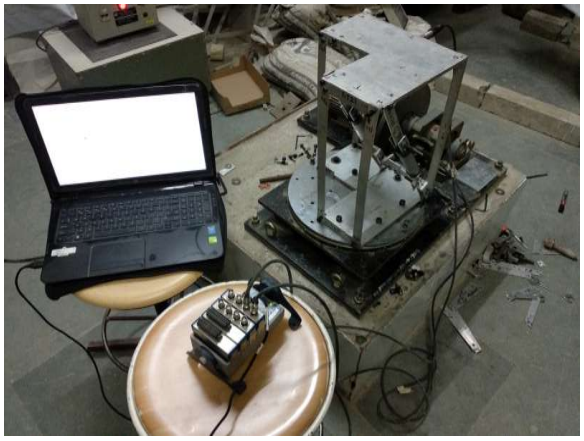

(b) Experimental setup of SDOF building model with Planar Asymmetry L Shape having double Pneumatic Damper

Figure 7.37: Experimental setup of SDOF system with Planar Asymmetry having Pneumatic Damper

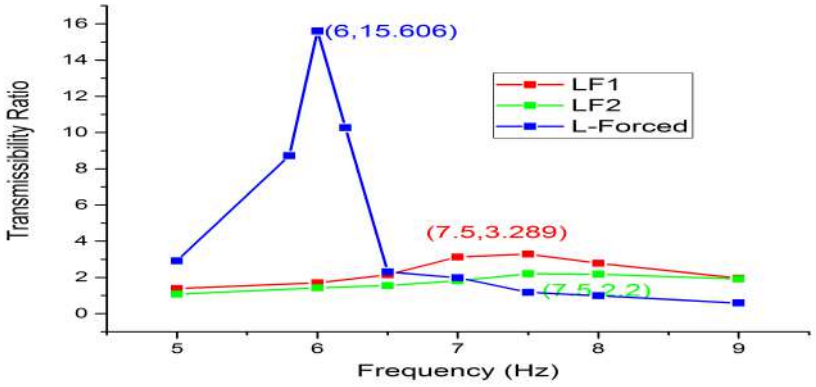

Figure 7.38: Comparison of Transmissibility Plot

In the above figure "LF 1" represents SDOF building model with Planar asymmetry L Shape having single Pneumatic Damper, also, LF 2 represents SDOF Building Models with Planar asymmetry L Shape with Double Pneumatic Damper and L Forced represents SDOF building model with Planar asymmetry L Shape without Dampers.

There is decrease in Response of SDOF building model with Planar asymmetry L Shape with double Pneumatic Damper compared with Single Pneumatic Damper and without Pneumatic Damper.

7.3.4 SDOF System having T-Planar As-symmetry with Pneumatic Damper

SDOF system with Planar Asymmetry T Shape was attached to Shake table using Allen screws and Harmonic excitation's were given to the SDOF system with Planar asymmetry with Planar Asymmetry T Shape.

Comparison of Transmissiblity ratio of SDOF Building model having Planar asymmetry T Shape with Single and Double pneumatic damper and also its comparison was done for SDOF Building Model having Planar asymmetry T Shape without Pneumatic Damper . Figure 7.40 shows the results of SDOF building model having Planar asymmetry T Shape with and without Pneumatic damper.

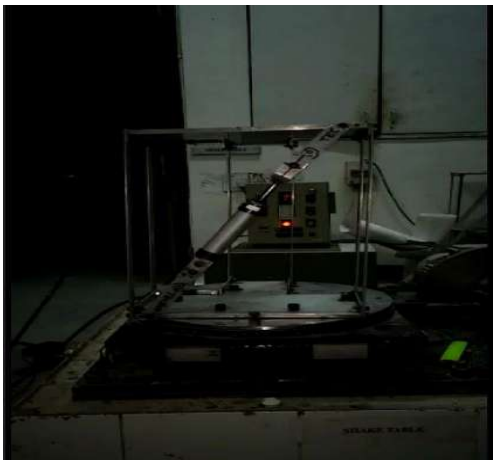

(a) Experimental setup of SDOF building model with Planar Asymmetry T Shape having single Pneumatic Damper

(b) Experimental setup of SDOF building model with Planar Asymmetry T Shape having double Pneumatic Damper

Figure 7.39: Experimental setup of SDOF building model with Planar Asymmetry L Shape having Pneumatic Damper

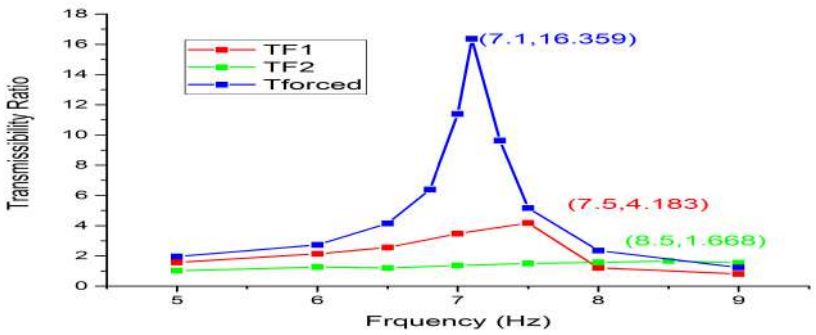

Figure 7.40: Comparison of Transmissibility plot

In the above figure "TF 1" represents SDOF building model with Planar asymmetry T Shape having single Pneumatic Damper, also, TF 2 represents SDOF Building Models with Planar asymmetry T Shape with Double Pneumatic Damper and T Forced represents SDOF building model with Planar asymmetry T Shape without Dampers.

There is decrease in Response of SDOF building model with Planar asymmetry T Shape with double Pneumatic Damper compared with Single Pneumatic Damper and without Pneumatic Damper.

7.4 Comparison of Damping of Building Model's With and Without Dampers

Comparison of Building model having irregularity with and without Pneumatic dampers under free vibrations are shown in below tables.

Table 7.1: SDOF Building Model

SDOF Building Model		
Cases	Damping	Natural Frequency (Hz)
Bare SDOF Model	.757 %	6.59
SDOF Model with Single Pneumatic Damper	23.55 %	8.49
SDOF Model with Double Pneumatic Damper	59.82 %	9.9

Table 7.2: SDOF Building Model with Material Irregularity

SDOF Building Model with Material Irregularity		
Cases	Damping	Natural Frequency (Hz)
Building Model	1.05 %	6.31
Building Model with Single Pneumatic Damper	24.085 %	7.76
Building Model with Double Pneumatic Damper	46.83 %	7.06

Table 7.3: SDOF Building Model with Planar irregularity L Shape

SDOF Building Model with Planar irregularity L Shape		
Cases	Damping	Natural Frequency (Hz)
Building Model	1.07 %	6.4
Building Model with Single Pneumatic Damper	21.11 %	8.37
Building Model with Double Pneumatic Damper	47.07 %	7.92

Table 7.4: SDOF Building Model with Planar irregularity T Shape

SDOF Building Model with Planar irregularity T Shape		
Cases	Damping	Natural Frequency (Hz)
Building Model	1.63 %	7.14
Building Model with Single Pneumatic Damper	24.105 %	7.4
Building Model with Double Pneumatic Damper	41.94%	8.42

Form the above table it can be concluded that there is increase in damping when Pneumatic dampers are introduced in the system and it can be concluded that there is decrease in response which is observed in the transmissibility plot shown in the Forced Vibration section above.

7.5 Summary

In this chapter results of experimental work has been presented.In this chapter, SDOF system with and without irregularities were introduced with Pneumatic damper and then comparison of dynamic properties such as damping ratio and transmissibility plots are presented.

Chapter 8

Conclusion and Future scope of work

8.1 Summary

The dynamic response of structures is an important topic in structural engineering field. Many a times to control the dynamic response of the structure various types of external dampers are provided.Which increases the damping and helps in resisting the dynamic forces acting on the system.

In this work, main focus was on evaluation of various dynamic properties of building models with and without irregularities and study the response of one storied building frame with planar asymmetry and material irregularity subjected to harmonic base motions.

Comparison of response of building model having planar and material irregularity when the angle of incidence of base motion is varied from 0 to $\pi/2$,and the results were compared experimentally and analytically .

Characterization of Pneumatic damper and piston type damper were evaluated,Then effectiveness of Pneumatic damper for structural response control of SDOF system having material and plan irregularity are found out.

8.2 Conclusion

Based on the work carried out, following conclusion were made.

- Modulus of Elasticity of Steel and Aluminum Material has been determined experimentally .

- Stiffness of Bare Aluminum Model is found out by experimental, theoretical and by using Shake Table and the results shows good agreement with each other.
- Frequency of Bare Aluminum Model is found out by experimental, theoretical and by using Shake Table and all the results shows good agreement with each other
- Damping Ratio of Aluminum and Steel material column strip through free Vibration is found out to be 0.4% and 0.7% respectively.
- Damping coefficient was evaluated for SDOF building model with material irregularity and planar irregularity i.e L-shape and T-shape,The results shows minor increment of damping coefficient in T-shape building model compared to other building models.
- Forced vibration study is carried out to understand the coupling behaviour of the SDOF model with irregularity. It has been found that no significant influence of angle of incident is observed for the SDOF models with asymmetry.
- Characterization of Pneumatic damper and Piston type damper is done, ζ_{avg} for Pneumatic damper was found out to be 0.267 and for Piston type damper ζ_{avg} was found out to be 0.0646.
- Damping ratio was observed to be very high when SDOF building model with and without irregularities were attached with single and double Pneumatic damper.
- The transmissibility plot depicts reduction in response for the SDOF test model with and without material and planar irregularities when attached with Pneumatic damper on comparison with the bare SDOF test model having Planar and material irregularities.

8.3 Future Scope of Work

- An experimental study comprising of MDOF building model with Passive damping devices like viscous damper, visco-elastic damper, etc. can be studied.
- Numerical validation of response of SDOF and MDOF building model with passive damping devices can be studied.

- Experimental study of various Intelligent material system like Electrorheological and Magnetorheological Dampers can be done.

Bibliography

[1] Manohar, C. S., and Venkatesha, S. (2006), *"Development of experimental setups for earthquake engineering education"*, Report National Program on Earthquake Engineering Education, MHRD, Government of India.

[2] Panchal, D. B. (2012), *"Experimental Evaluation of Dynamic Properties for Building Systems"*, M.Tech Thesis, Department of Civil Engineering, Institute of Technology, Nirma University.

[3] Patel H. Y. (2016), *"Dynamic Response Control of a Building Model"*, M.Tech Thesis, Department of Civil Engineering, Institute of Technology, Nirma University.

[4] Umashankar, K.S., Abhinav, A., Gangadharan, K.V. and Vijay, D., 2009. Damping behaviour of cast and sintered aluminium. ARPN Journal of Engineering and Applied Sciences, 4(6), pp.66-71

[5] Slifka D.L (2004), *"An Accelerometer based approach to measure the Displacement of a Vehicle body "*, M.Tech Thesis,University of Michigan – Dearborn,Department of Electrical and Computer Engineering

[6] Shah D (2017), *"Experimental Response of Irregular Building under Dynamic Loading"*, Institute of Technology, Nirma University.

[7] Aghlara, R., and Tahir, M. M. (2018). *"A passive metallic damper with replaceable steel bar components for earthquake protection of structures"*. Engineering Structures, 159, 185-197.

[8] Miyamoto, H. K., Gilani, A. S., and Wada, A. (2012). *" The Effectiveness of Viscous Dampers for Structures Subjected to Large Earthquakes"*. In Proceedings of the 15th World Congress on Earthquake Engineering.

[9] Mosqueda, G., Whittaker, A. S., Fenves, G. L., and Mellon, D. (2002). *"Performance characterization of fluid viscous dampers"*. In Seventh US National Conference on Earthquake Engineering

[10] IS 1893 (Part 1): 2002, *"Criteria for Earthquake Resistant Design of Structures"*, Part-1, General Provisions and Buildings, 5^{th} Revision, Bureau of Indian Standards, New Delhi.

[11] Clough R.W. and Penzien J.P. (2003). *"Dynamics of Structures"*, 2^{nd} Edition, Computers & Structures Inc.

[12] Chopra, A. K. (2007), *"Dynamics of Structures : Theory and Applications to Earthquake Engineering"*, 5^{th} Edition, Pearson Publication.

[13] Naeim, F. (1989), *"The Seismic Design Handbook"*, 1^{st} edition, Springer Science & Business Media, New York.

[14] Jeorme, J. (2010), *"Virtual Instrumentation Using LabVIEW"*, PHI Learning Private Limited.

[15] Manohar, C.S. *"NPTEL, Stochastic Structural Dynamics, IISc Bangalore"*.

Appendix A

Matlab Codes

A.0.1 MATLAB code for eigen value problem

```
m=[1.63345 0 0;0 1.63345 0;0 0 .01945884]
k=[3788.698 0 64.5826;0 263104.045 -9787.64045;64.5826 -9787.64045 5579.427327]
[eigenvector,w]=eig (k,m)
naturalfreq=sqrt(w)
NATFREQHZ=naturalfreq/(2*pi)
n = eigenvector
```

A.0.2 Matlab code for evaluation of response of SDOF system with Irregularities

```
c = ((1)/((38.787*38.787)-(43.9822*43.9822)+(i*2*38.787*.01*43.9822)))
+((0.00169*0.00169)/((427.326*427.326)-(43.9822*43.9822)
+(i*2*.01*427.326*43.9822)))+((.0339*.0339)/((288.1183*288.1183)
-(43.9822*43.9822)+(i*2*.01*288.1183*43.9822)))
c1 = c*exp(i*43.9822*0.1428)
c2 = abs(c1)
c3 = angle(c1)
d = ((-0.000424)/((38.787*38.787)-(43.9822*43.9822)
+ (i*2*38.787*.01*43.9822)))+((0.00169*-.0664)/((427.326*427.326)
-(43.9822*43.9822)+(i*2*.01*427.326*43.9822)))
+ ((.0339)/((288.1183*288.1183)-(43.9822*43.9822)+ (i*2*.01*288.1183*43.9822)))
```

```
d1 = d*exp(i*43.9822*0.1428)
d2 = abs(d1)
d3 = angle(d1)
e = ((-0.000943)/((38.787*38.787)-(43.9822*43.9822)+
(i*2*38.787*.01*43.9822)))+((0.00169*.239)/((427.326*427.326)
-(43.9822*43.9822)+(i*2*.01*427.326*43.9822)))
+((.0339)/((288.1183*288.1183)-(43.9822*43.9822) +(i*2*.01*288.1183*43.9822)))
e1 = e*exp(i*43.9822*0.1428)
e2 = abs(e1)
e3 = angle(e2)
```

Where c,d,e gives response in X,Y,θ Directions